

**Escuela Técnica Superior de Ingeniería
de Telecomunicación La Salle**

Trabajo Final de Máster

Máster Universitario en Ingeniería de Telecomunicación

**Virtual Antenna™ for Open-Source
Hardware Platforms:
IoT Smart-Tracking Applications**

Alumno

Roc Grados Luna

Profesores Ponentes

Dra. Aurora Andújar y Dr. Jaume Anguera

ACTA DEL EXAMEN DEL TRABAJO FIN DE MÁSTER

Reunido el Tribunal calificador en el día de la fecha, el alumno:

D. Roc Grados Luna

expuso su Trabajo Fin de Máster, el cual trató sobre el tema siguiente:

Virtual Antenna™ for Open-Source Hardware Platforms: IoT Smart-Tracking Applications

Acabada la exposición y contestadas por parte del alumno las objeciones formuladas por los Sres. miembros del tribunal, éste, valoró dicho Trabajo con la calificación de

Barcelona, a de..... de2019

VOCAL DEL TRIBUNAL

VOCAL DEL TRIBUNAL

PRESIDENTE DEL TRIBUNAL

La investigación realizada en este proyecto ha sido financiada por la empresa tecnológica Fractus Antennas.

Gracias al acuerdo de colaboración entre Ingeniería La Salle de la Universidad Ramon Llull – y Fractus Antennas, ambas en Barcelona.

The research done in this project has been funded by the technology company Fractus Antennas.

Thanks to the collaboration agreement between Ingeniería La Salle of the University Ramon Llull –and Fractus Antennas both in Barcelona.

La investigació realitzada en aquest projecte ha estat finançada per l'empresa tecnològica Fractus Antennas.

Gràcies a l'acord de col·laboració entre Enginyeria La Salle de la Universitat Ramon Llull – i Fractus Antennas a Barcelona.



ABSTRACT

In this project it has been searched a headliner IoT device and then, studied the applications and the bands which could be covered with a Virtual Antenna™ from Fractus Antennas Technology embedded into the selected device.

To achieve the main goal, first it has been defined the operating bands compatible with the chosen device needed to cover. Once the device and the frequency range to cover have been decided it has been studied various scenarios contemplating diverse antennas and designs.

The searched of the final solution it has had as a first step the electromagnetic simulation of a lot of set-ups which it helped to focalize in one direction and then, the physically implementation of the best performance set-ups simulated has been done in order to choose the better set-up for the embedding.

The conclusions obtained as a result of the study will allow to have an idea of the Virtual Antenna™ performance in an already commercialized device and the process to follow when the implementing of an embedded antenna is wanted in a small IoT device.

INDEX

1. INTRODUCTION	3
1.1 SCOPE AND OBJECTIVE.....	4
1.2 STRUCTURE.....	5
1.3 METHODOLOGY	6
1.4 ANTENNA PARAMETERS.....	7
1.5.1 Antenna Impedance	7
1.5.2 S parameters	8
1.5.3 Smith Chart.....	8
1.5.4 Antenna and Radiation Efficiency	9
2. BENCHMARKING	11
2.1 INDUSTRY 4.0 DEVICES ON THE MARKET.....	12
2.2 SIERRA WIRELESS: MANGO H DEVICES	12
2.3 MANGO H™ RED	13
3. ELECTROMAGNETIC SIMULATIONS	17
3.1 INTRODUCTION	18
3.2 CST SIMULATOR	19
3.3 ABOUT VIRTUAL ANTENNA™	20
3.4 FR01-S4-224 RUN mXTEND™	21
3.4.1 Experiment 1: 30x11mm Clearance Area and 5mm + 10mm of Feeding Line	22
3.4.2 Experiment 2: 30x11mm Clearance Area and 18mm + 11mm of Feeding Line	24
3.4.3 Experiment 3: 25x11mm Clearance Area and 13mm + 11mm of Feeding Line	26
3.4.4 Experiment 4: 20x11mm Clearance Area and 8mm + 11mm of Feeding Line	28
3.4.5 Comparison between Experiments	30
3.5 FR01-S1-210 TRIO mXTEND™	31
3.5.1 Experiment 1: 30x12mm Clearance Area Outside Main Board	31
3.5.2 Experiment 2: 31x12mm Clearance Area Inside Main Board	36

3.5.3 Experiment 3: 35x11mm Clearance Area Inside Main Board	38
3.5.4 Comparison between Experiments	41
3.6 NN03-320 DUO mXTEND™	43
3.7 Conclusions.....	49
4. EXPERIMENTAL VALIDATION	51
4.1 INTRODUCTION	52
4.2 PROTOTYPING	53
4.3 TRIO mXTEND™ PROTOTYPE	56
4.3.1 Experiment 1: 35 x 12mm ² Clearance Area and vertical pads for LTE and GNSS	56
4.3.2 Experiment 2: 35 x 12mm ² Clearance Area and horizontal pads for LTE and GNSS ..	63
4.4 DUO mXTEND™ PROTOTYPE	72
4.4.1 Experiment 3: 30 x 11mm ² Clearance Area and vertical pads for LTE and 7.5x4mm Clearance Area for GNSS.....	72
4.4.2 Experiment 4: 30 x 11mm ² Clearance Area and horizontal pads for LTE and 7.5x4mm Clearance Area for GNSS.....	79
4.4 COMPARISON BETWEEN EXPERIMENTS	86
4.5 EMBEDDING THE SOLUTION IN THE mangOH™ RED.....	89
5. CONCLUSIONS	97
6. BIBLIOGRAPHY.....	103

1. INTRODUCTION

1.1 SCOPE AND OBJECTIVE

Nowadays all the devices are connected between each other and all kinds of people is benefiting from it. The IoT (Internet of Things) could be defined as an interconnexion between devices through internet to transmit all kinds of data and without a human interaction.

Not only the most logical devices as sensors or telemetry objects are IoT devices, there are many devices which the society use during this routine without actually knowing they are IoT devices, as it can be the cars, access-control devices, the home automation, the mobile-phones, etc.

The total number of IoT devices currently active is massive but the growth of this technology is predicted to be even bigger. But not only the society is benefiting from the IoT growth, the industry is one of the most benefited fields from this massive growth.

Such is the revolution it has meant the Internet of Things for the industry that it is considered as the fourth industry revolution called as Industry 4.0.

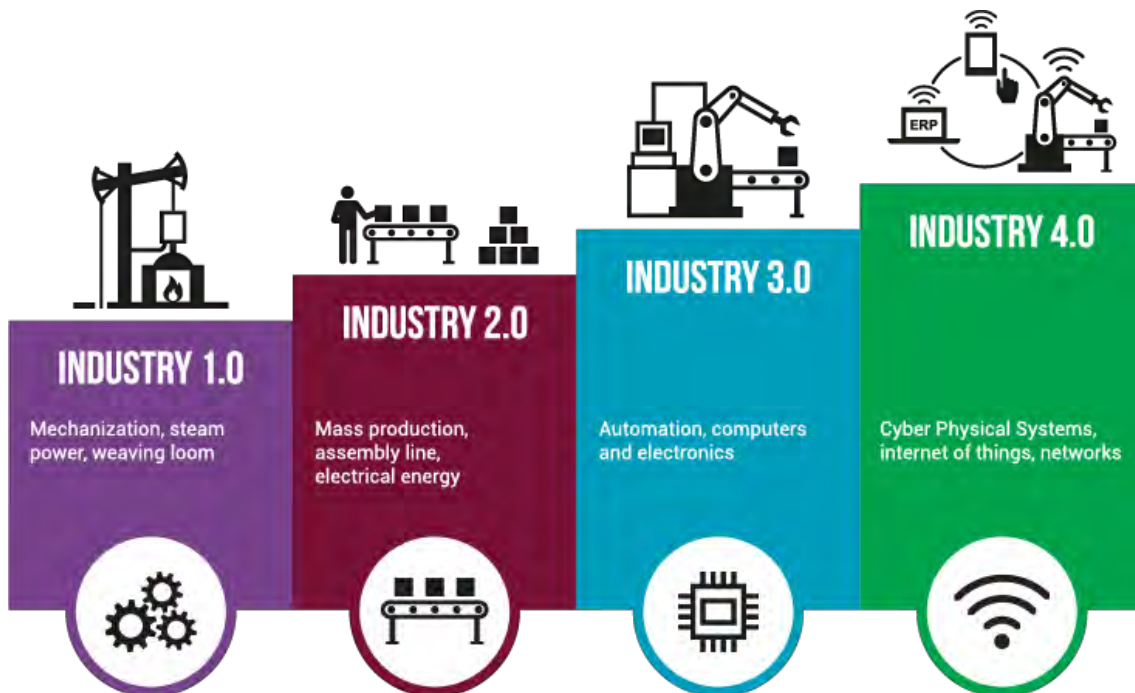


Figure 1 The four Industry revolution from the first (left) to the fourth (right) by accountancyresourcinggroup [1]

In the 1800s the steam powered machines were developed and increased the production capabilities making the first massive growth for the industry. In the late 19th century, electricity brought the standardization and the mass production increasing the productivity not only for the company, for the worker too. The Industry 3.0 started in the late 20th century with the inclusion of the electronic devices such as the integrate circuit chips, making possible to automatize machines and replace some operators. Finally, in the 21st century, the Industry 4.0 appeared along the Internet of Things with manufacturing methods enable to connect all the devices between each other and share information without the necessary of a human interaction.

Seen the importance of the Internet of Things in the Industry it has been searched a headliner device prepared for the Industry 4.0 field, to study the implementing of a VAT (Virtual Antenna Technology) product from Fractus Antennas company embedded into the selected device.

The objective of this project is to study the performance achievable for a Virtual Antenna in a device already designed and commercialized working in the IoT habit. An IoT device can work in several bands and applications, so it has been searched a solution able to cover the most important or used bands in an IoT device.

1.2 STRUCTURE

With the objective to find an antenna solution which could cover the most important bands for an IoT device already commercialized it has been done this project. First, a search of a device which it is already commercialized and used to not only for the IoT field but also for the Industrial Internet of Things, has been done in the Chapter 2 of this project. The bands which the antenna must cover it have been decided in the same Chapter, after the election of the device.

Once the device and the bands to cover has been decided, the project has been divided in 2 big blocks which are the third chapter called as “Electromagnetic Simulations” and the fourth chapter called as “Experimental Validation”.

The third chapter is a set of simulations testing various antennas in a set-up the most similar possible to the real device. These simulations have been done in order to know the most quickly possible the performance achievable by the antennas tested and to decide some critical parameters of the set-up design such as the Clearance Area available for the antenna, the length of the feeding line, the antenna location, etc. To evaluate the antenna performance of each

scenario simulated it has been calculated the reflection coefficient and the antenna and radiation efficiency. Thanks to that, it has been possible to decide which antenna and which scenario it would be physically implemented in Chapter 4.

The fourth chapter is the physically implementation of the scenarios chosen in the third chapter. To implement these scenarios, it has been mounted prototypes the closest possible to the original device selected in order to see the approximate performance of the antenna in the IoT device. Finally, it has been selected one of the prototypes solutions to be embedded into the original device and it has been calculated and compared the performance achieved.

1.3 METHODOLOGY

This project has been separated in four steps which have been followed by order to the achieve the final result.

First of all, a Documentation process has been realized. In this first step, it has been decided, at the beginning, the objectives and the scope of the project. Once the scope has been decided, the search of a device adjusted to the project scope has been done, with the result of the election of the mangOH™ RED device by Sierra Wireless company which fulfill all the specification defined at the scope. Then, a benchmarking of the product has been done to know which applications and bands frequency are the most common used for this kind of products.

The second step of the project, it has been the Simulation period where the firsts approximation designs have been done for three different antennas and various scenarios for each antenna. This process it helped to discard and as consequence, to select, the antennas to test and the set-up to mount physically.

The simulations done for this step have been realized with the CST Simulator software from Dassault Systems. The simulations done with this Electromagnetic Simulator it has helped to see the performance of various scenarios with the three antennas simulated and have a first approximation of the matching network topology it has been needed to tune the matching network physically. It is important to note, the values achieved in the Simulator will be probably higher than the achieved ones when the solution is mounted due to is only an, very good one, approximation of the reality. With the CST Simulator has been measured the Reflection

Coefficients and the Antenna and Radiation Efficiencies, for the frequencies specified in the simulation.

Then, the third step it has been the prototyping process where it has been physically mounted, the solution chosen at the simulation period. For the prototyping process, first it has been created a PCB (Printed Circuit Board) in-house at the Fractus Antennas installations with the footprint needed and simulated. After the PCB in-house creation, the antenna has been soldered into the board with a shot gun applying 420 °C heat to the antenna meanwhile is pushed to the board with a tweezer. Once the antenna is soldered into the board, the connectors and coaxial cables necessary to measure the antenna performance has been implements into the board. Finally, the matching network solution components has been put on the required pads.

Finally, the last step consists in measuring the performance of the set-up mounted. First, the Reflection Coefficient is measured at the Network Analyzer knowing if the antenna is tuned at the desired frequency bands, and then the Antenna Efficiency is measured in a Stargate 32 Satimo anechoic chamber from Microwave Vision Company. It is important to note, the matching network implemented is readjusted with the Smith Chart help seen in the Network analyzed so, the prototyping step and the measuring step will be continuously changing in order to tune the matching network.

After the PCB in-house solution decided, it has been embedded the solution into the mangOH™ RED device following the same steps as it has been followed for the PCB in-house solutions.

1.4 ANTENNA PARAMETERS

Some antenna concepts appear through the project, so for a better understanding and the clarification of all these concepts, it has been explained what it has been considered the basics as far as the antenna parameters.

1.5.1 Antenna Impedance

The input impedance of an antenna is defined as the relation between the voltage and the current of the antenna in question. The antenna impedance has a real/resistive part (R_a) which is dependent to the frequency and an imaginary part (X_a) which also depends to the frequency

(1.1)

$$Z_a = \frac{V_{in}}{I_{in}} \quad \Rightarrow \quad Z_a = R_a + jX_a \quad I. \quad 1$$

Regarding the resistive part, is the result of sum between the radiation resistance (R_r) which is caused by the radiation of electromagnetic waves from the antenna, and the loss resistance which is caused by electrical resistance and is converted into heat (1.2).

$$R_a = R_r + R_{\Omega} \quad II. \quad 2$$

On the other hand, when the imaginary part is equal to 0 ($X_a = 0$), the antenna is considered to be in resonance.

1.5.2 S parameters

The S parameters are defined as the relation between an input voltage wave and the voltage wave, which is returning from an impedance changing point of the system. This returning voltage wave is caused by the impedance untuning between where the input voltage wave is coming (in our case the impedance of the antenna Z_L) and the mentioned specific point (in our case the impedance of the signal generator Z_0).

$$S_{11} = \frac{V_{in}^-}{V_{in}^+} = \frac{Z_L - Z_0}{Z_L + Z_0} \quad S_{11}|_{dB} = 20 \log|S_{11}| \quad III. \quad 3$$

When the antenna impedance and the generator impedance are equal, then the antenna is tuned and therefore, the S_{11} is zero (there is no returning signal).

The S parameters are referred to two sub-indexes (S_{nm}), where “n” is the output port and “m” is the input port, where the measure has been done. Consequently, S_{21} is considered the coefficient transmission or the coupling between port 2 (output signal) and the port 1 (input signal).

1.5.3 Smith Chart

The Smith Chart is a polar diagram which shows how the complex impedance of a transmission line or a matching circuit, changes along the frequency spectrum.

The Smith Chart can be normalized for the impedance, admittance or both at the same time. The most common normalization impedance is 50Ω which is located at the center of the diagram.

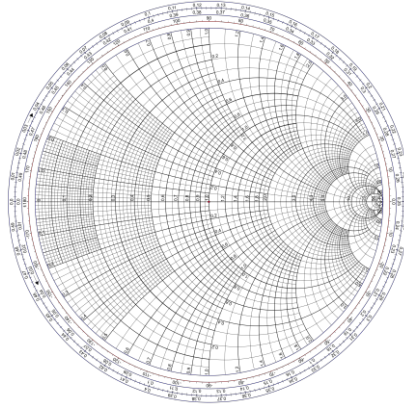


Figure 2 Smith Chart normalized for the impedance

1.5.4 Antenna and Radiation Efficiency

The Radiation Efficiency (1.4) is defined by the ratio of the power radiated over the input power.

$$\eta_r = \frac{P_{radiated}}{P_{input}} = \frac{P_r}{P_r + P_\Omega} = \frac{\frac{1}{2} I^2 R_r}{\frac{1}{2} I^2 (R_r + R_\Omega)} = \frac{R_r}{R_r + R_\Omega} \quad IV. 4$$

On the other hand, the Antenna Efficiency is the ratio of the power delivered to the antenna and the power radiated for the antenna. Therefore, it takes into consideration the Radiation Efficiency and the untuning of the matching network.

For an ideal case where the matching network is totally tuned at the specific working band of the antenna ($S_{11} = 0$ in lineal), the Radiation Efficiency and the Antenna Efficiency have the same value.

$$\eta_a = \eta_r \cdot (1 - |S_{11}|^2) \quad V. 5$$

2. BENCHMARKING

2.1 INDUSTRY 4.0 DEVICES ON THE MARKET

Nowadays the IoT market is expanding very fast and the Industry has been one of the most favored fields by this new technology. A lot of devices oriented to the called Industry 4.0 has been recently appeared in the market and with so many devices to choose, it can be difficult to find the most appropriate for your project.

Consequently, is important to mark the stronger priorities for your project and search a device which can fulfill your requirements. Not only the hardware requirements are important, the software could be a problem if you are not familiarized with this kind of solution and some of the open-software devices which are more friendly for a started, could not be enough for an industrial-grade IoT project.

So, it has been searched a device with an industrial-grade components hardware, friendly software for a starter in the IIoT field (Industrial Internet of Things), small and with a high battery life expectancy. The bands wanted to work are also important due to not all the devices are compatible with the LTE bands, GNSS bands or Bluetooth bands.

The result of the searching it has been the mangOH™ devices from Sierra Wireless.

2.2 SIERRA WIRELESS: MANGOH DEVICES

The mangOH™ devices from Sierra Wireless company, has 3 kind of devices centered in the IoT development field: mangOH™ Green, mangOH™ Red and finally the mangOH™ Yellow.

Being the mangOH™ Green the first device of the series, is a product which main objective is to provide a sensor-to-cloud platform with a fast prototype step ready for the industrialization. The mangOH™ Green as well as the other products of the series, is an open hardware product and in the mangOH™ Green case, compatible with other open hardware products as Arduino.

The development environment for the device is an open source Legato Linux platform, developed for Sierra Wireless which guarantees a robust API and making easy connect to cellular networks and to the cloud.

After the mangOH™ Green comes the mangOH™ Red device. Sierra Wireless designed the evolution of the mangOH™ Green as a smaller option (120 mm x 100 mm for the mangOH™ Green vs the 69 mm x 61 mm of the mangOH™ Red), less expensive but as capable as the mangOH™ Green.

With a battery life of approximate 10 years, this device support 2G, 4G, LTE-M, Bluetooth 4.0, Wi-Fi b/g/n capabilities and GNSS. The development platform is the same Legato Linux used for the mangOH™ Green and includes an accelerometer, a gyroscope, temperature and pressure sensors, as well as light sensors and a 26-pin Raspberry Pi compatible connector.

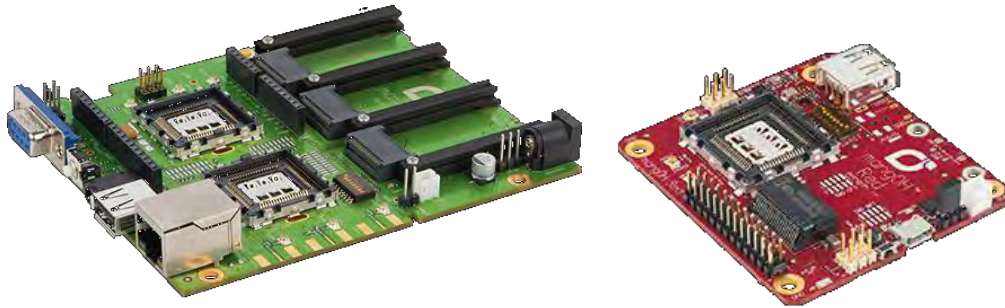


Figure 3 At the left, mangOH Green device from Sierra Wireless and at the right, mangOH™ Red device from Sierra Wireless

Finally, the recently commercialized last product from the series, is the mangOH™ Yellow. Smaller and lighter, mangOH™ Yellow is targeted at IoT applications where compactness and low-power consumption are critical parameters. The portability between all the mangOH™ products can be easily done thanks to the developing platform Legato open source, so do an update of any of the older devices to the newest one is not a problem.

2.3 MANGO™ RED

The device selected from the mangOH™ series of Sierra Wireless it has been the mangOH™ Red device. Is smaller and cheaper than mangOH™ Green, a critical parameter in the IoT field nowadays and is compatible with many applications where the implementation study of the Virtual Antenna Technology can be done.

Apart from the already mentioned application included on the device, mangOH™ Red is based on the CF3 modules engine from Sierra Wireless. This means with the same mangOH™ Red device you are able to put the desired module depending on the applications and features you need to work. As a consequence, the module needed changes depending on the target of the project and can be change for another module, making the mangOH™ Red device usable for future projects prototypes working in the different applications.

There are five different sizes. The smaller size modules are though for wearables and sensors working at WiFi, BLE and LPWA (Low Power Wide Area). On the other hand, the bigger size modules are though for automotive applications with additional bands requirements.

As the solution searched in this project wants to fulfill the maximum amount of the mangOH™ Red devices without the necessary of an antenna changing, it has been done a comparison between the 19 modules available for the mangOH™ Red (see Table 1) and after that, it has been counted for every module parameter how many modules uses that parameter (Table 2).

Therefore, the frequency bands which the Virtual Antenna covers, have been decided considering the most used bands.

For the LTE bands, the low frequency range (LFR) covers from 824MHz – 960MHz (B5, B8 and GSM-900) and the high frequency range (HFR) covers from 1710MHz – 2170MHz (B1, B3, B4 and GSM-1800). As far as the GNSS bands, it has been decided to full cover it: 1561MHz for BeiDou E1 band, 1575 MHz for GPS L1 band and from 1598 MHz to 1606 MHz for GLONASS L1 band.

VAT for Open-Source Hardware Platforms: IoT Smart-Tracking Applications

WP Series									
Module PN	Regions	4G LTE Category	4G LTE Bands	3G Bands	2G Bands	Satellite Systems	Dimensions	Diversity/MIMO	Price
WP7700	Global	Cat-M1/NB1	B1, B2, B3, B4, B5, B8, B12, B13, B17, B18, B19, B20, B26, B28	-	-	GPS, Galileo, Glonass, Beidou	22x23x2.5mm	NO	\$129.00
WP7702	Global	Cat-M1/NB1	LTE: B1, B2, B3, B4, B5, B8, B12, B13, B17, B18, B19, B20, B26, B28	-	850, 900, 1800, 1900	GPS, Galileo, Glonass, Beidou	22x23x2.5mm	NO	\$129.00
WP7601-1	Americas	Cat-1	LTE: B4, B13	-	-	GPS, Galileo, Glonass, Beidou	22x23x2.5mm	YES	\$139.00
WP7603-1	Americas	Cat-1	LTE: B2, B4, B5, B12	B2, B4, B5	-	GPS, Galileo, Glonass, Beidou	22x23x2.5mm	YES	\$139.00
WP7607-1	EMEA	Cat-1	LTE: B1, B3, B7, B8, B20, B28	B1, B8	900, 1800	GPS, Galileo, Glonass, Beidou	22x23x2.5mm	YES	-
WP7608-1	India, China	Cat-1	LTE: B1, B3, B5, B8, B40, B41*	B1, B8	900, 1800	GPS, Galileo, Glonass, Beidou	22x23x2.5mm	YES	-
WP7601	Americas	Cat-4	LTE: B4, B13	-	-	GPS, Galileo, Glonass, Beidou	22x23x2.5mm	YES	-
WP7603	Americas	Cat-4	LTE: B2, B4, B5, B12	B2, B4, B5	-	GPS, Galileo, Glonass, Beidou	22x23x2.5mm	YES	\$139.00
WP7605	Japan	Cat-4	LTE: B1, B3, B8, B11, B18, B19, B21	B1, B6, B19	-	GPS, Galileo, Glonass, Beidou	22x23x2.5mm	YES	-
WP7607	EMEA	Cat-4	LTE: B1, B3, B7, B8, B20, B28	B1, B8	900, 1800	GPS, Galileo, Glonass, Beidou	22x23x2.5mm	YES	\$139.00
WP7608	India, China	Cat-4	LTE: B1, B3, B5, B8, B40, B41*	B1, B8	900, 1800	GPS, Galileo, Glonass, Beidou	22x23x2.5mm	YES	\$139.00
WP7609	Australia, Brazil	Cat-4	LTE: B1, B3, B5, B7, B8, B28	B1, B5, B8	900, 1800	GPS, Galileo, Glonass, Beidou	22x23x2.5mm	YES	-
WP7610	Americas	Cat-4	LTE: B2, B4, B5, B12, B13, B14, B17, B66	B2, B4, B5	-	GPS, Galileo, Glonass, Beidou	22x23x2.5mm	YES	-
WP7502	EMEA	Cat-3	LTE: B1, B3, B7, B8, B20	B1, B8	900, 1800	GPS, Galileo, Glonass	22x23x4.4mm	YES	-
WP7504	Americas	Cat-3	LTE: B2, B4, B5, B12, B17, B25, B26	B2, B4, B5, BC0, BC1, BC10	BC0, BC1, BC10	GPS, Galileo, Glonass	22x23x4.4mm	YES	-
WP7504-1	Americas	Cat-3	LTE: B2, B4, B5, B12, B17, B25, B26	B2, B4, B5	-	GPS, Galileo, Glonass	22x23x4.4mm	YES	-
WP8548	Global	-	-	B1, B2, B5, B6, B8, B19	850, 900, 1800, 1900	Galileo, Glonass, GPS	22x23x4.4mm	YES	\$137.00
HL Series *Only these 2 models are compatible with manHOH Red									
HL7800	Global	Cat-M1/NB1	B1, B2, B3, B4, B5, B8, B9, B10, B12, B13, B14, B17, B18, B19, B20, B25, B26, B27, B28, B66	-	-	GPS+Glonass	15x18x2.4mm	NO	\$139.00
HL7802	Global	Cat-M1/NB1	B1, B2, B3, B4, B5, B8, B9, B10, B12, B13, B14, B17, B18, B19, B20, B25, B26, B27, B28, B66	-	850, 900, 1800, 1900	GPS+Glonass	15x18x2.4mm	NO	-

Table 1 Comparison between all the modules compatibles with the mangOH™ Red device

VAT for Open-Source Hardware Platforms: IoT Smart-Tracking Applications

Number of Modules utilizing the following 4G bands:										
B1	B2	B3	B4	B5	B7	B8	B11	B12	B13	B14
11	9	11	11	12	4	11	1	9	7	3
B17	B18	B19	B20	B25	B26	B28	B40	B41	B66	
7	5	5	7	4	6	7	2	2	3	
Number of Modules utilizing the following LTE Categories:										
Cat-M1	Cat-1	Cat-3	Cat-4							
4	4	3	7							
Number of Modules per region:										
Global	Americas	EMEA	India, China	Japan	Australia, Brazil					
5	12	8	7	6	6					
Number of Modules utilizing the following 3G bands:										
B1	B2	B4	B5	B6	B8	B19	BC0	BC1	BC10	
8	6	5	7	2	7	2	1	1	1	
Number of Modules utilizing the following 2G bands:										
850	900	1800	1900	BC0	BC1	BC10				
3	9	9	3	1	1	1				
Number of Modules utilizing the following GNSS bands:										
GPS	Galileo	Glonass	Beidou							
19	17	19	13							
Number of Modules utilizing the following Dimensions:										
22x23x2.5mm	22x23x4.4mm	15x18x2.4mm								
7	4	2								

Table 2 Number of modules using the different parameters. In blue, the most used parameters by category and used in the solution

3. ELECTROMAGNETIC SIMULATIONS

3.1 INTRODUCTION

In the current chapter is explained the simulation design process as a first approximation to the final set-up mounted in the mangOH™ RED device. These simulations have helped to discard and choose some critical design parameters as which antenna has been tested, the clearance area dimensions, the feeding line dimensions or the antenna location.

Three antennas have been simulated in different scenarios: first the RUN mXTEND™ antenna booster placed at the top right corner working at LTE band (824MHz-960MHz & 1710MHz-2170MHz), then the TRIO mXTEND™ antenna booster at the top right corner working at LTE band in one port and working at GNSS band (1561MHz-1606MHz) in the other port, and finally one DUO mXTEND™ antenna booster placed at the top right corner working at LTE band and another DUO mXTEND™ placed at the bottom middle working at GNSS band.

The RUN mXTEND™ can only work at application per antenna as the DUO mXTEND™, but this last one, due to its small dimension can be placed vertically at the bottom middle of the PCB without occupying a high amount of space.

For every antenna it has been tested different Clearance Area antenna dimensions, searching an equilibrate solution between good performance and small dimension occupied. It has been decided to place in every antenna simulation, the LTE antenna in the top right corner because is where the original mangOH™ RED device places the connectors to its antennas and where there is more free space to place the supposed antenna.

As far as the DUO mXTEND™ antenna for GNSS placed at the bottom middle, it has been searched a place at the PCB border where the antenna could be fit.

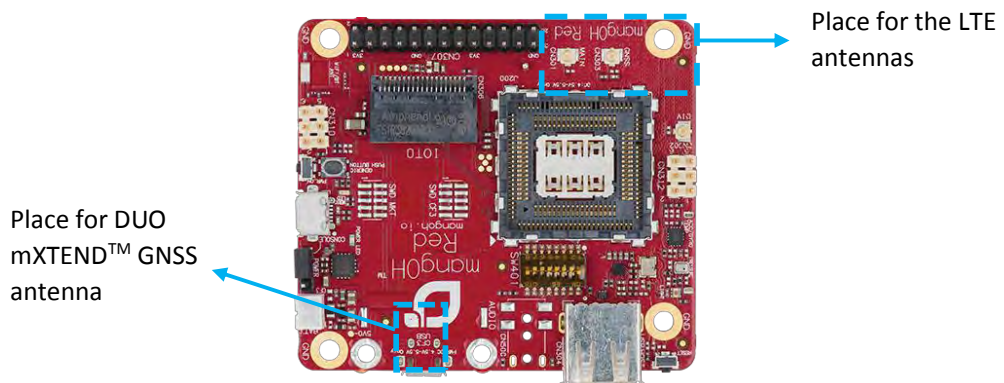


Figure 4 Areas reserved to place the antenna in the original mangOH™ RED device.

3.2 CST SIMULATOR

In order to reduce all the set-ups and scenarios possibilities for the prototyping process, it has been used an Electromagnetic Simulator able to simulate all the device to simulate. The Electromagnetic Simulator used it has been the CST Simulator which is a high-performance 3D EM analysis software package for designing, analyzing and optimizing electromagnetic (EM) components and systems. The Fractus Antennas' CST license has been used.

It has been simulated a 1mm width, 69mm x 61mm dimensions (the same as the original mangOH™ RED device) FR4 PCB with a Loss tangent of 0.014 at 1GHz and a Permittivity of 4.3, the same used at the Prototyping process which is used to be a PCB standard properties. Then all the top PCB layer it has been covered by copper and after that, some copper it has been removed on the Clearance Area antenna space. Once the PCB footprint is done, the antenna to simulate has been added to the design next to its respective feeding line. At the end of all the feeding lines created just before the ground plane area, a port has been created where all the antenna performance will be measured (the Reflection Coefficient and the Antenna and Radiation Efficiency).

It is important to note the mesh on the design is very important due to it will rule how precise is the simulation launched and how long it will be (the more mesh, more time to simulate). Furthermore, the Virtual Antennas design used for the simulations, have a very precise structure where every detail count, so is very important to realize a restrictive mesh in the sensible areas if a realistic performance is wanted.

The number of monitors used in the simulation will restrict the accuracy of some measures like the Antenna and Radiation Efficiency, so if it is put monitors every 10MHz (for example), then it will be obtained the exact Antenna or Radiation Efficiency value for every 10MHz, and the values between each monitor it will be calculated like an interpolation. As it happened with the meshing, the more monitors more long the simulation will be, but more accurate measure it will be obtained.

3.3 ABOUT VIRTUAL ANTENNA™

Nowadays the devices need an antenna capable to operate in several frequency regions. To cover these several regions, it has been used antennas having self-resonant performance. But these kinds of antennas have some limitations with the technology tendency such as the small size of the devices or the embedding of the antenna in the device.

But a different kind of antennas have surged where the radiator element is not the antenna self-resonating. Substituting these self-resonant antennas, it has appeared a small non-resonant element in charge of exciting the efficient modes of the ground plane to become the main radiator. These small non-resonant elements have a very small electrical length and its location on the board which is radiating is an essential parameter to correctly excite the radiating modes of the ground plane [2]-[16].

Therefore, a multiband frequency range can be covered using a non-resonant element called as antenna booster, matched by multiband matching network operating in a small volume ground plane.

The antennas used for this project has been the Virtual Antenna™ technology antennas which acts like the non-resonant element antenna booster previously described.

In order to tune the matching to cover a multiband frequency range, it must be observed the antenna booster response which will defer depending on the booster location and ground plane extension. Consequently, it can be said Virtual Antenna™ itself is not a conventional antenna, is a system where every element described have an effect to the final radiator element.

From the antenna booster response, it can be tuned the matching network in order to cover only the desired frequencies. To do that, is necessary to observe the moves in the Smith Chart done from the system measured in every component introduced in the matching network. It is important to note there are four possible moves it can be done in a matching network: a serial inductor, a serial capacitor, a parallel inductor and a parallel inductor (see Figure 5). But not all the moves are equal for every frequency, when a serial capacitors or a parallel inductor is placed in the matching network the moves for the lower frequencies are quicker than the moves for the high frequency, due to the characteristic impedance of the component is bigger when the frequency is low and thus the impact of the component is bigger to.

On the other hand, for the serial inductors and parallel capacitors the effect is the opposite. As bigger is the frequency observed, bigger it is the effect of those components.

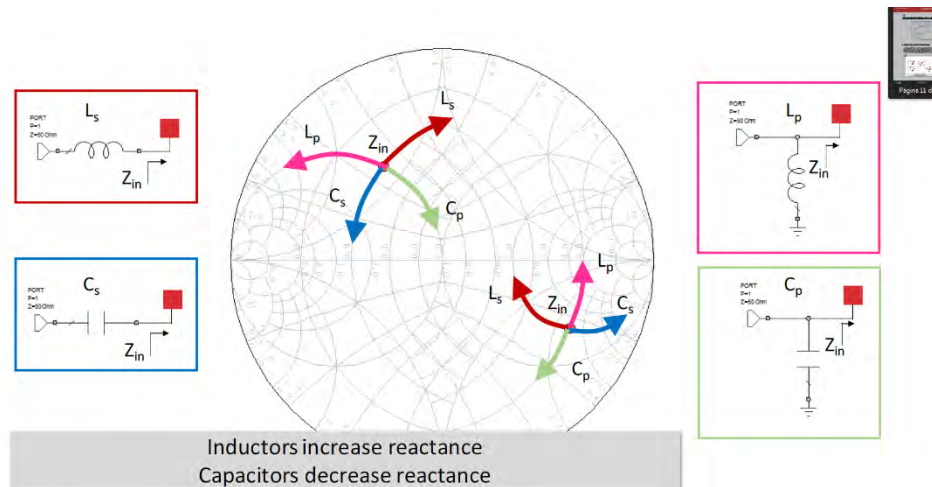


Figure 5 Moves on the Smith Chart done by the components of the Matching network [17]

3.4 FR01-S4-224 RUN mXTEND™

The first antenna booster tested with the CST Simulator it has been the RUN mXTEND™ featuring a size of 12 mm x 3 mm x 2.4 mm [18]. All the set-ups simulated with this antenna have the Clearance Area outside the main board. It is important to note, only difference between all the scenarios simulated is the feeding line length due to if the simulation is done on a free space area and the Clearance Area is outside the main board, then it does not matter the quantity of Clearance Area simulated with FR4, all the space around the main board is considered Clearance Area.

So, the most important thing to study with this Experiment, is the importance of the feeding line length. The first Experiment has the recommended feeding line length for the antenna working at LTE mobile bands, but considering the PCB is very small, with the original feeding line length, the LTE low band (824MHz-960MHz) will be very restrictive. So, the more feeding line, better will be the performance at the lower band but is important not put too much feeding line or the LTE higher band (1710MHz-2170MHz) will be affected too.

3.4.1 Experiment 1: 30x11mm Clearance Area and 5mm + 10mm of Feeding Line

In this chapter, as it has been said, the RUN mXTEND™ antenna booster has been simulated into a 30mm x 11mm Clearance Area and with a feeding line of 5mm + 10mm outside the main PCB.

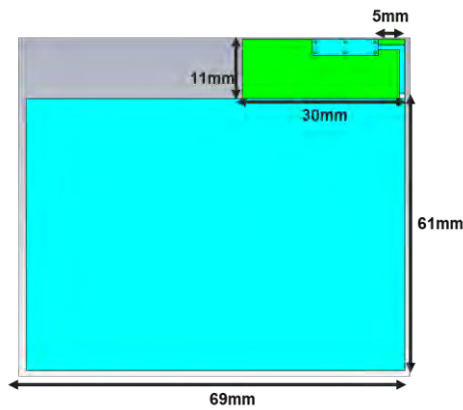


Figure 6 Set-up simulated for Experiment 1 with a 1mm width and 69mm x 61mm FR4 PCB with a Loss tangent of 0.014 at 1GHz and a relative permittivity of 4.3.

On the set-up analyzed the proposed matching network shown in Table 3 has been implemented with the matching network topology seen at Figure 7 and then, the Reflection Coefficient and the Antenna and Radiation Efficiency have been measured.

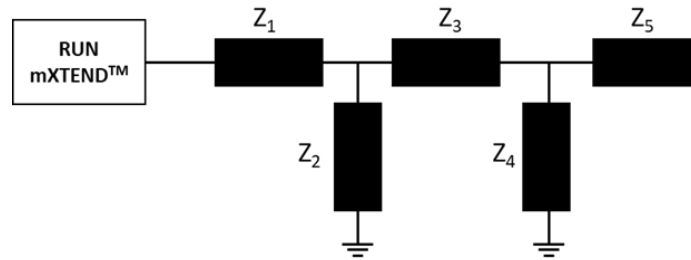


Figure 7 Matching network topology for the RUN mXTEND™ Experiment 1 MN1 at LTE band

Component	Value	Part Number
Z1	0Ω Resistor	-
Z2	15nH	LQW18AN15NG80
Z3	1.0pF	GJM1555C1H1R0WB01
Z4	6.3nH	LQW15AN6N3G80
Z5	3.0pF	GJM1555C1H3R0WB01

Table 3 Build of materials (BoM) used to obtain for the RUN mXTEND™ Experiment 1 MN1 at LTE band

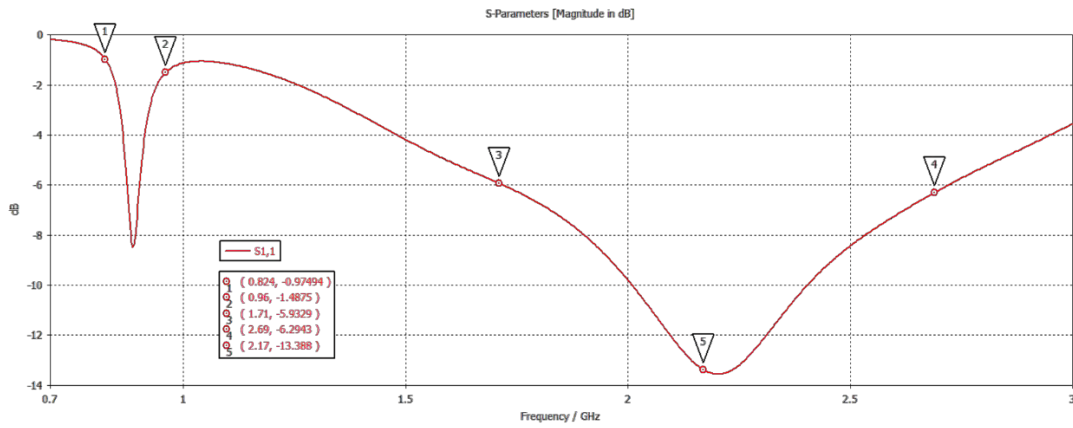


Figure 8 S_{11} obtained for the RUN mXTEND™ Experiment 1 MN1 at LTE band

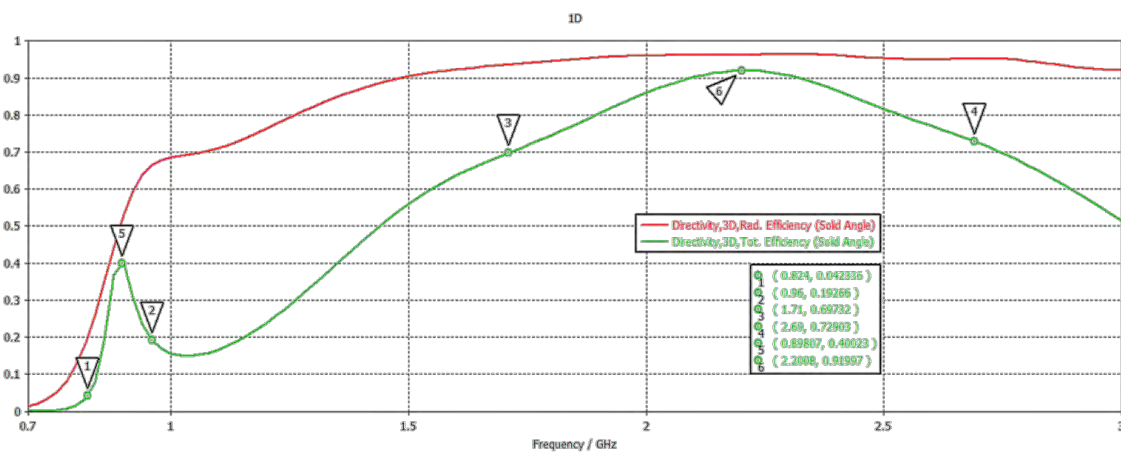


Figure 9 Antenna and Radiation Efficiency obtained for the RUN mXTEND™ Experiment 1 MN1 at LTE band

Experiment	ANTENNA EFFICIENCY (%)					
	824MHz	960MHz	Avg 824-960MHz	1710MHz	2170MHz	Avg 1710-2170MHz
Experiment 1 – MN1	4.2	19.3	22.6	69.7	91.7	82.0

Table 4 Efficiency values obtained for the RUN mXTEND™ Experiment 1 MN1 at LTE band

As it is shown at Table 4, for this first set-up analyzed the higher band achieves very good values of efficiency and a bandwidth much wider than the necessary but for the lower band, the bandwidth obtained is too much narrow and a good tuning for all the band cannot be achieved. The 824MHz frequency is the lower efficiencies value obtained, which it means it is necessary to increase the feeding line in order to sacrifice a little of the higher band in order to gain on the lower band.

3.4.2 Experiment 2: 30x11mm Clearance Area and 18mm + 11mm of Feeding Line

With the same Clearance Area extension as Experiment 1, 30mm x 11mm, it has been tested to expand the maximum possible the feeding line in order to see clearly the difference with the first Experiment. So, a feeding line of 18mm + 11mm has been tested in the set-up seen in the Figure 10.

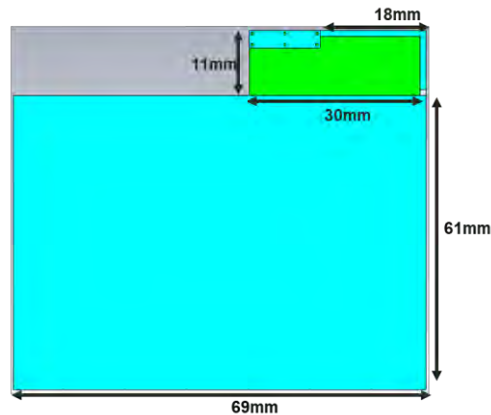


Figure 10 Set-up simulated for Experiment 2 with a 1mm width and 69mm x 61mm FR4 PCB with a Loss tangent of 0.014 at 1GHz and a relative permittivity of 4.3.

On the set-up analyzed the proposed matching network shown in Table 5 has been implemented with the matching network topology seen at Figure 7 and then, the Reflection Coefficient and the Antenna and Radiation Efficiency have been measured.

Component	Value	Part Number
Z1	0Ω Resistor	-
Z2	11nH	LQW18AN11NG80
Z3	1.3pF	GJM1555C1H1R3WB01
Z4	2.0pF	GJM1555C1H2R0WB01
Z5	10nH	LQW18AN10NG10

Table 5 Build of materials (BoM) used to obtain for the RUN mXTEND™ Experiment 2 MN1 at LTE band

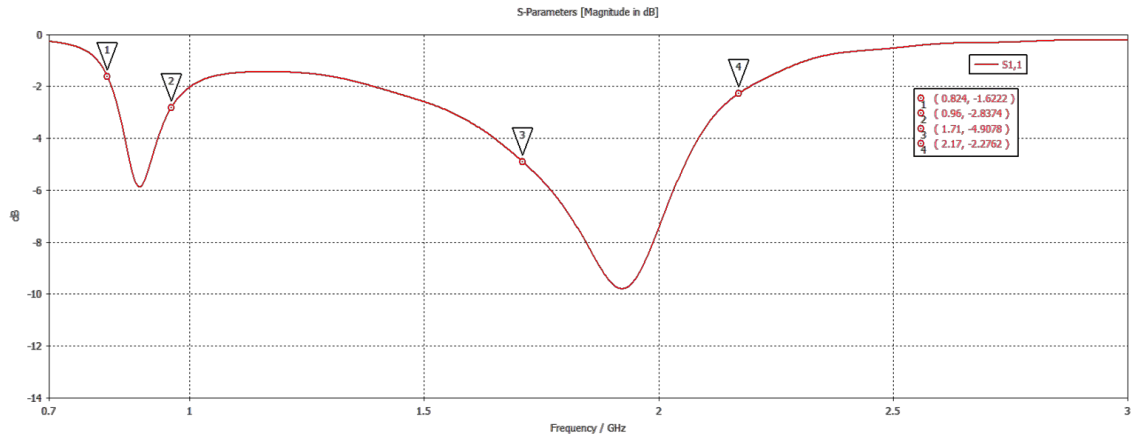


Figure 11 S₁₁ obtained for the RUN mXTEND™ Experiment 2 MN1 at LTE band

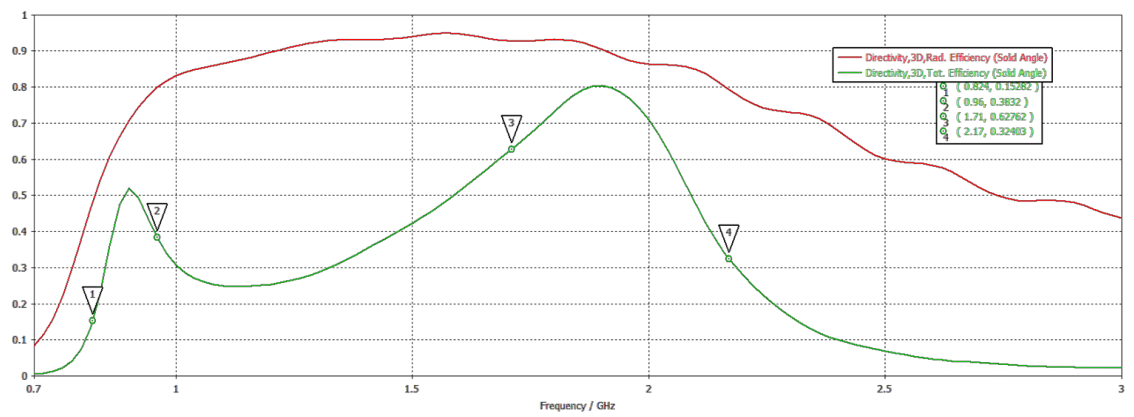


Figure 12 Antenna and Radiation Efficiency obtained for the RUN mXTEND™ Experiment 2 MN1 at LTE band

Experiment	ANTENNA EFFICIENCY (%)					
	824MHz	960MHz	Avg 824-960MHz	1710MHz	2170MHz	Avg 1710-2170MHz
Experiment 2 – MN1	15.3	38.3	37.9	62.7	32.4	64.5

Table 6 Efficiency values obtained for the RUN mXTEND™ Experiment 2 MN1 at LTE band

As can be seen in the Figure 11, now the Reflection Coefficient is narrower at the higher band but a lot better performance at the lower band is achieved. Although the performance at the lower band has become better, the higher band values has been too much affected, specially at the 2170MHz frequency where the efficiency value has decreased from 91.7% (Experiment 1) to the current 32.4%.

So, as it has been already said, an equality between both extremes must to searched. Then the next step is to put a lengthier feeding line than Experiment 1 but shorter than Experiment 2.

3.4.3 Experiment 3: 25x11mm Clearance Area and 13mm + 11mm of Feeding Line

With a new testing feeding line of 13mm + 11mm, the required Clearance Area to place the antenna has been reduced, so a new Clearance Area of 25mm x 11mm has been simulated in the set-up mounted at Figure 13.

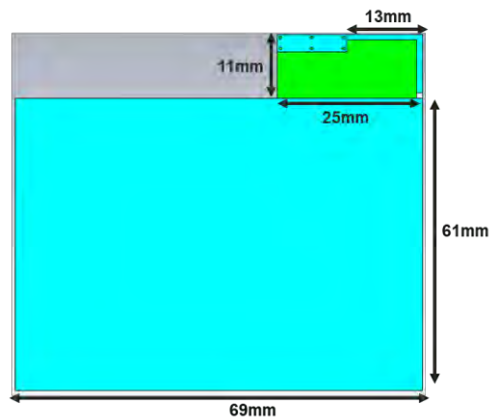


Figure 13 Set-up simulated for Experiment 3 with a 1mm width and 69mm x 61mm FR4 PCB with a Loss tangent of 0.014 at 1GHz and a relative permittivity of 4.3.

On the set-up analyzed the proposed matching network shown in Table 7 has been implemented in a new matching network topology shown at Figure 14 and then, the Reflection Coefficient and the Antenna and Radiation Efficiency have been measured.

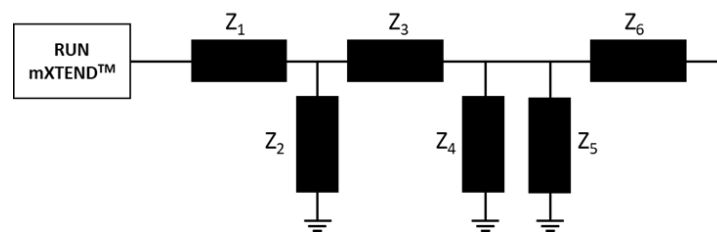


Figure 14 Matching network topology for the RUN mXTEND™ Experiment 3 MN3 at LTE band

Component	Value	Part Number
Z1	0Ω Resistor	-
Z2	15nH	LQW18AN15NG80
Z3	1.0pF	GJM1555C1H1R0WB01
Z4	6.3nH	LQW15AN6N3G80
Z5	0.5pF	GJM1555C1HR50WB01
Z6	3.5pF	GJM1555C1H3R5WB01

Table 7 Build of materials (BoM) used to obtain for the RUN mXTEND™ Experiment 3 MN3 at LTE band

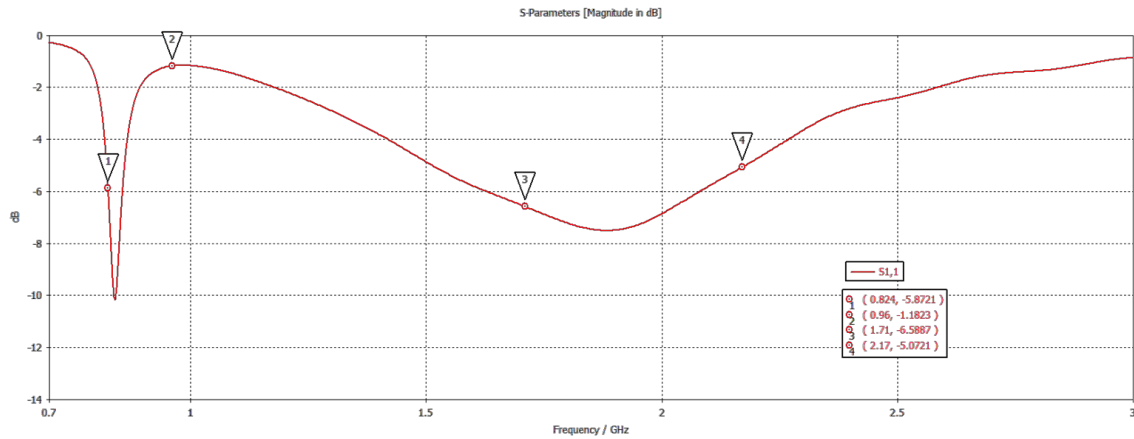


Figure 15 S₁₁ obtained for the RUN mXTEND™ Experiment 3 MN3 at LTE band

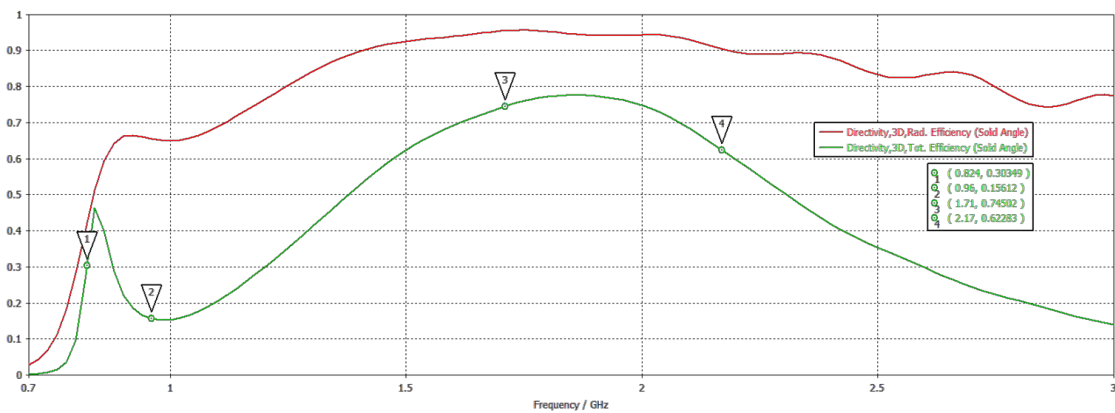


Figure 16 Antenna and Radiation Efficiency obtained for the RUN mXTEND™ Experiment 3 MN3 at LTE band

Experiment	ANTENNA EFFICIENCY (%)					
	824MHz	960MHz	Avg 824-960MHz	1710MHz	2170MHz	Avg 1710-2170MHz
Experiment 3 – MN3	30.3	15.6	26.8	74.5	62.3	73.4

Table 8 Efficiency values obtained for the RUN mXTEND™ Experiment 3 MN3 at LTE band

As it is shown at the Figure 16, now the higher band has a wide bandwidth again and although the lower band is narrower than the simulated in the Experiment 2, the values achieved are much better than the Experiment 1 values. It has been prioritized the 824MHz in the matching network tuning process due to the radiation efficiency is very low in this frequency, but quickly increases to a very high radiation efficiency values in the next frequencies, which means that without an excellent S₁₁ response in the frequencies with a high radiation efficiency value, the antenna efficiency values achieved it will be good enough.

3.4.4 Experiment 4: 20x11mm Clearance Area and 8mm + 11mm of Feeding Line

A last Experiment with the RUN mXTEND™ has been done in order to test if a similar solution as Experiment 3 can be achieved with a smaller Clearance Area and feeding line. The size of the area occupied is a critical part when the final solution it must be decided, so as smaller the space occupied with a good performance is achieved, better will be.

In this Experiment a feeding line of 8mm + 11mm and a 20mm x 11mm Clearance Area have been considered.

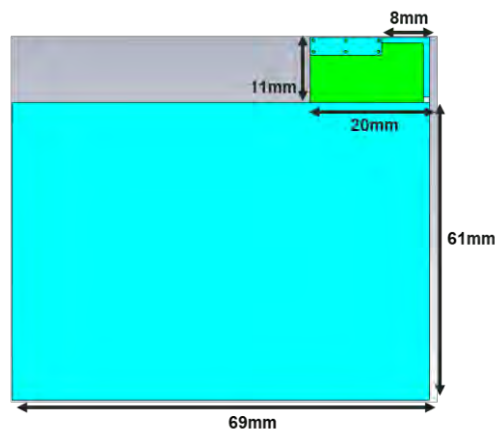


Figure 17 Set-up simulated for Experiment 3 with a 1mm width and 69mm x 61mm FR4 PCB with a Loss tangent of 0.014 at 1GHz and a relative permittivity of 4.3.

On the set-up analyzed the proposed matching network shown in Table 7 has been implemented in a new matching network topology shown at Figure 14 and then, the Reflection Coefficient and the Antenna and Radiation Efficiency have been measured.

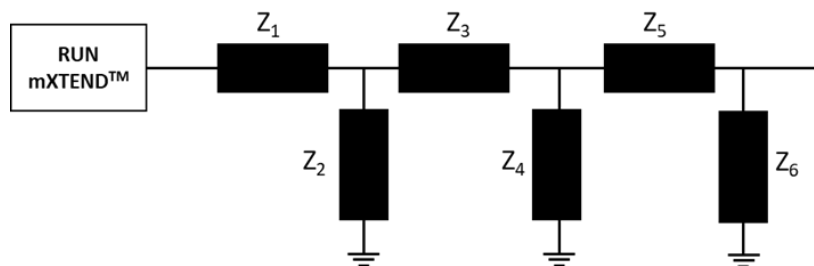


Figure 18 Matching network topology for the RUN mXTEND™ Experiment 4 MN2 at LTE band

Component	Value	Part Number
Z1	0Ω Resistor	-
Z2	15nH	LQW18AN15NG80
Z3	1.0pF	GJM1555C1H1R0WB01
Z4	6.3nH	LQW15AN6N3G80
Z5	3.0pF	GJM1555C1H3R0WB01
Z6	20nH	LQW18AN20NG00

Table 9 Build of materials (BoM) used to obtain for the RUN mXTEND™ Experiment 4 MN2 at LTE band

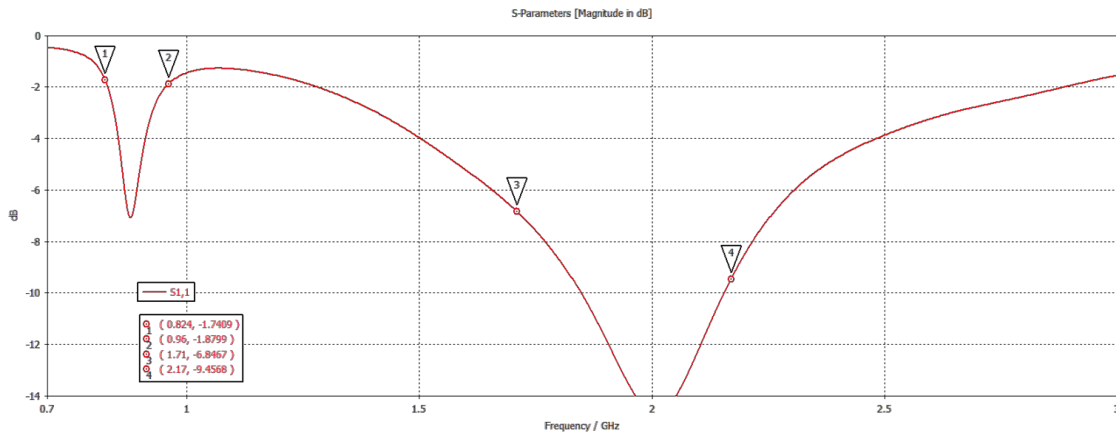


Figure 19 S₁₁ obtained for the RUN mXTEND™ Experiment 4 MN2 at LTE band

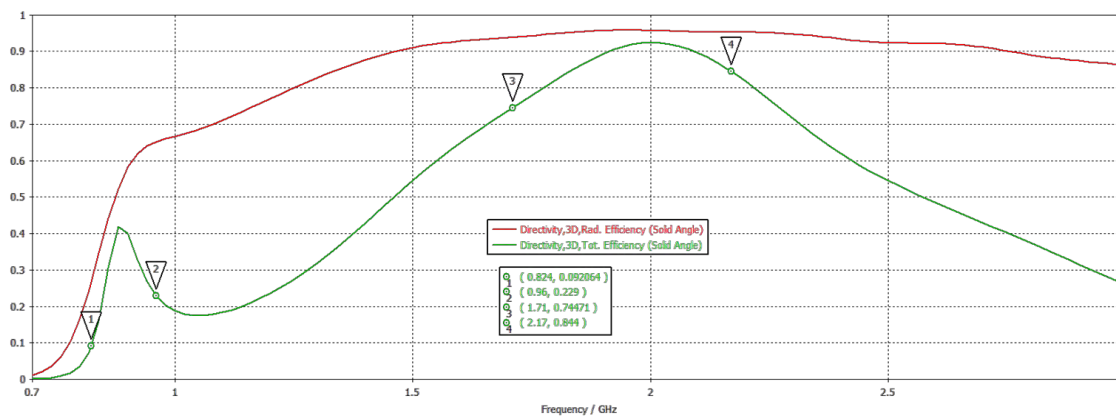


Figure 20 Antenna and Radiation Efficiency obtained for the RUN mXTEND™ Experiment 4 MN2 at LTE band

Experiment	ANTENNA EFFICIENCY (%)					
	824MHz	960MHz	Avg 824-960MHz	1710MHz	2170MHz	Avg 1710-2170MHz
Experiment 4 – MN2	9.2	22.9	27.3	74.4	84.4	86.8

Table 10 Efficiency values obtained for the RUN mXTEND™ Experiment 4 MN2 at LTE band

Although the efficiency value achieved at 824MHz frequency is much lower than the obtained in the Experiment 3, the average efficiency values for the lower band and the higher band are higher with a feeding line shorter.

3.4.5 Comparison between Experiments

As it has been explained through all the experiments realized for the RUN mXTEND™ antenna booster, the feeding line length is a critical parameter for the bandwidth obtained at the LTE lower band and LTE higher band.

The more feeding line the set-up measured has, more inductive will be the antenna response. So, for feeding line very long, the performance at the lower band will achieve better efficiency values and will have a wider bandwidth, and as contraposition, the higher band will obtain worse performance and will have a narrower bandwidth.

For a better understanding, a comparison between all the Experiments in terms of antenna efficiency have been done as it is shown at Figure 21.

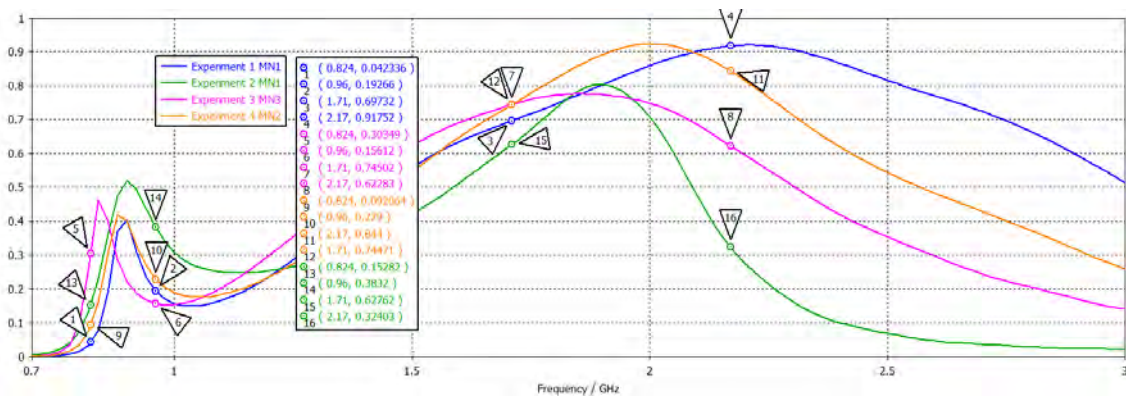


Figure 21 Comparison between the four Experiments done for the RUN mXTEND™ antenna booster.

Experiment	ANTENNA EFFICIENCY (%)					
	824MHz	960MHz	Avg 824-960MHz	1710MHz	2170MHz	Avg 1710-2170MHz
Experiment 2 – MN1	15.3	38.3	37.9	62.7	32.4	64.5
Experiment 3 – MN3	30.3	15.6	26.8	74.5	62.3	73.4
Experiment 4 – MN2	9.2	22.9	27.3	74.4	84.4	86.8
Experiment 1 – MN1	4.2	19.3	22.6	69.7	91.7	82.0

Table 11 Efficiency values for the four Experiments done for the RUN mXTEND™ antenna booster

In Table 11 Efficiency values for the four Experiments done for the RUN mXTEND™ antenna booster Table 11 it can be seen the antenna efficiency values for the four Experiments order from feeding line longer to the feeding line shorter. The better performance achieved at LTE low band (824MHz-960MHz) is the Experiment 2 which is the Experiment with the longer feeding line, and as contraposition, the one with the worse efficiency performance and the narrower bandwidth at the LTE high band (1710MHz-2170MHz).

Consequently, Experiment 1 is the Experiment with the shorter feeding line, the worse performance and narrower bandwidth at LTE low band, and the second-best scenario at performance efficiency values at the higher band with the wider bandwidth.

Experiment 4 which has an 11mm + 8mm feeding line achieves a really good values at the LTE low band and high band, so is the most equilibrated Experiment and best-case scenario for this antenna.

3.5 FR01-S1-210 TRIO mXTEND™

In this Chapter, the TRIO mXTEND™ has been tested with the CST Simulator. One set-up has been mounted with the Clearance Area antenna outside the main board as the Experiments seen at Chapter 3.4, and two Experiments has been designed with the Clearance Area antenna inside the main PCB. Putting the Clearance Area outside the main PCB will give a better performance due in the design simulated, it is considered to be in a free space area, so an infinite Clearance Area is considered at the borders and furthermore, a bigger ground plane area will be considered.

But putting the Clearance Area inside the main PCB represent a more realistic and compact option in a device like the mangOH™ RED where every millimeter is approached at maximum. In these scenarios the Clearance Area considered changes and is a critical parameter of the design.

It has been added the GNSS application (1561MHz-1606MHz) apart from the same LTE bands simulated in the last Chapter (824MHz-960MHz), but only one antenna is considered (one application per port).

3.5.1 Experiment 1: 30x12mm Clearance Area Outside Main Board

The first Experiment done with the TRIO mXTEND™ has been simulated into a 30mm x 12mm Clearance Area outside the main board, with one port for LTE (824MHz-960MHz & 1710MHz-2170MHz) and another port working at GNSS (1561MHz-1606MHz), both ports with a 9mm feeding line [19].

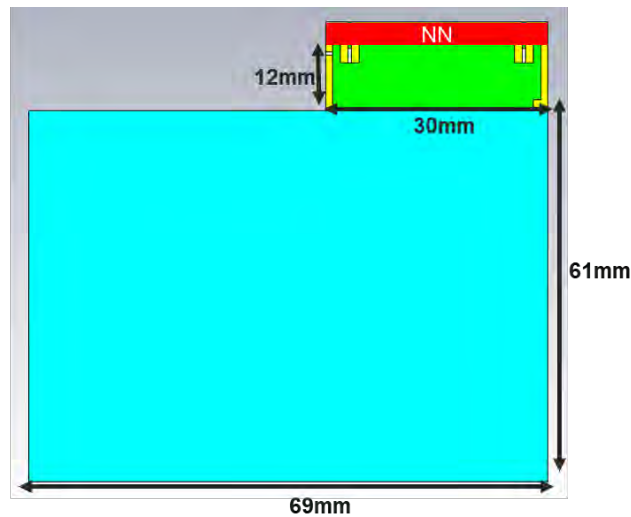


Figure 22 Set-up simulated for Experiment 1 with a 1mm width and 69mm x 61mm FR4 PCB with a Loss tangent of 0.014 at 1GHz and a relative permittivity of 4.3.

The TRIO mXTEND™ when is working at LTE used to have two matching network sections (see Figure 23 for a better understanding). Section A is where the LTE matching network topology is placed, and Section B is used for an optional filter which will separate the coupling effect between the lower frequency range (LFR: 824MHz-960MHz) and the higher frequency range (HFR: 1710MHz-2170MHz).



Figure 23 Clarification of Section A and Section B on the CST Simulations

Two matching networks have been tested for LTE band Section A (Figure 23), considering the same matching network topology (see Figure 24) and components (see Table 12) for the LTE Filter.

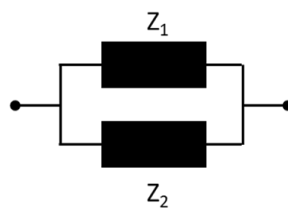


Figure 24 Matching network topology for Experiment 1 LTE band Section B

Component	Value	Part Number
Z1	8.0nH	LQW15AN8NG80
Z2	0.8pF	GJM1555C1HR80WB01

Table 12 Build of materials (BoM) used to obtain the LTE filter for Experiment 1 at LTE band Section B.

For both matching networks obtained, it has been measured the Reflection Coefficient and the Antenna and Radiation Efficiency. On the other hand, one GNSS matching network has been designed and measured as well as the LTE band.

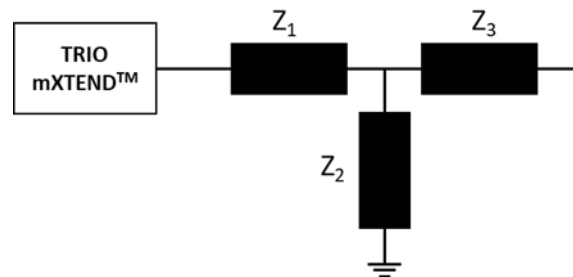


Figure 25 Matching network topology for the TRIO mXTEND™ Experiment 1 MN1 at LTE band

Component	Value	Part Number
Z1	4.3nH	LQW15AN4N3B80
Z2	5.5nH	LQW18AN5N5B80
Z3	2.3pF	GJM1555C1H2R3WB01

Table 13 Build of materials (BoM) used to obtain for the TRIO mXTEND™ Experiment 1 MN1 at LTE band

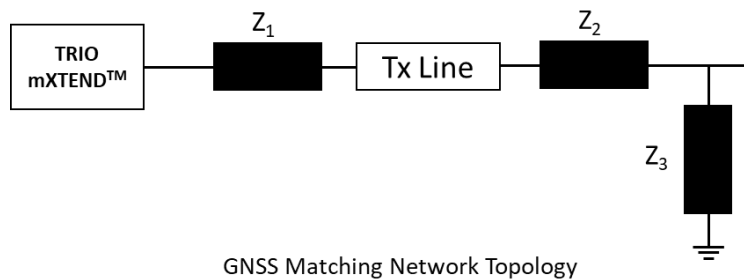


Figure 26 Antenna and Radiation Efficiency obtained for the RUN mXTEND™ Experiment 1 MN1 at GNSS band

Component	Value	Part Number
Z1	0.1pF	GJM1555C1HR10WB01
Z2	22nH	LQW18AN22NG80
Z3	4.3nH	LQW15AN4N3B80

Table 14 Build of materials (BoM) used to obtain for the TRIO mXTEND™ Experiment 1 MN2 at LTE band

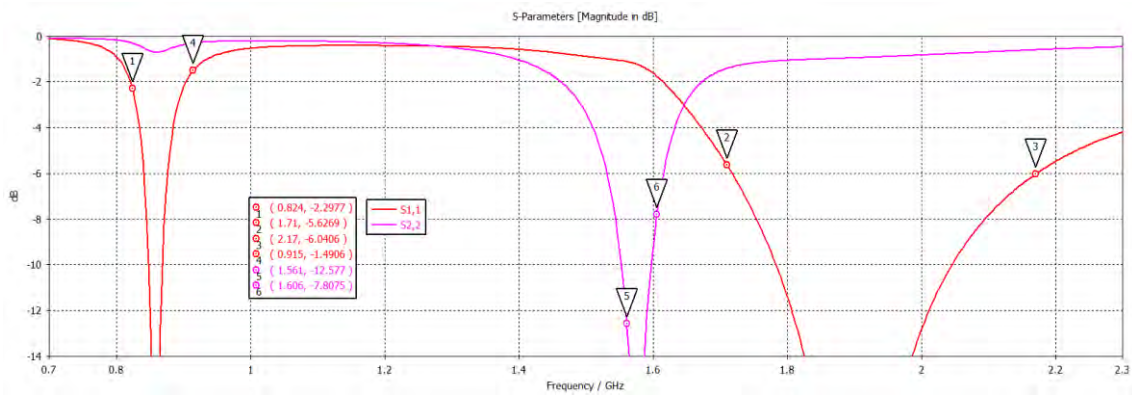


Figure 27 S_{11} obtained for the TRIO mXTEND™ Experiment 1 for the MN1 at LTE band (in red) and for MN1 at GNSS band (in pink).

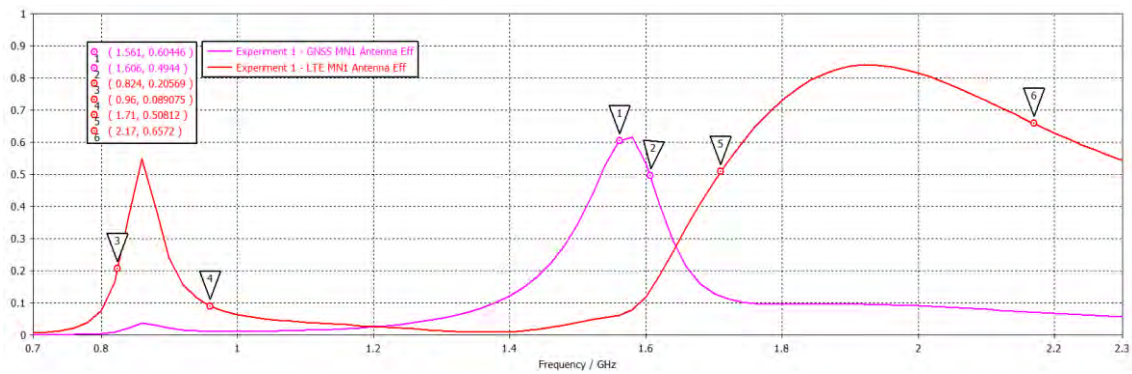


Figure 28 Antenna Efficiencies obtained for the TRIO mXTEND™ Experiment 1 for the MN1 at LTE band (in red) and for MN1 at GNSS band (in pink).

Experiment 1	ANTENNA EFFICIENCY (%)					
	824MHz	960MHz	Avg 824-960MHz	1710MHz	2170MHz	Avg 1710-2170MHz
LTE – MN1	20.5	8.9	25.9	50.8	65.7	74.7
Experiment 1	1561MHz			1575Mhz		Avg 1598-1606Mhz
GNSS – MN1	60.4			61.1		52.1

Table 15 Antenna Efficiency values for Experiment 1 MN1 at the LFR (824MHz-960MHz) and HFR (1710MHz-2170MHz) of the LTE band and for Experiment 1 MN1 at 1561MHz (BeiDou E1 band), 1575 MHz (GPS L1 band) and from 1598 MHz to 1606 MHz (GLONASS L1 band).

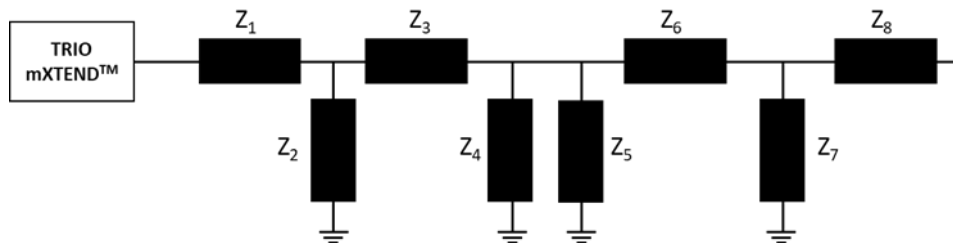


Figure 29 Matching network topology for the TRIO mXTEND™ Experiment 1 MN2 at LTE band

Component	Value	Part Number
Z1	0Ω Resistor	-
Z2	8.1nH	LQW18AN8N1G80
Z3	2.2pF	GJM1555C1H2R2WB01
Z4	0.6pF	GJM1555C1HR60WB01
Z5	8.9nH	LQW15AN8N9G80
Z6	2.0pF	GJM1555C1H2R0WB01
Z7	8.8nH	LQW15AN8N8G80
Z8	2.5pF	GJM1555C1H2R5WB01

Table 16 Build of materials (BoM) used to obtain for the TRIO mXTEND™ Experiment 1 MN2 at LTE band

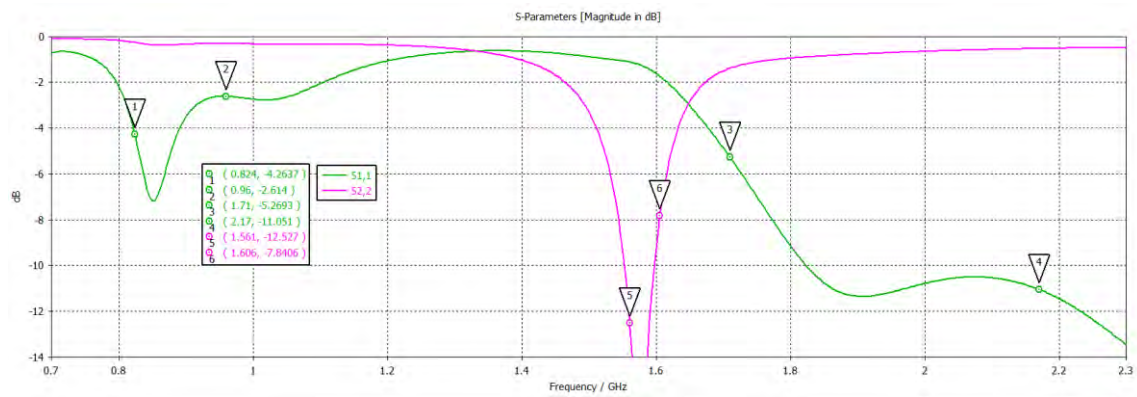


Figure 30 S₁₁ obtained for the TRIO mXTEND™ Experiment 1 for the MN2 at LTE band (in green) and for MN1 at GNSS band (in pink).

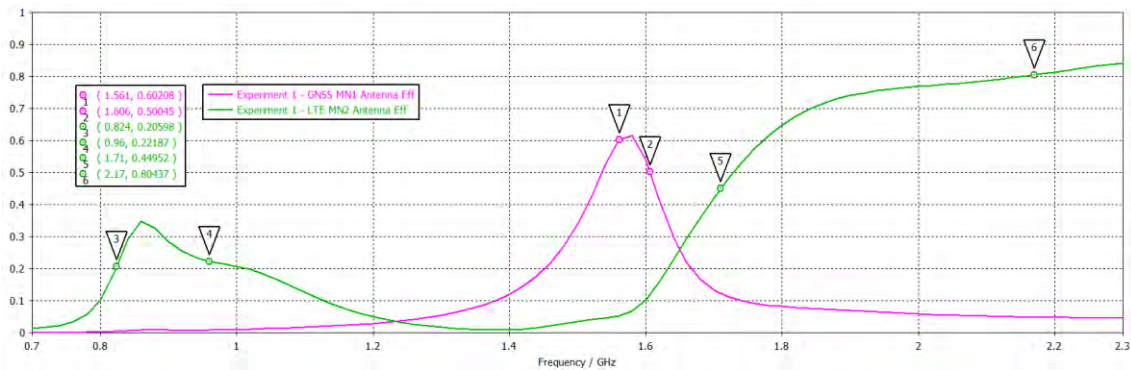


Figure 31 Antenna Efficiencies obtained for the TRIO mXTEND™ Experiment 1 for the MN2 at LTE band (in green) and for MN1 at GNSS band (in pink).

Experiment 1	ANTENNA EFFICIENCY (%)					
	824MHz	960Mhz	Avg 824-960MHz	1710MHz	2170MHz	Avg 1710-2170MHz
LTE – MN2	20.6	22.2	27.3	44.9	80.4	70.9
Experiment 1	1561MHz		1575Mz		Avg 1598-1606Mhz	
GNSS – MN1	60.2		61.1		52.3	

Table 17 Antenna Efficiency values for Experiment 1 MN2 at the LFR (824MHz-960MHz) and HFR (1710MHz-2170MHz) of the LTE band and for Experiment 1 MN1 at 1561MHz (BeiDou E1 band), 1575 MHz (GPS L1 band) and from 1598 MHz to 1606 MHz (GLONASS L1 band).

As it can be observed at Table 15 and Table 17, the antenna efficiency average is very similar for both matching networks. For the first Matching network, MN1, the antenna efficiency at the higher band is slightly better than the second matching network mounted, MN2, but this last one is slightly better at the lower band, specially at the 960MHz frequency where the MN1 efficiency is very low.

As far as the GNSS band, due to the matching network mounted is the same in both cases, the results are almost the same. The slightly difference between both cases is produced for the LTE matching network impact into the GNSS band.

3.5.2 Experiment 2: 31x12mm Clearance Area Inside Main Board

In order to do a more realistic scenario, the Clearance Area and the antenna has been placed inside the main board, making a much more compact design but a more restrictive one also.

In this set-up designed, almost the same Clearance Area as Experiment 1 (now has 31mm x 12mm dimensions) has been placed at the top right corner of the main board. The Clearance is 1 mm wider in order to not make a short circuit between the antenna and the ground plane area next to the antenna. The feeding line length for both ports keeps being the same as the Experiment 1 ones.

So, in this Experiment it will be possible to see clearly the differences between having the Clearance Area outside the board, and as a consequence having a free space next your antenna, and having the Clearance Area inside the main board and therefore having your antenna very close to metallic component as it is the ground plane area.

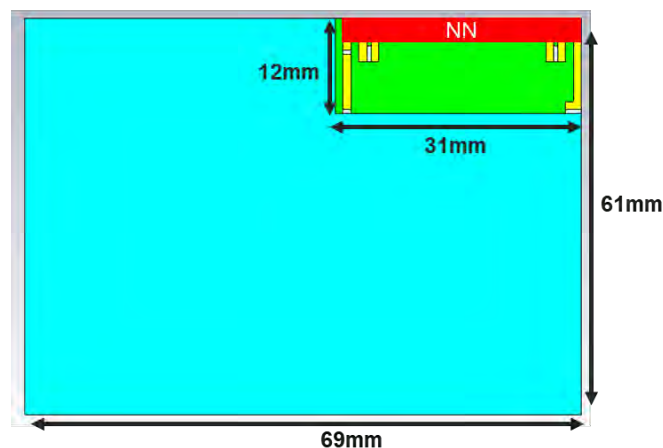


Figure 32 Set-up simulated for Experiment 2 with a 1mm width and 69mm x 61mm FR4 PCB with a Loss tangent of 0.014 at 1GHz and a relative permittivity of 4.3.

One matching network has been tested for LTE band Section A (Figure 23), considering a different matching network topology (Figure 33) meanwhile for Section B, the filter used is the same seen in the Figure 24 and Table 12. As far as the GNSS band, one Matching network has been tested with the same matching network topology as the seen in the Figure 26. For every matching networks obtained, it has been measured the Reflection Coefficient and the Antenna and Radiation Efficiency.

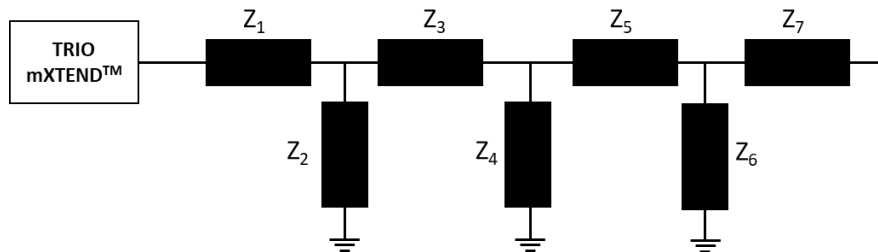


Figure 33 Matching network topology for the TRIO mXTEND™ Experiment 2 MN1 at LTE band

Component	Value	Part Number
Z1	2.2nH	LQW15AN2N2B80
Z2	10nH	LQW18AN10NG10
Z3	3.0pF	GJM1555C1H3R0WB01
Z4	12nH	LQW18AN12NG10
Z5	2.5pF	GJM1555C1H2R5WB01
Z6	1.0pF	GJM1555C1H1R0WB01
Z7	0Ω Resistor	-

Table 18 Build of materials (BoM) used to obtain for the TRIO mXTEND™ Experiment 2 MN1 at LTE band

Component	Value	Part Number
Z1	0.1pF	GJM1555C1HR10WB01
Z2	16nH	LQW18AN16NG80
Z3	2.2nH	LQW18AN2N2B80

Table 19 Build of materials (BoM) used to obtain for the TRIO mXTEND™ Experiment 2 MN1 at GNSS band

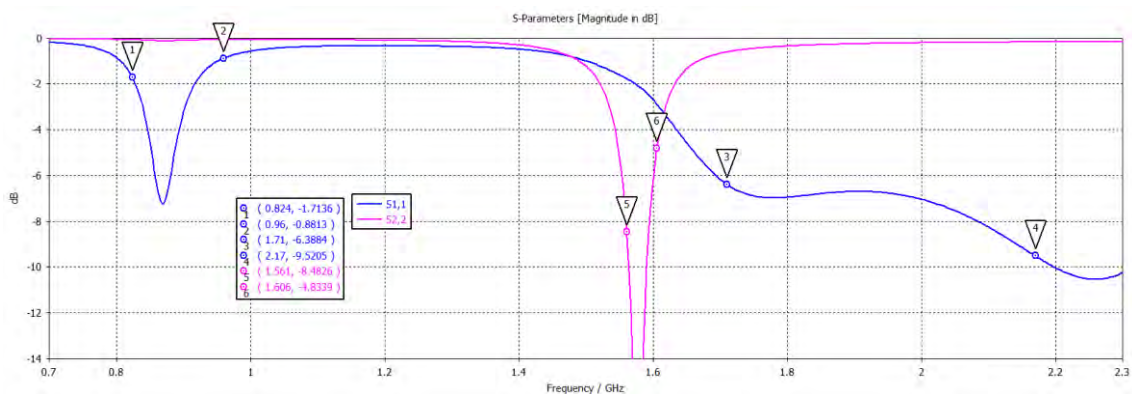


Figure 34 S_{11} obtained for the TRIO mXTEND™ Experiment 2 for the MN1 at LTE band (in blue) and for MN1 at GNSS band (in pink).

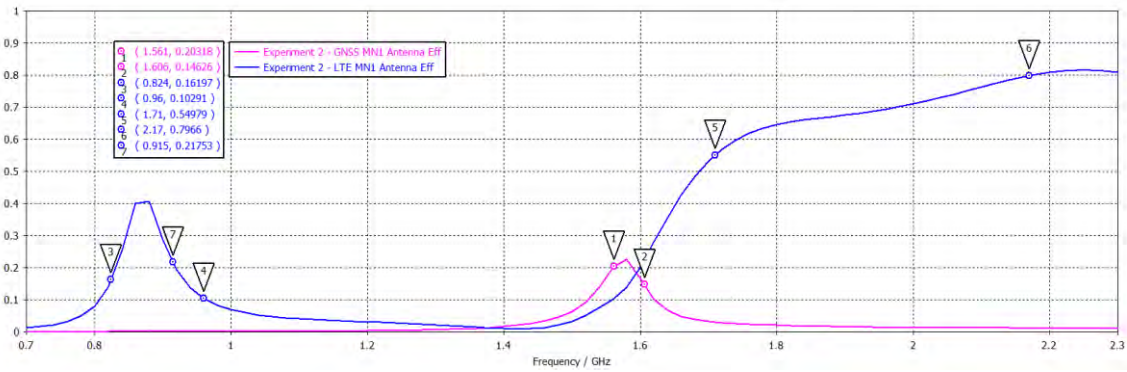


Figure 35 Antenna Efficiencies obtained for the TRIO mXTEND™ Experiment 1 for the MN1 at LTE band (in blue) and for MN1 at GNSS band (in pink).

Experiment 2	ANTENNA EFFICIENCY (%)					
	824MHz	960MHz	Avg 824-960MHz	1710MHz	2170MHz	Avg 1710-2170MHz
LTE – MN1	16.2	10.3	24.3	55.0	79.7	69.0
Experiment 2	1561MHz			1575Mz		Avg 1598-1606Mhz
GNSS – MN1	20.3			21.9		15.9

Table 20 Antenna Efficiency values for Experiment 2 MN1 at the LFR (824MHz-960MHz) and HFR (1710MHz-2170MHz) of the LTE band and for Experiment 2 MN1 at 1561MHz (BeiDou E1 band), 1575 MHz (GPS L1 band) and from 1598 MHz to 1606 MHz (GLONASS L1 band).

As it can be observed at Table 20 the most affected band it has been the GNSS due to is the port closer to the ground plane area between both ports. Although the S_{11} response at GNSS is totally tuned, the efficiency has been reduced a lot in comparison to the previous Experiment.

As far as the LTE band, the most affected part it has been the lower band (824MHz-960MHz), specially at the frequency extremes of the band. At the higher band (1710MHz-2170MHz) the performance is almost the same as the previous Experiment where the Clearance Area was outside the main board.

It is important to note, not only the antenna is now surrounded by a ground plane area, the ground plane area available to radiate it has been reduced which affects to the final antenna performance.

3.5.3 Experiment 3: 35x11mm Clearance Area Inside Main Board

A last Experiment with the TRIO mXTEND™ has been simulated working at LTE band in one port and GNSS band on the other port. The feeding lines length is the same as the previous Experiments. A 35mm x 11mm Clearance Area has been designed in order to move away the GNSS port from the ground plane area.

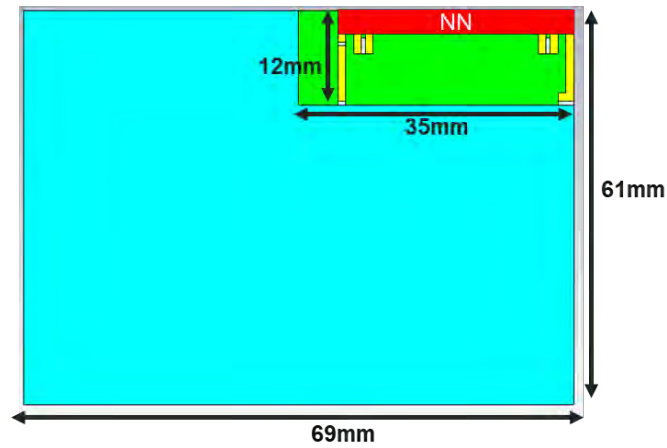


Figure 36 Set-up simulated for Experiment 3 with a 1mm width and 69mm x 61mm FR4 PCB with a Loss tangent of 0.014 at 1GHz and a relative permittivity of 4.3.

One matching network has been tested for LTE band Section A (Figure 23), considering a different matching network topology (Figure 37) meanwhile for Section B, the filter used is the same seen in the Figure 24 and Table 12. As far as the GNSS band, one matching network has been tested with the same matching network topology as the seen in the Figure 26. For every matching networks obtained, it has been measured the Reflection Coefficient and the Antenna and Radiation Efficiency.

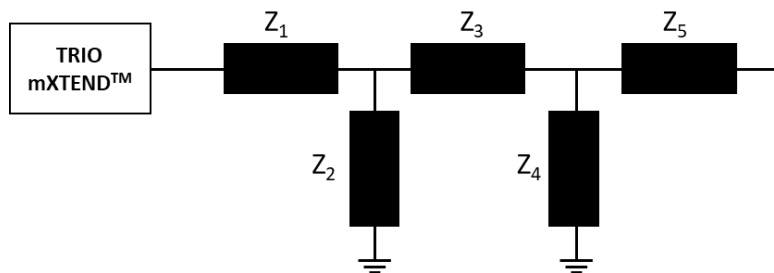


Figure 37 Matching network topology for the TRIO mXTEND™ Experiment 3 MN1 at LTE band

Component	Value	Part Number
Z1	4.3nH	LQW15AN4N3B80
Z2	10nH	LQW18AN10NG10
Z3	3.4pF	GJM1555C1H3R4WB01
Z4	12nH	LQW18AN12NG10
Z5	2.2pF	GJM1555C1H2R2WB01

Table 21 Build of materials (BoM) used to obtain for the TRIO mXTEND™ Experiment 2 MN1 at LTE band

Component	Value	Part Number
Z1	0.1pF	GJM1555C1HR10WB01
Z2	19nH	LQW18AN19NG80
Z3	2.2nH	LQW18AN2N2B80

Table 22 Build of materials (BoM) used to obtain for the TRIO mXTEND™ Experiment 2 MN1 at GNSS band

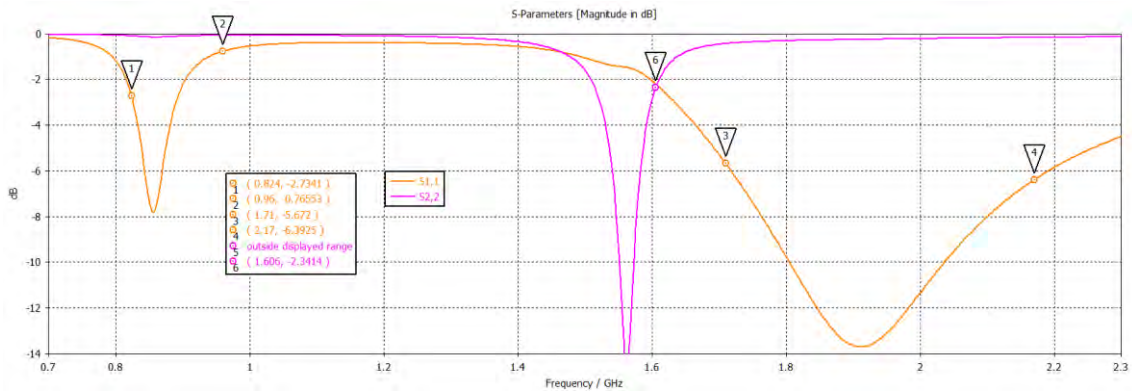


Figure 38 S₁₁ obtained for the TRIO mXTEND™ Experiment 3 for the MN1 at LTE band (in orange) and for MN1 at GNSS band (in pink).

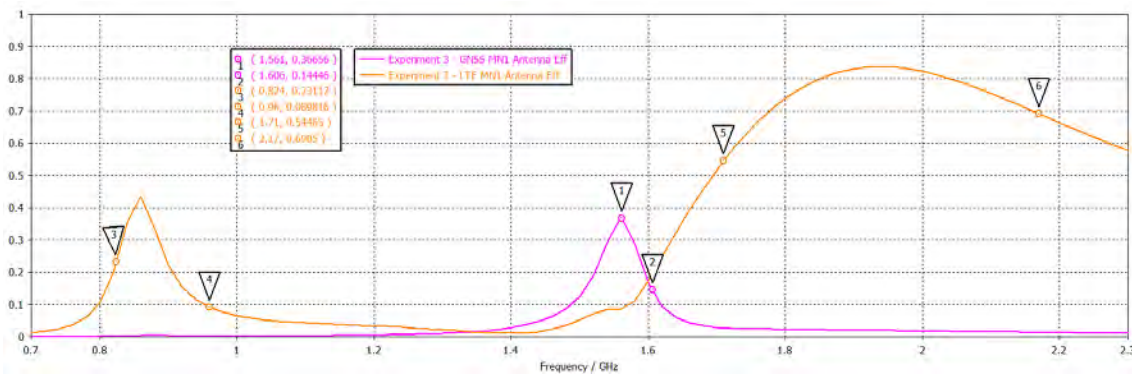


Figure 39 Antenna Efficiencies obtained for the TRIO mXTEND™ Experiment 3 for the MN1 at LTE band (in orange) and for MN1 at GNSS band (in pink).

Experiment 3	ANTENNA EFFICIENCY (%)					
	824MHz	960MHz	Avg 824-960MHz	1710MHz	2170MHz	Avg 1710-2170MHz
LTE – MN1	23.1	9.0	24.2	54.5	69.0	75.1
Experiment 3	1561MHz			1575Mz		Avg 1598-1606MHz
GNSS – MN1	36.7			31.0		16.2

Table 23 Antenna Efficiency values for Experiment 3 MN1 at the LFR (824MHz-960MHz) and HFR (1710MHz-2170MHz) of the LTE band and for Experiment 3 MN1 at 1561MHz (BeiDou E1 band), 1575 MHz (GPS L1 band) and from 1598 MHz to 1606 MHz (GLONASS L1 band).

As it is shown in Table 23, the efficiency in the lower band is almost the same as the seen for the Experiment 2. It has been prioritized the 824MHz frequency and for that reason the efficiency at 960MHz frequency is slightly lower than the previous Experiment.

As far as the higher band, the average efficiency value has increased a 5% in comparison to Experiment 2, although the 2170MHz frequency has a lower performance.

On the other hand, for GNSS band the improvement is the most notorious one. If in Experiment 2 the feeding line and the port for GNSS is 1 mm far from the ground plane area, now the distance has been increased to 5mm.

So, it is very important to note the negative effect produced by a metallic component as it is the ground plane area, when is too close to the antenna, and specially, when is too close to the feeding line of the port measured.

3.5.4 Comparison between Experiments

So, to see clearly the differences between the three Experiments simulated for the TRIO mXTEND™ antenna, a comparison between all the Experiments has been done.

One design change has been done in every design from the first Experiment in order to see step by step, which is the effect of these design changes in the antenna performance. The original set-up, Experiment 1, has a 30mm x 11mm Clearance placed above the top right PCB corner, outside the main board, as an additional PCB embedded to the original PCB.

In this first design, it has been changed the matching network topology of the first matching network, MN1, to a matching network topology with more components and consequently, more complex.

For the second design, Experiment 2, the Clearance Area before outside the main board it has been considered in the main board, just below where the additional PCB is placed in Experiment 1. So, in this Experiment it can be observed the difference between having the antenna in free space to having the antenna inside a board where a metallic component like is the ground plane area, is considered very close to the antenna.

Finally, for the Experiment 3, the Clearance Area has been increased to 35mm x 11mm dimensions, to see the which is the effect of having a bigger Clearance Area inside the main board.

In every Experiment it has been studied the changes in the design set-up for the two bands simulated, LTE (824MHz-960MHz & 1710MHz-2170MHz) and GNSS (1561MHz-1606MHz). For every band a comparison between antenna efficiencies has been done (Figure 40 for LTE band and Figure 41 for the GNSS band).

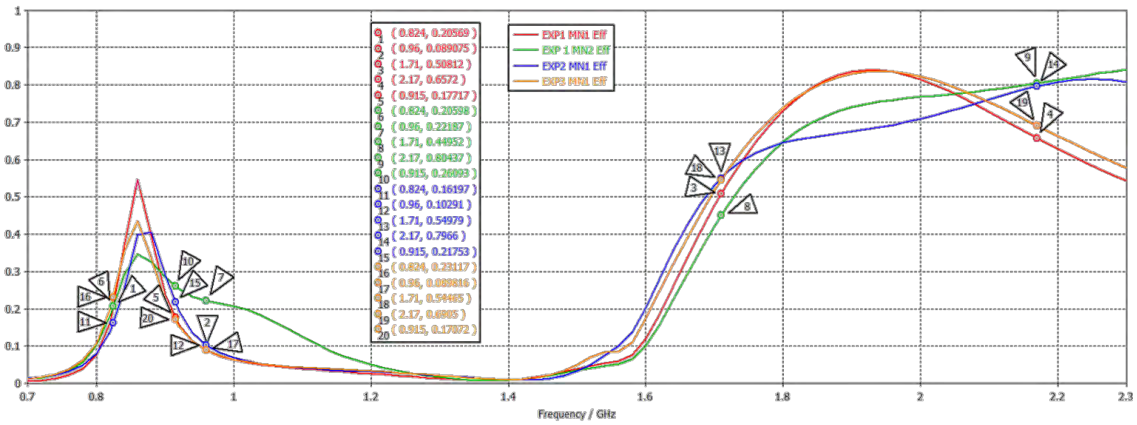


Figure 40 Antenna Efficiency comparison between the three Experiments done for the TRIO mXTEND™ chip antenna at LTE band

Experiment	ANTENNA EFFICIENCY (%)					
	824MHz	960MHz	Avg 824-960MHz	1710MHz	2170MHz	Avg 1710-2170MHz
Experiment 1 – MN1	20.5	8.9	25.9	50.8	65.7	74.7
Experiment 1 – MN2	20.6	22.2	27.3	44.9	80.4	70.9
Experiment 2 – MN1	16.2	10.3	24.3	55.0	79.7	69.0
Experiment 3 – MN1	23.1	9.0	24.2	54.5	69.0	75.1

Table 24 Antenna efficiency values for the three Experiments done for the TRIO mXTEND™ chip antenna at LTE band

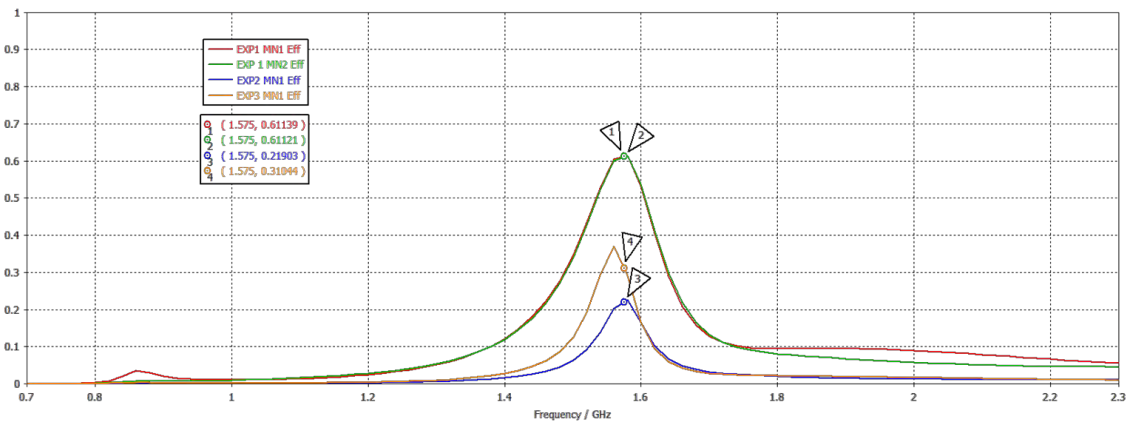


Figure 41 Antenna Efficiency comparison between the three Experiments done for the TRIO mXTEND™ chip antenna at GNSS band

GNSS	ANTENNA EFFICIENCY (%)		
	1561MHz	1575MHz	Avg 1598-1606MHz
Experiment 1 – MN1	60.4	61.1	52.1
Experiment 1– MN2	60.4	61.1	52.1
Experiment 2 – MN1	20.3	21.9	15.9
Experiment 3 – MN1	36.7	31.0	16.2

Table 25 Antenna efficiency values for the three Experiments done for the TRIO mXTEND™ chip antenna at GNSS band

For the first Experiment with different matching network topologies, it can be seen at Table 24 that the MN1 has a better performance at the higher frequency but a worse performance at LTE lower band is obtained in comparison to MN2. With MN2 it has been searched a tuning more focused in the lower band due to the values for high band are already very high.

It is important to note these are the values achieved in a simulation, although the components considered in the simulation has introduce their Q factor and their losses tangent, in mounted solution many factors will affect to the matching network tuning. As long is the matching network topology, the less will be the losses introduced by the components, but for a matching network which has very few components and where the Reflection Coefficient obtained is very accurate, the tolerances of the components will shift the antenna response more than a larger matching network, so the repeatability of the matching network will be worse. These are considerations important to note but not reflexed in the CST Simulation results.

On the other hand, regarding the Experiment 2 differences between the results obtained in Experiment 1, it can be observed how the antenna performance at the LTE band is very similar in the higher band and slightly different in the lower band, specially at the 824MHz frequency. But the most notorious change is in the GNSS band, which is the port closer to the ground plane area and therefore, the most affected for the set-up design change. So, it can be observed the negative effect produced by a metallic component to the antenna performance.

Finally, the last Experiment, Experiment 3, which introduces a more Clearance Area than Experiment 2, improve a lot the results at the GNSS band due to the GNSS port is now 5 mm far from the ground plane area. Then, it can be seen the importance of the Clearance Area for the antenna performance, and the negative effect produced by the metallic components to the antenna performance when are placed close to the antenna.

3.6 NN03-320 DUO mXTEND™

In this Chapter it has been simulated one DUO mXTEND™ working at the LTE band placed at the top right PCB corner as it has been done with the DUO mXTEND™ and TRIO mXTEND™ Experiments, and another DUO mXTEND™ placed at the bottom middle of the pcb working at the GNSS band [20].

After seeing the Clearance Area importance in the last Chapter conclusion, a study with the DUO mXTEND™ antenna booster has been done comparing the same scenario but modifying the Clearance Area length of the LTE antenna, to see if the change is critical. In the same set-up, as it has been said, another antenna placed far from the LTE one has been simulated working for the GNSS band.

The antenna working at the GNSS band does not work as a monopole antenna as it does the corner one, the antenna is working like a slot antenna and for that reason as closer to the middle of the board is the antenna, the better will be the performance.

As the project objective is to embed the solution to a mangOH™ RED device, is important to search where the antenna could realistically fit in the device without modifying too much the original device. So, for that reason, the GNSS antenna is not placed exactly in the middle of the board where the performance would be the maximum, is shifted to the left where no components are placed in the original device.

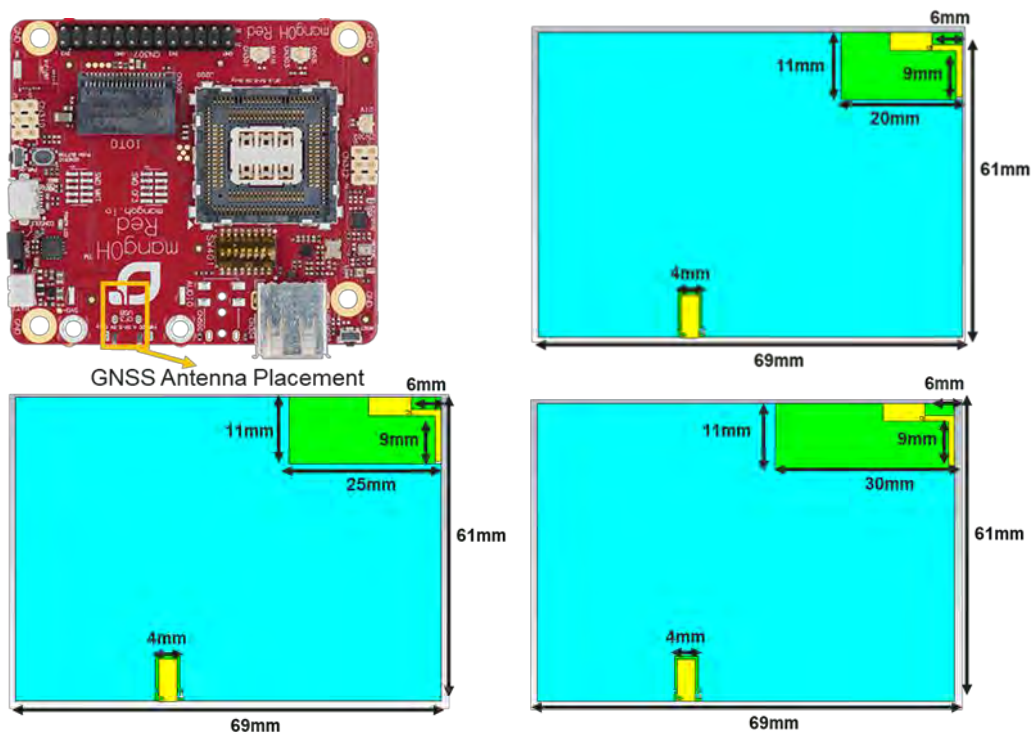


Figure 42 At top left the original device with the GNSS antenna placement indicated; at top right the Experiment 1 with the DUO mXTEND™ antenna booster; at bottom left the Experiment 2 with the DUO mXTEND™ antenna booster; at bottom right the Experiment 3 with the DUO mXTEND™ antenna booster

Three set-ups have been simulated modifying the Clearance Area dimension (see Figure 42) and with the same matching network topology (Figure 43) and matching network components (Table 26) a comparison of the Reflection Coefficient and the Antenna Efficiency between the three scenarios have been done.

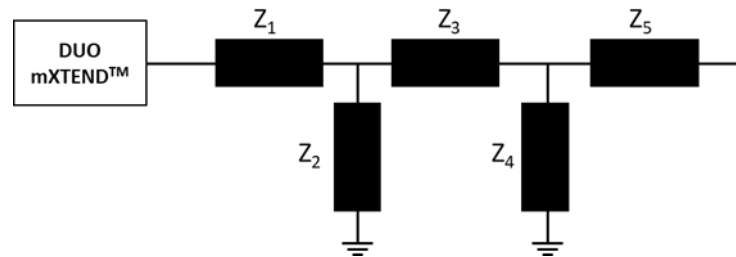


Figure 43 Matching network topology for the DUO mXTEND™ Experiments working at LTE band

Component	Value	Part Number
Z1	25nH	LQW18AN25NG80
Z2	15nH	LQW18AN15NG80
Z3	1.2pF	GJM1555C1H1R2WB01
Z4	2.0pF	GJM1555C1H2R0WB01
Z5	0Ω Resistor	-

Table 26 Build of materials (BoM) used to obtain for the DUO mXTEND™ Experiments MN2 at LTE band

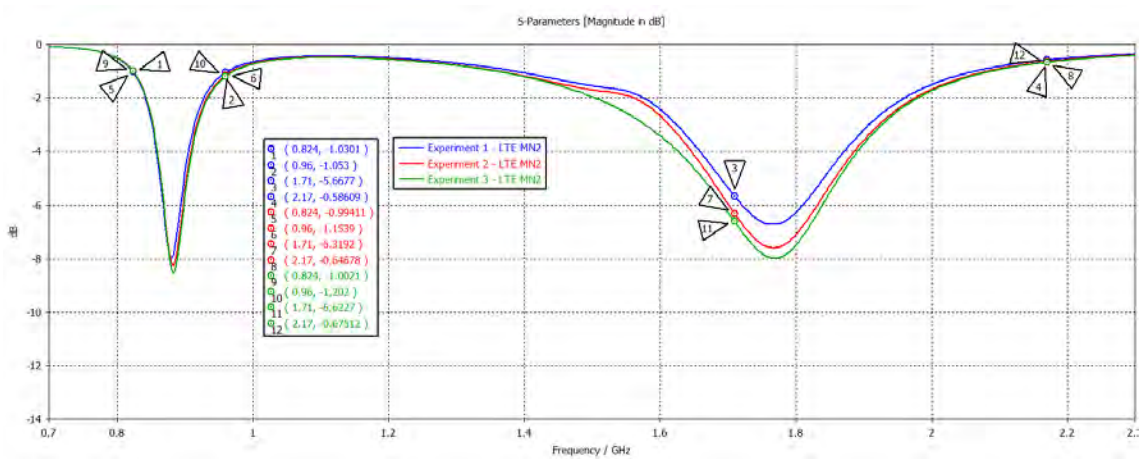


Figure 44 S parameters comparison between the three Experiments done for the DUO mXTEND™ booster antenna at LTE band

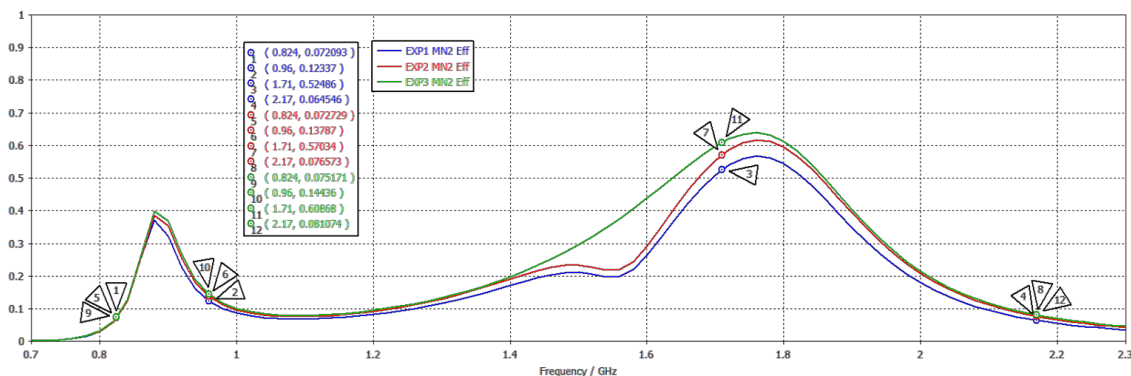


Figure 45 Antenna Efficiency comparison between the three Experiments done for the DUO mXTEND™ booster antenna at LTE band

Experiment	ANTENNA EFFICIENCY (%)					
	824MHz	960MHz	Avg 824-960MHz	1710MHz	2170MHz	Avg 1710-2170MHz
Experiment 1 – MN2	7.2	12.3	20.6	52.5	6.5	31.3
Experiment 2 – MN2	7.3	13.8	22.0	57.0	7.7	33.8
Experiment 3 – MN2	7.5	14.4	22.8	60.9	8.1	35.0

Table 27 Antenna efficiency values for the three Experiments done for the DUO mXTEND™ booster antenna at LTE band

As it is shown at Table 27, the efficiency values increase as many Clearance Area is simulated. This increase is a little higher at the higher band than at the lower band, but in both bands the improvement between the worst-case scenario (20mm x 11mm Clearance Area) and the best case (30mm x 11mm Clearance Area) is very low. At the lower band the difference is 2% and at the higher band the difference is 4%.

The improvement is lower than the seen in the last Chapter, because the previous scenario the feeding line is placed next to the ground plane area and in this scenario, the feeding line is placed at the edge of the board, as far as it can be to the ground plane area.

As the results in the higher band are a little low, specially at the 2170MHz frequency, another matching network (Table 28) with the same matching network topology (Figure 43) has been simulated in order to improve the results obtained in Experiment 3.

Component	Value	Part Number
Z1	25nH	LQW18AN25NG80
Z2	15nH	LQW18AN15NG80
Z3	1.0pF	GJM1555C1H1R0WB01
Z4	1.3pF	GJM1555C1H1R3WB01
Z5	0Ω Resistor	-

Table 28 Build of materials (BoM) used to obtain for the DUO mXTEND™ Experiments MN3 at LTE band

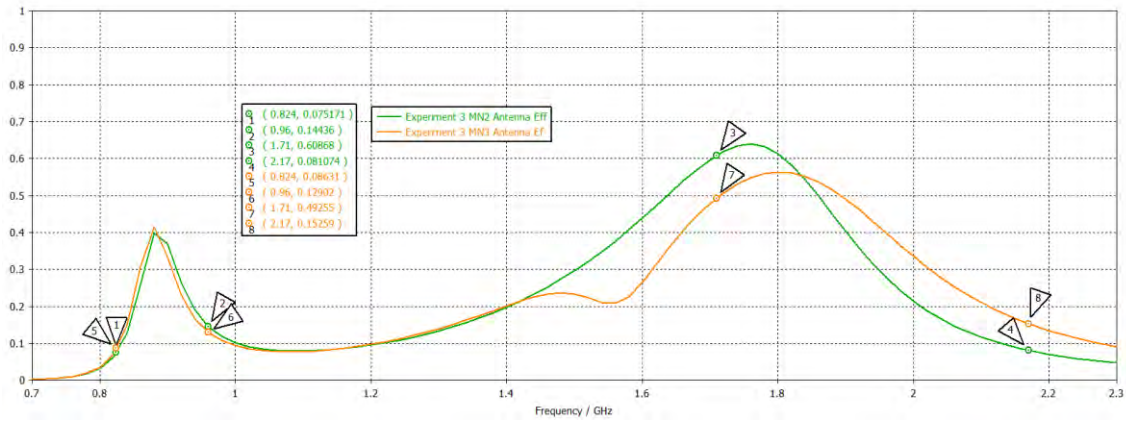


Figure 46 Antenna Efficiency comparison between MN2 and MN3 of the Experiment 3 done for the DUO mXTEND™ booster antenna at LTE band

Experiment	ANTENNA EFFICIENCY (%)					
	824MHz	960MHz	Avg 824-960MHz	1710MHz	2170MHz	Avg 1710-2170MHz
Experiment 3 – MN2	7.5	14.4	22.8	60.9	8.1	35.0
Experiment 3 – MN3	8.6	12.9	22.7	49.3	15.3	39.2

Table 29 Antenna efficiency values for MN2 and MN3 of the Experiment 3 done for the DUO mXTEND™ booster antenna at LTE band

The higher band average efficiency has been improved, specially at the 2170MHz frequency although the 1710MHz frequency value has decreased a little.

On the other hand, a GNSS matching network has simulated for every Experiment but the performance is the same in all the Experiments due to the LTE Clearance Area does not affect to the GNSS antenna. The GNSS antenna Clearance Area has 4mm x 7.5mm dimensions, which it means is only 0.5mm higher than the antenna footprint for every antenna side next to the ground plane area.

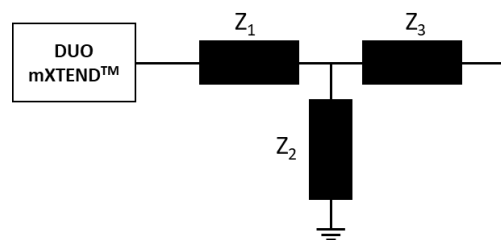


Figure 47 Matching network topology for the DUO mXTEND™ Experiments working at GNSS band

Component	Value	Part Number
Z1	1.2pF	GJM1555C1H1R2WB01
Z2	4.6pF	GJM1555C1H14R6WB01
Z3	0Ω Resistor	-

Table 30 Build of materials (BoM) used to obtain for the DUO mXTEND™ Experiments MN1 at GNSS band

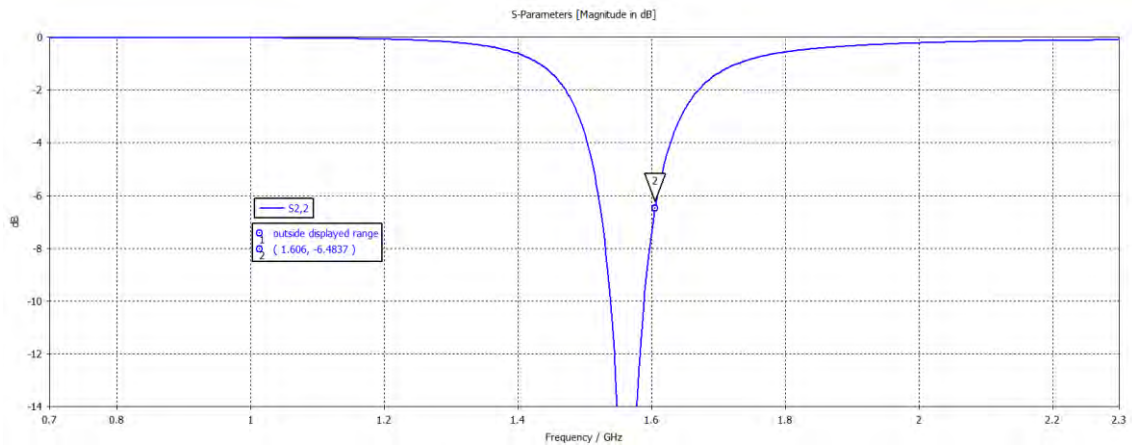


Figure 48 S parameters for the Experiments done for the DUO mXTEND™ booster antenna MN1 at GNSS band

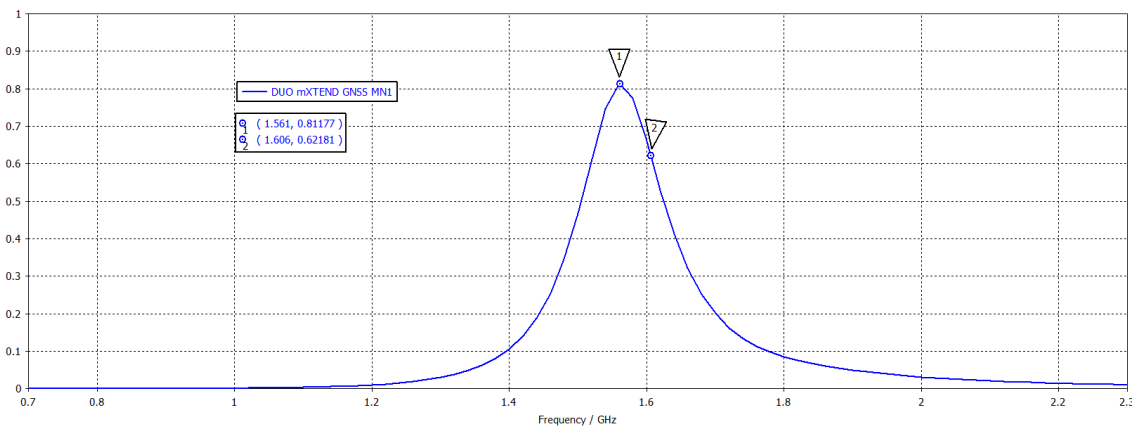


Figure 49 Antenna Efficiency for the Experiments done for the DUO mXTEND™ booster antenna MN1 at GNSS band

GNSS	ANTENNA EFFICIENCY (%)		
	1561MHz	1575MHz	Avg 1598-1606MHz
Experiment 1 – MN1	81.1	78.5	64.8

Table 31 Antenna efficiency values for the Experiments done for the DUO mXTEND™ booster antenna MN1 at GNSS band

The results obtained for the GNSS band are much higher than the results seen in the last Chapter using the TRIO mXTEND™ chip antenna, and the space used for the antenna, including the Clearance Area is very small.

As big is the Clearance Area for the GNSS solution with the DUO mXTEND™, better will be the performance, but the results obtained are already very good, so is better to stay with a very small space occupied than increase the Clearance Area to improve the performance.

3.7 Conclusions

In Chapter 3, it has been simulated three different antennas, everyone with its pros and cons. As big is the antenna, better the efficiency at the lower band and wider the bandwidth has been.

So, the logical says the TRIO mXTEND™ should be the antenna with the better performances but, the RUN mXTEND™ seems to have similar results if not better. This is caused by the fact RUN mXTEND™ only works at LTE band and the antenna is placed outside the main PCB, meanwhile the TRIO mXTEND™ works at LTE and GNSS bands at the same time and the most of the experiments has been done inside the PCB in order to search a more compact and realistic solution.

On the other hand, there is the DUO mXTEND™ which is very small antenna with a considerably lower efficiency values at LTE band but with a very high performance for the GNSS band.

It has been observed that the antennas inside the main PCB, with the feeding line close to the ground plane area, are very affected in the antenna performance. So, the TRIO mXTEND™ in a prototype PCB mounted, should need a high Clearance Area in order to work well in the band placed next to the ground plane area.

As the RUN mXTEND™ is an antenna that only can work at one band at the same time due only has one port, like the DUO mXTEND™, and the original device pcb does not has a realistic space to locate another RUN mXTEND™ antenna booster to work at GNSS, it has been the antenna discarded for the prototyping process.

As far as the solutions selected, the TRIO mXTEND™ and the DUO mXTEND™, each solution is very different from the other one. The TRIO mXTEND™ chip antenna has a better LTE performance and only needs one antenna to work with both bands, but it requires a bigger space to place the antenna and a Clearance Area which guarantees a good performance at the GNSS band.

For the DUO mXTEND™ antenna booster, the performance at LTE band is considerably lower and it is necessary to place two antennas in a different location of the PCB but, the space occupied to for its correct working is smaller and the GNSS band performance is better.

4. EXPERIMENTAL VALIDATION

4.1 INTRODUCTION

This chapter proposes a compact embedded antenna solution for the mangOH™ RED device. To arrive at this point it will be necessary to choose the scenario, including antenna and location, which will be the final solution.

In the last chapter conclusions, it can be seen the selected antennas to prototype, the TRIO mXTEND™ and the DUO mXTEND™, so in this chapter it will be necessary to know which antenna will be the used for the final device. To know the final scenario chosen, a PCB in house prototype it will be mounted for each scenario and then, a comparison between all the PCB's mounted will be done in order to choose the most optimal solution for the embedded mangOHTM RED solution.

The measurements done to compare each solution have been the same as the last chapter: the reflection coefficient of each band, and the antenna and radiation efficiency of each band.

As far as the solutions mounted, four total solutions have been mounted: two solution with the TRIO mXTEND™ and two solutions with the DUO mXTEND™. Each antenna has a scenario with the LTE matching network pads located vertically and another scenario with the LTE pads located horizontally. This difference in the set-ups mounted it has an impact to the final antenna performance and both solutions, the vertically and the horizontally, have their own pros and cons.

Furthermore, in the two TRIO mXTEND™ experiments exist another difference between scenarios. In the first experiment mounted (see Figure 54) the GNSS feeding line is vertically located and it measures 9mm. The second experiment mounted with the TRIO mXTEND™ (see Figure 67) the GNSS feeding line is horizontally located and it measures 5mm. As a consequence of this design change, the performance will be different between both GNSS solutions.

4.2 PROTOTYPING

The MangOH™ RED is an already commercialized device though time ago for its optimal utilization and with a closed antenna design. So, as it is not possible mounting both antennas simulated to the final device due to lack of all the characteristics supposed in the simulations, a PCB in house for each solution it has been mounted, in order to create a physical scenario as closer as it can be done to the MangOH™ RED device.

A PCB in house is, as the name indicates, a PCB realized without any industrial manufacturing process. So, the PCB is made of a standard FR4 dielectric, the same used in the Electromagnetic Simulation and a copper top layer to make connectivity. The objective in the PCB in house realization is to remove some parts of the top copper layer, having the same antenna footprint as the simulated and the matching network footprint to put all the components in order to tune our antenna.

To achieve that purpose, it will be necessary to use an UV contact copier and mask to protect the copper that it must remain in the board. Then with a created acid, the non-desirable copper will be removed. So, see below the step by step guide followed for the PCB in house manufacturing:

1. Realization of the black mask with AutoCAD. It is important to note the black color printed it must be a pure black color. In a non-industrial printer, the quantity of ink used by the printer is not enough because in the UV contact copier process, the mask will not protect the desired copper zones.

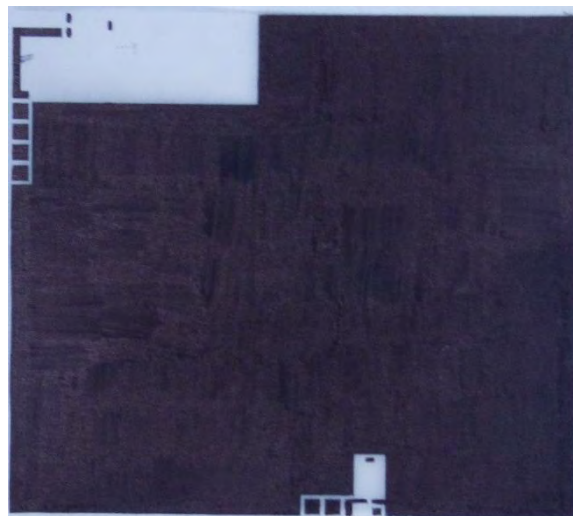


Figure 50 Mask used for Experiment 1 of the DUO mXTEND™ seen in chapter 4.4.1

2. At the chemical lab open the yellow light. It is important to note the natural light accelerates the revelation process, so the yellow light help to slow down the reveal.
3. Cut off a piece of substrate bigger than the mask made. The substrate used for the experiment is the same as the supposed in Chapter 3: Electromagnetic Analysis, a 1mm width FR4 with a Loss tangent of 0.014 at 1GHz and a Permittivity of 4.3.
4. Put off the fiber protection showing the top layer copper.



Figure 51 Piece of FR4 substrate used for the Prototyping making off, without a piece of protective fiber, which shows the top layer copper.

5. Put the board on the UV contact printer with the footprint mask done right above the board. It is important to note the darker face of the mask must to be in contact with the board, so the footprint mask drawing must to be the mirror of the footprint PCB wanted.
6. Making it empty with the board and the mask above. Therefore, push down the lid and apply the UV light the PCB during 3'30".
7. Once the time is over, take the PCB and apply the positive revelator to the board no more than 5-10 seconds, until the shadow of the footprint appears.
8. Wash with water the board and then make the acid needed the remove the copper. That acid is compound by (in a total of 100ml):
 - a. 25% of Hydrochloric acid.
 - b. 25% of Hydrogen peroxide.
 - c. 50% water.

9. Tip out the created acid until the copper is totally removed from the board. Then it can be cleaned with Acetone.



Figure 52 From left to right, the components used to create the PCB in the chemical lab: Hydrochloric acid, Hydrogen peroxide, Acetone.

10. Cut off the substrate not necessary of the PCB. This last point is not mandatory due to the most important is the surface covered by copper, the substrate without copper have not any impact on the antenna performance.

So, once all the points have been followed step by step the result it will be the PCB desired, like the seen in the Figure 53.

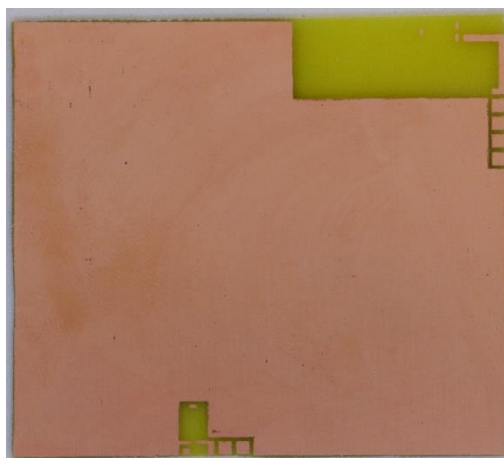


Figure 53 PCB board created with a 1mm width and 69mm x 61mm FR4 PCB with a Loss tangent of 0.014 at 1GHz and a relative permittivity of 4.3, for the Experiment 1 seen in the Chapter 4.4.2

4.3 TRIO mXTEND™ PROTOTYPE

Two prototypes using TRIO mXTEND™ antenna have been mounted, using a PCB with the same dimensions, 69mm x 61mm, and the same clearance area for both antennas have been considered, 35mm x 12mm. The same bands are covered by the two experiments: LTE B1, B3, B4, B5, B8 (824MHz-960MHz and 1710MHz-2170MHz) and GNSS (1561MHz-1606MHz).

4.3.1 Experiment 1: 35 x 12mm² Clearance Area and vertical pads for LTE and GNSS

In this Chapter it can be observed a solution working in two ports for the already described bands, LTE and GNSS. As far as the feeding lines length, LTE and GNSS have a similar feeding line of 9mm x 1mm but as per GNSS, the feeding line is separated in two parts. The first part measures 0.5mm x 1mm followed by a gap of the same dimensions and then, the remaining 8mm x 1mm.

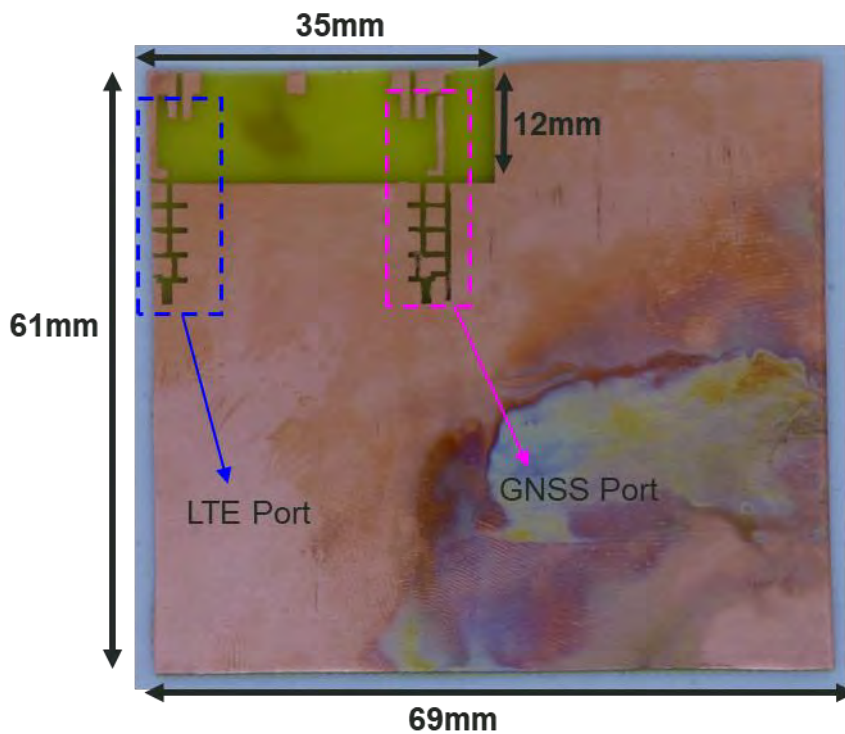


Figure 54 PCB in house used for Experiment 1. LTE port is placed at left and GNSS port is placed at right.

On the other hand, the matching network footprint is the same for both bands like it can be seen in Figure 54.

The antenna booster TRIO mXTEND™ has been soldered to the board using a hot gun like is explained in the methodology process (1.3 Methodology), furthermore, a SMA connector compatible with the Network Analyzers used for measurements, alongside a micro coaxial cable have been implemented on the board, following the same methodology process.

In order to tune the interest bands at the minimum Reflection Coefficient possible, it has been measured the antenna 0 ohms response in each port.

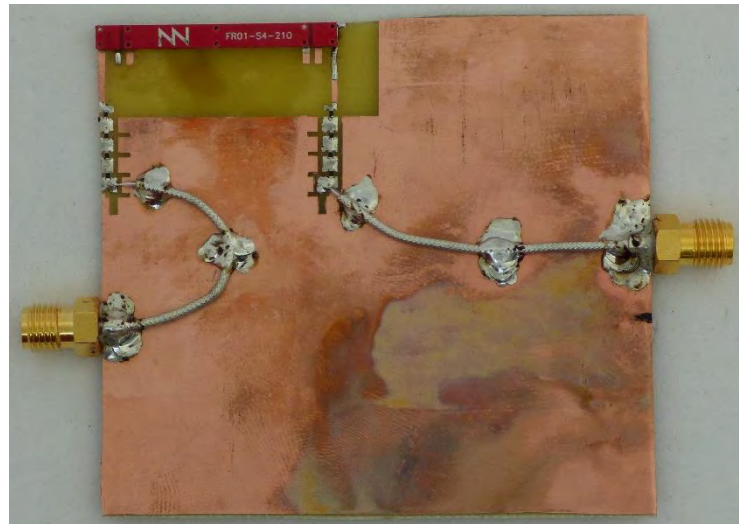


Figure 55 PCB in house used for Experiment 1, with the TRIO mXTEND™ antenna booster (30mm x 3mm x 1mm) and 0 ohms matching network connected to the SMA connectors [1]- [22]

The antenna 0 ohms response is shifted in phase due to the pads and coaxial cables length, so it is important first to correct the phase with Network Analyzer. Once the phase is corrected and the real antenna response is seen in the Network Analyzer, the tune process can be started.

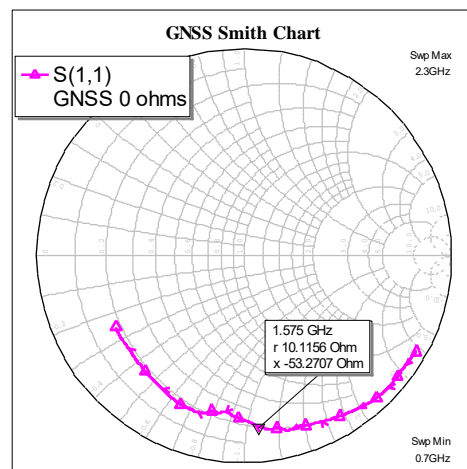


Figure 56 0 ohms antenna response measured in the Network Analyzed and the phase corrected for Experiment 1. At the left it is shown LTE port, at right GNSS port.

The tune process it has been done with an engineering process which consist in build the matching network component by component, observing the response given in the Network Analyzer and then, decide the following component as a consequence of the response achieved, as it is explained at Chapter 3.3 (see Figure 5).

It is important to note, the moves realized by the components are not the same in an Electromagnetic Simulator or any other matching network tuner tool than the real component response, due to the losses introduced by the components are used to be higher than ideally would be and the PCB in house created is nothing else than an approximation to what we are simulated before. Any change on the footprint antenna or pads geometry caused by the PCB in house creation process, could affect to the characteristic impedance we are looking at the Network Analyzer.

As is explained at Chapter 3.5.1, the TRIO mXTEND™ when is working at LTE used to have two matching network sections (see Figure 57 for a better understanding). Section A is where the LTE matching network topology is placed, and Section B is used for an optional filter which will separate the coupling effect between the lower frequency range (LFR: 824MHz-960MHz) and the higher frequency range (HFR: 1710MHz-2170MHz).

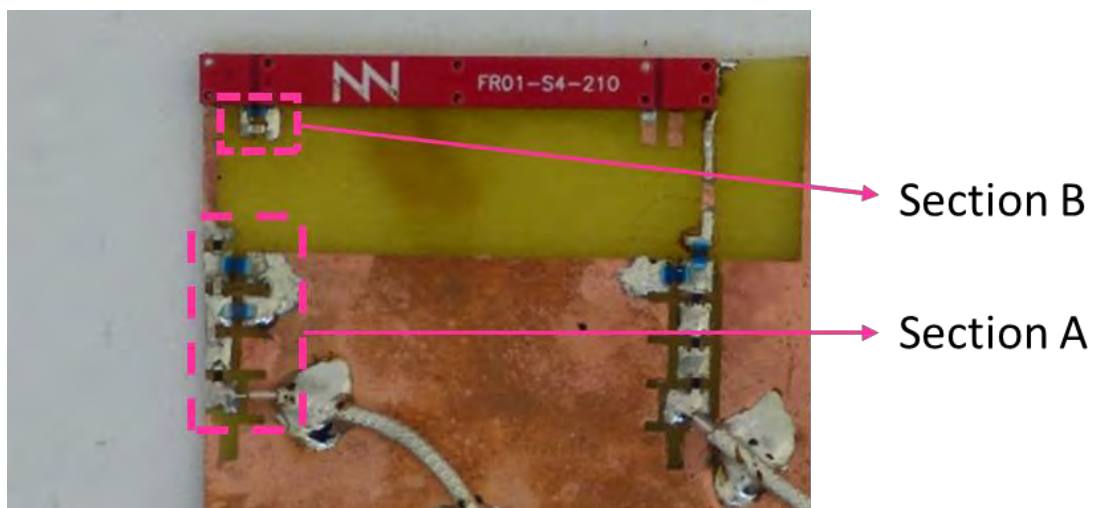


Figure 57 Clarification of Section A and Section B on the Experiment 1 with MN2 for LTE band mounted

Three matching networks have been tested for LTE band Section A, considering the same matching network topology for each band (Figure 58). For every matching network obtained, it has been measured the reflection coefficient and the Antenna and Radiation Efficiency:

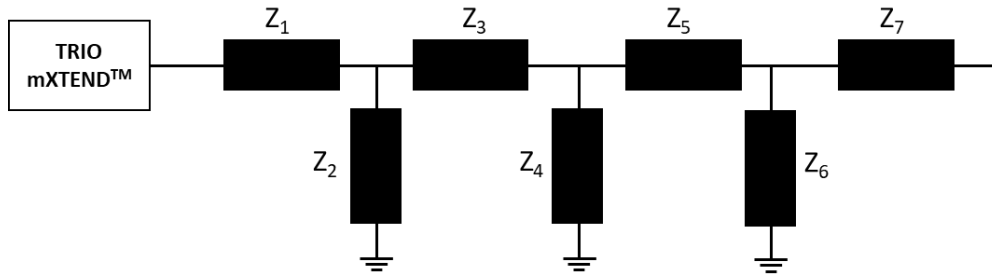


Figure 58 Matching network topology for Experiment 1 at LTE band Section A

MN	Component	Value	Part Number
MN1	Z1	0Ω Resistor	-
	Z2	10nH	LQW18AN10NG10
	Z3	0Ω Resistor	-
	Z4	Empty	-
	Z5	0Ω Resistor	-
	Z6	Empty	-
	Z7	0Ω Resistor	-

Table 32 Build of materials (BoM) used to obtain MN1 for Experiment 1 at LTE band Section A

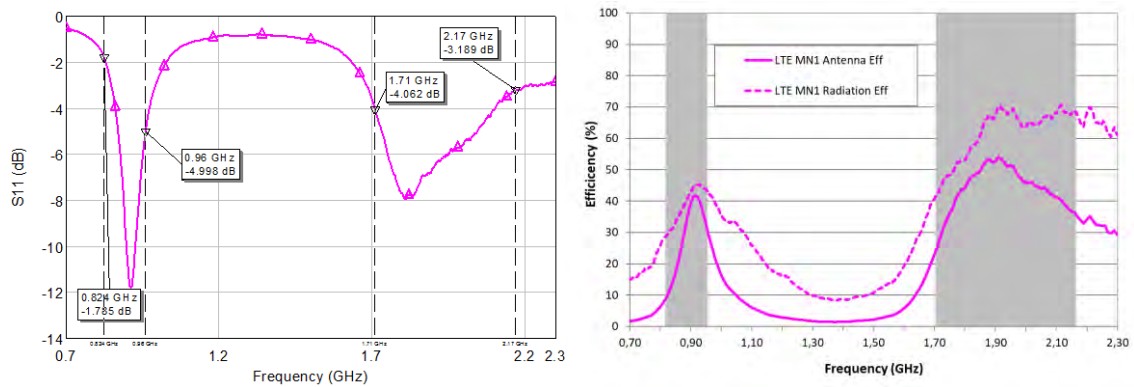


Figure 59 Measured S_{11} at left and Antenna and Radiation Efficiency at right, for Experiment 1 MN1 at LTE band.

MN	Component	Value	Part Number
MN2	Z1	0Ω Resistor	-
	Z2	9.1nH	LQW15AN9N1G80
	Z3	2.0pF	GJM1555C1H2R0WB01
	Z4	12nH	LQW18AN12NG10
	Z5	2.0pF	GJM1555C1H2R0WB01
	Z6	Empty	-
	Z7	0Ω Resistor	-

Table 33 Build of materials (BoM) used to obtain MN2 for Experiment 1 at LTE band Section A

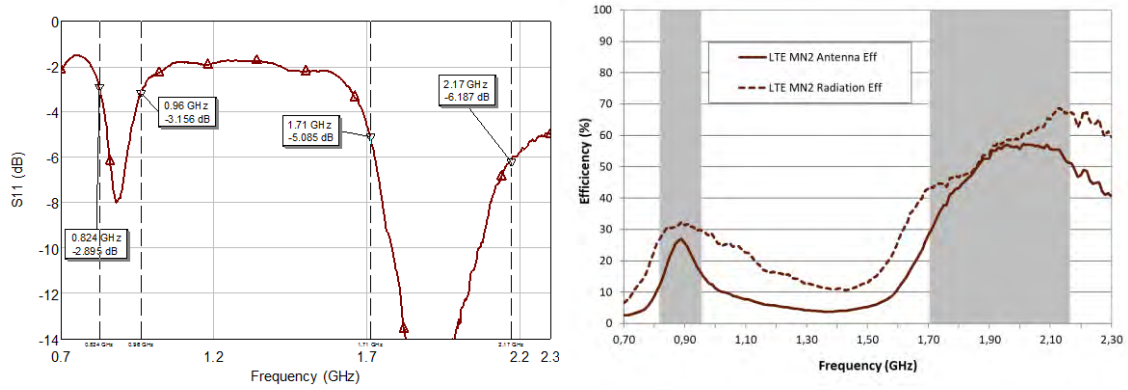


Figure 60 Measured S_{11} at left and Antenna and Radiation Efficiency at right, for Experiment 1 MN2 at LTE band.

MN	Component	Value	Part Number
MN3	Z1	0Ω Resistor	-
	Z2	9.1nH	LQW15AN9N1G80
	Z3	2.0pF	GJM1555C1H2R0WB01
	Z4	12nH	LQW18AN12NG10
	Z5	2.3pF	GJM1555C1H2R3WB01
	Z6	18nH	LQW18AN18NG10
	Z7	0Ω Resistor	-

Table 34 Build of materials (BoM) used to obtain MN3 for Experiment 1 at LTE band Section A

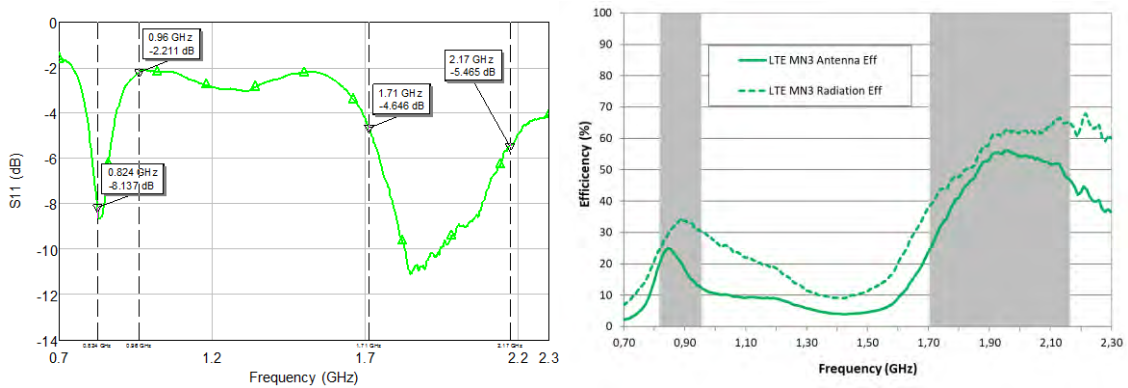


Figure 61 S_{11} at left and Antenna and Radiation Efficiency at right, for Experiment 1 MN3 at LTE band.

Working on the same port but changing to Section B matching network, the values used to make the filter have been the observables on Table 35.

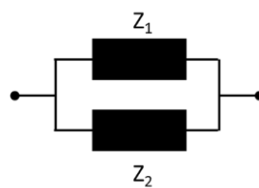


Figure 62 Matching network topology for Experiment 1 LTE band Section B

Component	Value	Part Number
Z1	8.0nH	LQW15AN8NG80
Z2	0.8pF	GJM1555C1HR80WB01

Table 35 Build of materials (BoM) used to obtain the LTE filter for Experiment 1 at LTE band Section B.

To determine which performance will be better, it is important to compare the Reflection Coefficient (Figure 63) and Antenna Efficiency (Figure 64) between all cases.

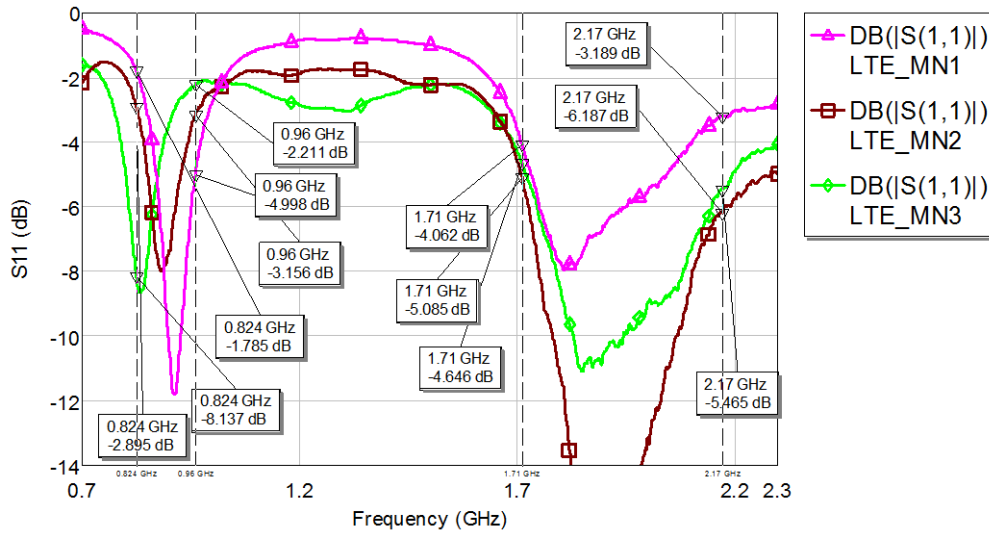


Figure 63 S parameters comparison between all the matching networks for Experiment 1 at LTE band.

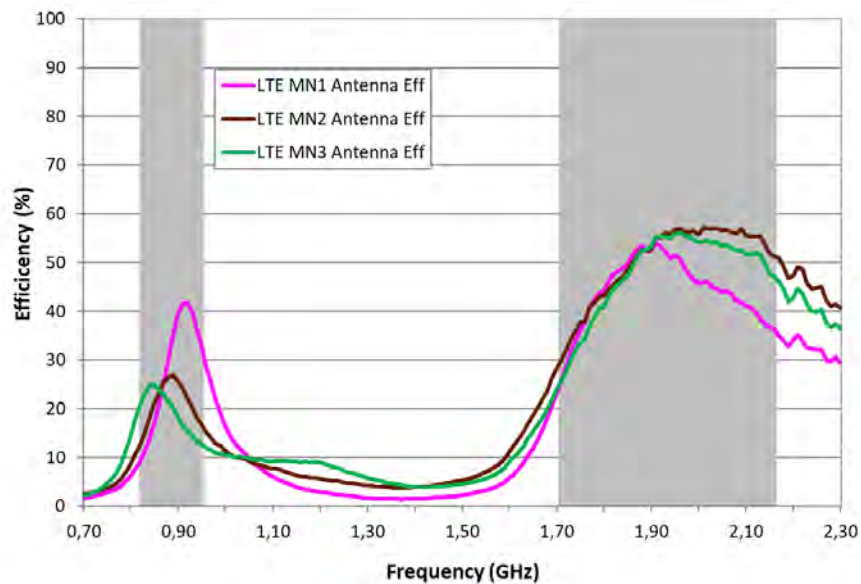


Figure 64 Measured Antenna Efficiency comparison between all the Matching Networks for Experiment 1 at LTE band

LTE	ANTENNA EFFICIENCY (%)					
	824MHz	960MHz	Avg 824-960MHz	1710MHz	2170MHz	Avg 1710-2170MHz
MN1	8.9	30.9	28.6	24.3	35.7	44.2
MN2	12.3	16.0	21.3	29.1	51.2	50.3
MN3	20.3	12.4	19.4	24.7	46.6	48.1

Table 36 Antenna Efficiency values for Experiment 1 at the LFR (824MHz-960MHz) and HFR (1710MHz-2170MHz) of the LTE band.

As it can be seen in Table 36, the three matching networks have similar Antenna Efficiency values at the HFR (1710MHz-2170MHz), but at as far as the LFR (824MHz-960MHz), the Antenna Efficiency for each matching network is pretty different. In the first matching network analyzed, MN1, the average efficiency and the 960MHz value are the higher, then for MN2 the average efficiency is lower than the first matching network but has the extremes of the band more equilibrated. Finally, for MN3, the average efficiency at LFR is the lower but at 824MHz has the higher antenna efficiency.

It is important to note the LFR band analyzed is formed by two LTE bands: B5 and B8. Every LTE band is divided in Uplink band (824MHz-849MHz for B5 and 880MHz-915MHz for B8) and Downlink band (869MHz-894MHz for B5 and 925-960MHz for B8). In IoT, Smart cities and the new technologies in general, the lifetime is one of the most important things to have into account and the consumption of battery in reception is way lower than the battery consumption at transmitting. For this reason, in some cases, it is more important to prioritize the uplink bands than the downlink bands, although that means having less antenna efficiency average value at the band.

On the other hand, for GNSS band, one matching network has been obtained (Figure 65).

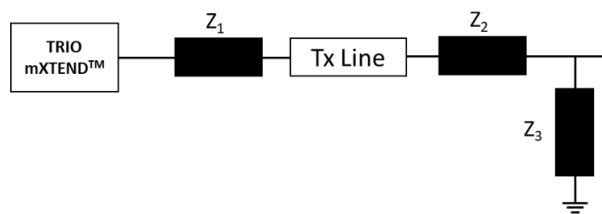


Figure 65 Matching network topology for Experiment 1 GNSS band

Component	Value	Part Number
Z1	0.1pF	GJM1555C1HR10WB01
Z2	18nH	LQW18AN18NG10
Z3	16nH	LQW18AN16NG80

Table 37 Build of materials (BoM) used to obtain MN1 for Experiment 1 at GNSS band

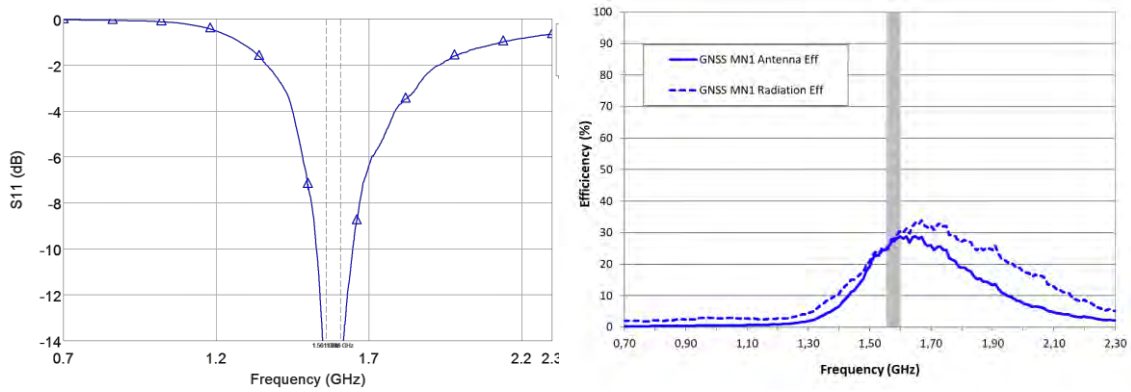


Figure 66 S_{11} at left and Antenna and Radiation Efficiency at right, for Experiment 1 MN1 at GNSS band.

ANTENNA EFFICIENCY (%)			
GNSS	1561MHz	1575MHz	Avg 1598-1606MHz
MN1	24.7	27.1	28.6

Table 38 Antenna Efficiency values for 1561MHz (BeiDou E1 band), 1575 MHz (GPS L1 band) and from 1598 MHz to 1606 MHz (GLONASS L1 band).

4.3.2 Experiment 2: 35 x 12mm² Clearance Area and horizontal pads for LTE and GNSS

This Chapter proposes a solution operating with two ports for LTE and GNSS. As far as the feeding lines length, LTE keep having a feeding line of 9mm x 1mm but as per GNSS, the feeding line now is horizontal and is separated in two parts as Experiment 1. The first part measures 0.5mm x 1mm followed by a gap of the same dimensions and then, the remaining 4mm x 1mm. The antenna location has been changed to the right part of the PCB (the original simulated position) which will not do any effect in terms of antenna performance.

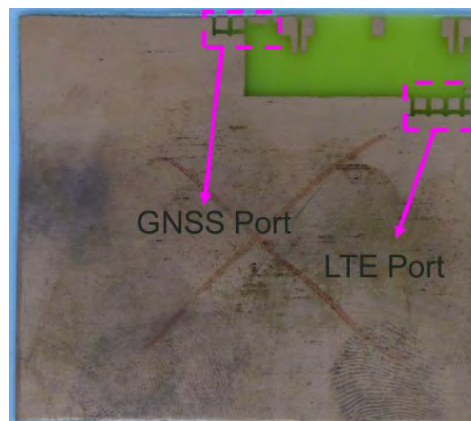


Figure 67 PCB in house used for Experiment 2. LTE port is placed at right and GNSS port is placed at left.

Regarding the matching network topologies, LTE keeps having the same topology as Experiment 1 but for GNSS the matching network topology it has been reduced because, as it can be seen in Chapter 4.3.1, it is no necessary to have a matching network topology with so many components.

As it is shown in Figure 68, the 0 ohms antenna response has changed in comparison to the 0 ohms antenna response from Experiment 1, in both bands. At GNSS band the changed of topology have had a big impact on the antenna response due to less pads are considered now, and the feeding line is shorter. At LTE band, the 0 ohms response is different to the seen in the Experiment 1 due to LTE filter is already implemented on the board, being the same as the Experiment 1 LTE filter (Figure 62 and Table 35).

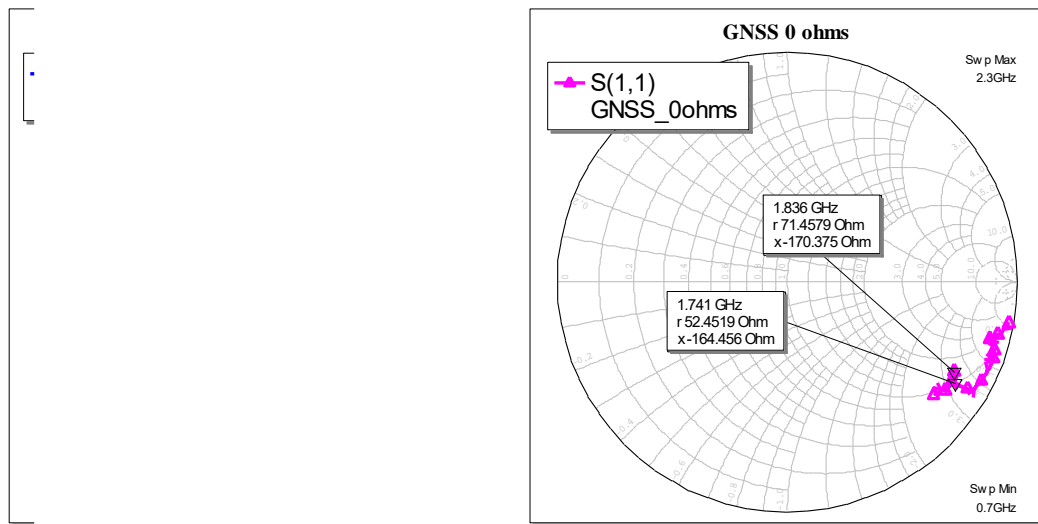


Figure 68 0 ohms antenna response measured in the Network Analyzed and the phase corrected for Experiment 2. At the left it is shown LTE port, at right GNSS port.

Four matching networks have been tested for LTE band Section A (Figure 57), considering the same matching network topology for each band (the same as Experiment 1 Figure 58). For every matching network obtained, it has been measured the Reflection Coefficient and the Antenna and Radiation Efficiency:

MN	Component	Value	Part Number
MN1	Z1	0Ω Resistor	-
	Z2	18nH	LQW18AN18NG10
	Z3	0Ω Resistor	-
	Z4	Empty	-
	Z5	0Ω Resistor	-
	Z6	Empty	-
	Z7	0Ω Resistor	-

Table 39 Build of materials (BoM) used to obtain MN1 for Experiment 2 at LTE band Section A

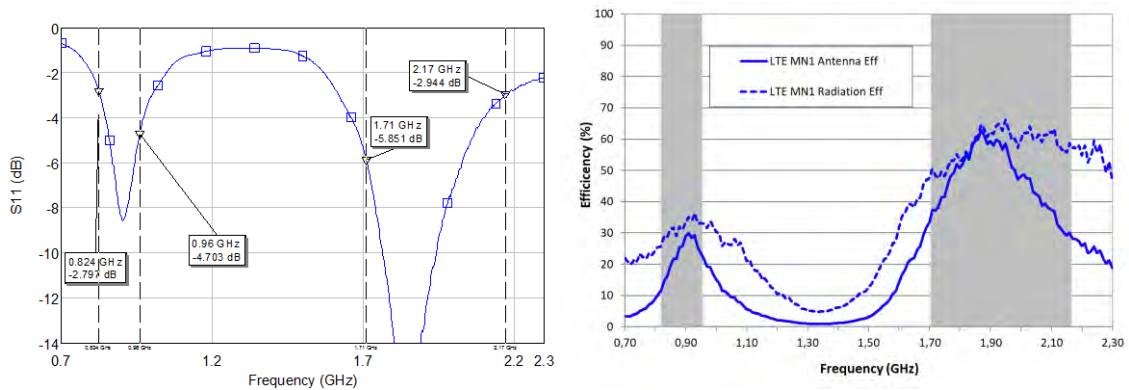


Figure 69 S_{11} at left and Antenna and Radiation Efficiency at right, for Experiment 2 MN1 at LTE band.

MN	Component	Value	Part Number
MN2	Z1	0Ω Resistor	-
	Z2	6.5nH	LQW15AN6N5G80
	Z3	2.0pF	GJM1555C1H2R0WB01
	Z4	18nH	LQW18AN18NG10
	Z5	0Ω Resistor	-
	Z6	Empty	-
	Z7	0Ω Resistor	-

Table 40 Build of materials (BoM) used to obtain MN2 for Experiment 2 at LTE band Section A

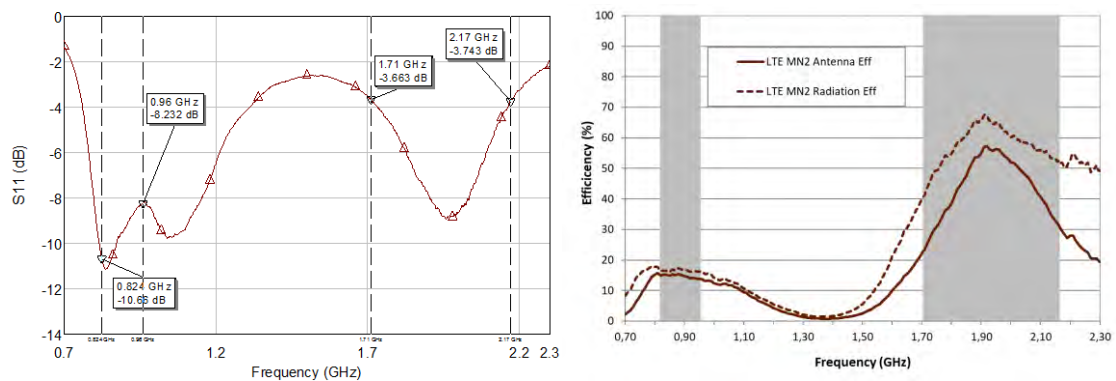


Figure 70 S_{11} at left and Antenna and Radiation Efficiency at right, for Experiment 2 MN2 at LTE band.

MN	Component	Value	Part Number
MN3	Z1	0Ω Resistor	-
	Z2	6.5nH	LQW15AN6N5G80
	Z3	2.0pF	GJM1555C1H2R0WB01
	Z4	18nH	LQW18AN18NG10
	Z5	2.0pF	GJM1555C1H2R0WB01
	Z6	Empty	-
	Z7	0Ω Resistor	-

Table 41 Build of materials (BoM) used to obtain MN3 for Experiment 2 at LTE band Section A

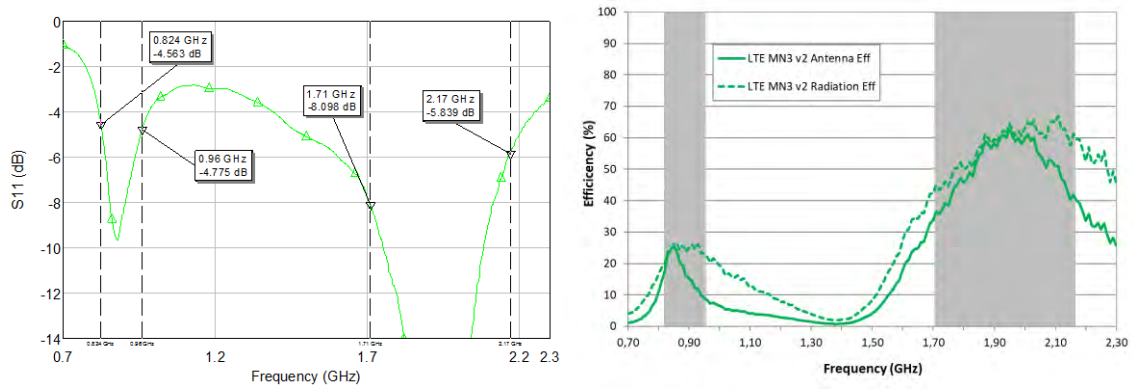


Figure 71 S_{11} at left and Antenna and Radiation Efficiency at right, for Experiment 2 MN3 at LTE band.

MN	Component	Value	Part Number
MN4	Z1	0Ω Resistor	-
	Z2	6.5nH	LQW15AN6N5G80
	Z3	2.0pF	GJM1555C1H2R0WB01
	Z4	18nH	LQW18AN18NG10
	Z5	2.4pF	GJM1555C1H2R4WB01
	Z6	Empty	-
	Z7	0Ω Resistor	-

Table 42 Build of materials (BoM) used to obtain MN4 for Experiment 2 at LTE band Section A

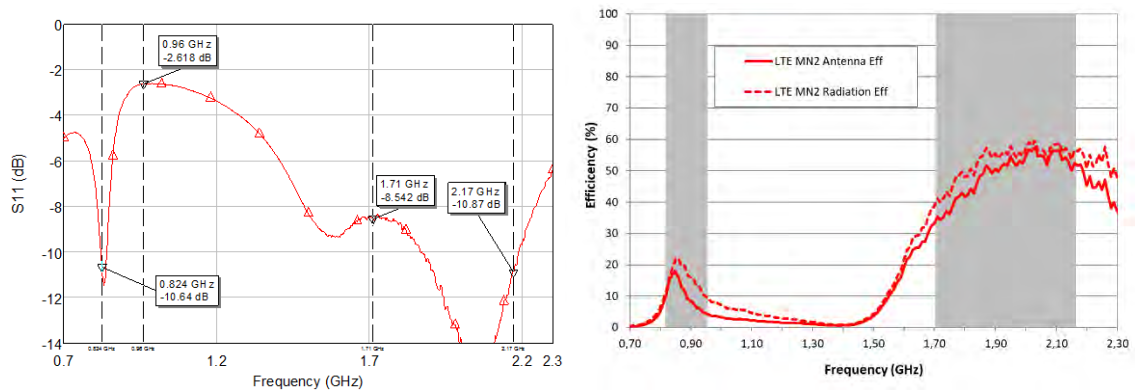


Figure 72 S_{11} at left and Antenna and Radiation Efficiency at right, for Experiment 2 MN4 at LTE band.

To see clearly which performance will be better, it is important to do a comparison in Reflection Coefficient (see Figure 73) and Antenna Efficiency (see in Figure 74) between all the performances obtained.

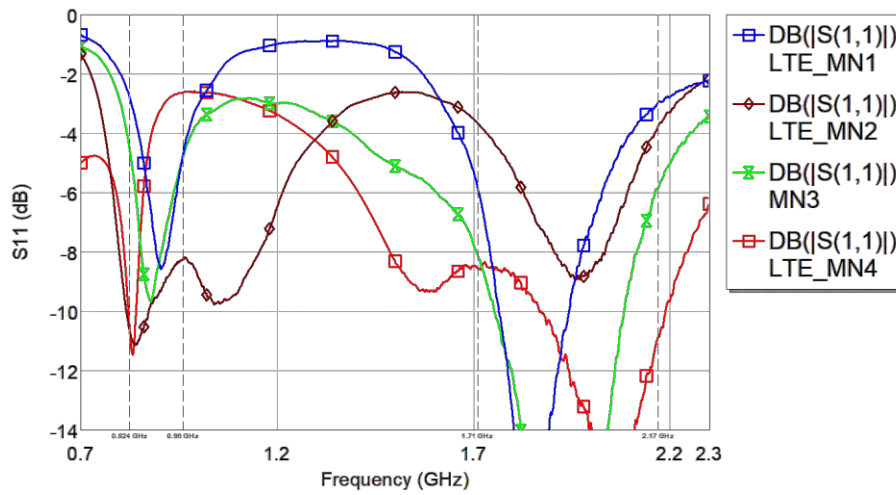


Figure 73 S parameters comparison between all the matching networks for Experiment 2 at LTE band.

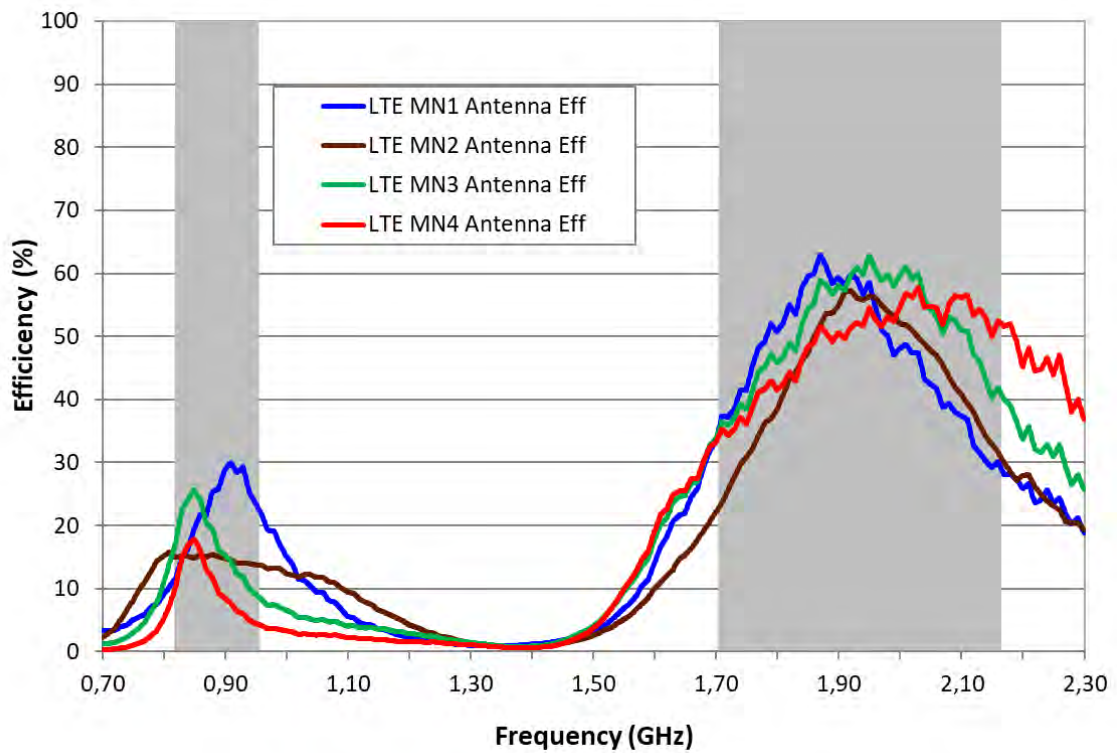


Figure 74 Antenna Efficiency comparison between all the matching networks for Experiment 1 at LTE band.

LTE	ANTENNA EFFICIENCY (%)					
	824MHz	960MHz	Avg 824-960MHz	1710MHz	2170MHz	Avg 1710-2170MHz
MN1	11.5	22.7	23.3	35.4	29.1	47.3
MN2	15.0	13.7	14.7	22.8	30.8	44.2
MN3	16.9	8.7	17.3	35.1	40.9	51.4
MN4	10.0	4.3	10.6	34.3	52.0	49.1

Table 43 Antenna Efficiency values for Experiment 2 at the LFR (824MHz-960MHz) and HFR (1710MHz-2170MHz) of the LTE band.

As it can be observed in Table 43 the four matching networks tested have a good performance in the higher band (1710MHz-2170MHz), although in the 2170MHz frequency the first two matching networks have a notably lower performance than MN3 and MN4. In the low band the performance is lower in comparison to the high band, being MN1 and MN3 the matching network with better efficiency values.

First, a high efficiency at LFR (824MHz-960MHz) in MN1 has been achieved, but the Uplink frequencies for B5 (824MHz-849MHz) are lower in comparison to the rest of the LFR band. At the high band, the average efficiency is high but at 2170MHz frequency, the worst efficiency value of all the matching networks tested has been obtained.

In MN2 it has been tested a topology to improve the performance in the Uplink B5 band respect MN1 and try to get an equilibrate Reflection coefficient through all the LFR (see Figure 70), but the efficiency values do not correspond to the theoretically S_{11} seen in the figure. It may be for the losses in the set-up measured which are making the efficiency values lower than what it should be and making the Reflection coefficient better. At the higher band, the worst average efficiency values are obtained which makes sense with the loss's situation seen in the lower band.

Then, for MN3 the best average efficiency values at HFR and at the best values at 824MHz are achieved, although its LFR average efficiency is lower than the seen in MN1.

Finally, for MN4, it has been designed a matching network to increase the efficiency at 2170MHz and prioritize the 824MHz frequency with respect to 960MHz at LFR. The values obtained at HFR are very good, being the efficiency at 2170MHz the better of all the matching networks tested. Regarding the LFR, the efficiency values obtained are the worst.

On the other hand, for GNSS band, the same topology as Experiment 1 has been applied (see Figure 65), and one matching network has been tested:

Component	Value	Part Number
Z1	0.1pF	GJM1555C1HR10WB01
Z2	27nH	LQW18AN27NG10
Z3	Empty	-

Table 44 Build of materials (BoM) used to obtain MN1 for Experiment 2 at GNSS band

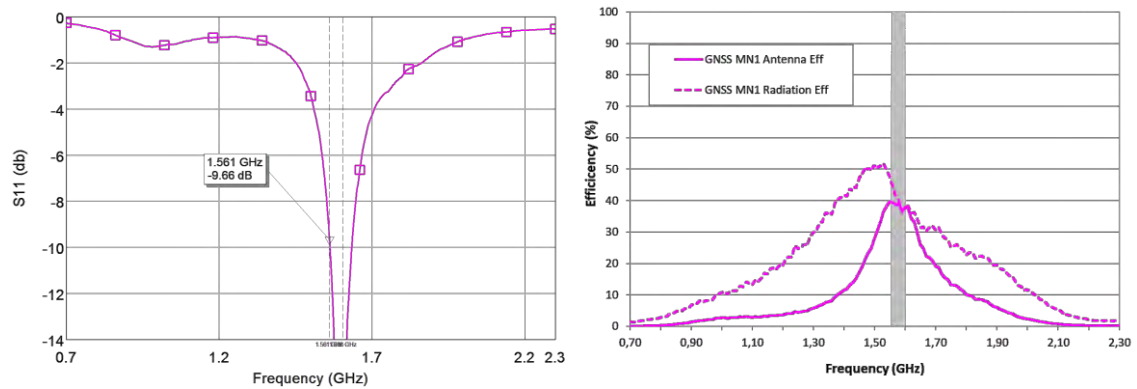


Figure 75 S_{11} at left and Antenna and Radiation Efficiency at right, for Experiment 2 MN1 at GNSS band.

GNSS	ANTENNA EFFICIENCY (%)		
	1561MHz	1575MHz	Avg 1598-1606MHz
MN1	39.5	38.7	37.4

Table 45 Antenna Efficiency values for 1561MHz (BeiDou E1 band), 1575 MHz (GPS L1 band) and from 1598 MHz to 1606 MHz (GLONASS L1 band).

And additional experiment for this set-up has been done in order to improve the LTE efficiency values even though the GNSS deteriorate, due to the high values achieved. So, a filter for GNSS to avoid the coupling effect for both bands it has been used.

To implement that filter, two ways are possible: make a filter with the same components as the matching network ones, just before the antenna tuning or buy a SAW filter designed specifically for the band.

The first option it would introduce a lot of losses to the GNSS band and the filter it would not be as selective as SAW filter specially designed. So, this first option could be a good option if the efficiency values achieved at GNSS are higher than minimum desired, and if the coupling effect is very notorious. Regarding the SAW filter option, it would be a better option but an

expensive one, that is why it is good idea to simulate if the SAW filter will contribute enough to be profitable in the mounted set-up.

So, to see this SAW filter impact, one of the matching networks tested (MN3) has been remeasured considering the coupling effect at the Radiation Efficiency calculation. The Antenna Efficiency keeps being the same, so if s_{21} is included in the equation, the Radiation Efficiency becomes higher:

$$Radiation\ Efficiency = \frac{Antenna\ Efficiency}{1 - |s_{11}|^2 - |s_{21}|^2} \quad VI. 6$$

So, to measure the new antenna efficiency it must be considered the dropping of the coupling effect (s_{21}) and the LTE S_{11} change, due to the SAW filter considered which is the SF2385H from Murata Manufacturing.

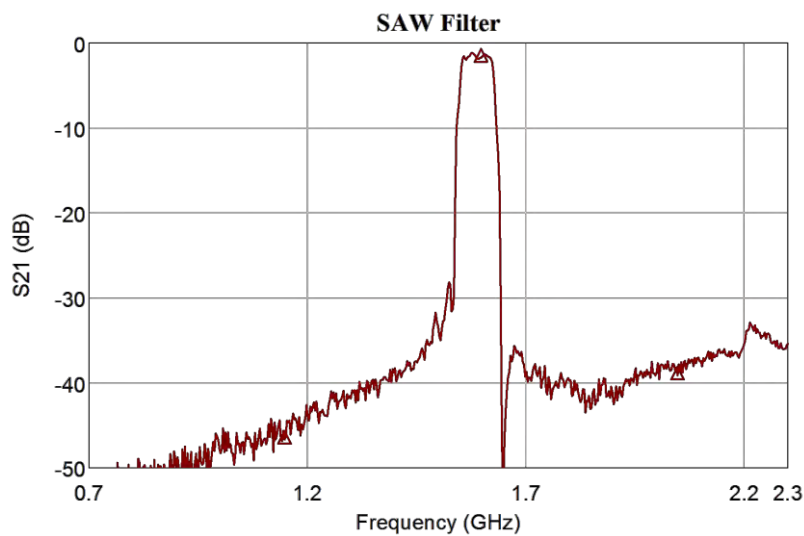


Figure 76 SAW Filter SF2385H from Murata manufacturing response.

The new S parameters will be obtained simulating the SAW filter effect to the Experiment 2 MN3 S parameters with the Microwave Office software.

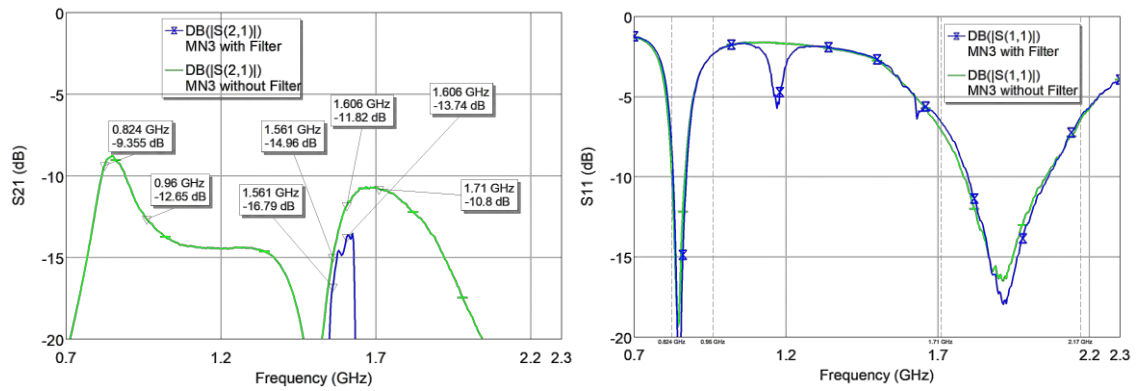


Figure 77 At left the coupling between GNSS port and LTE port without considering the filter (green) and considering the filter (blue). At right, the LTE S₁₁ without considering the filter (green) and considering the filter (blue).

So, once the new S parameters with the SAW filter effect is considered and the previous Radiation Efficiency calculated with the coupling effect considered, the Antenna Efficiency can be calculated with the formula seen before (70VI).

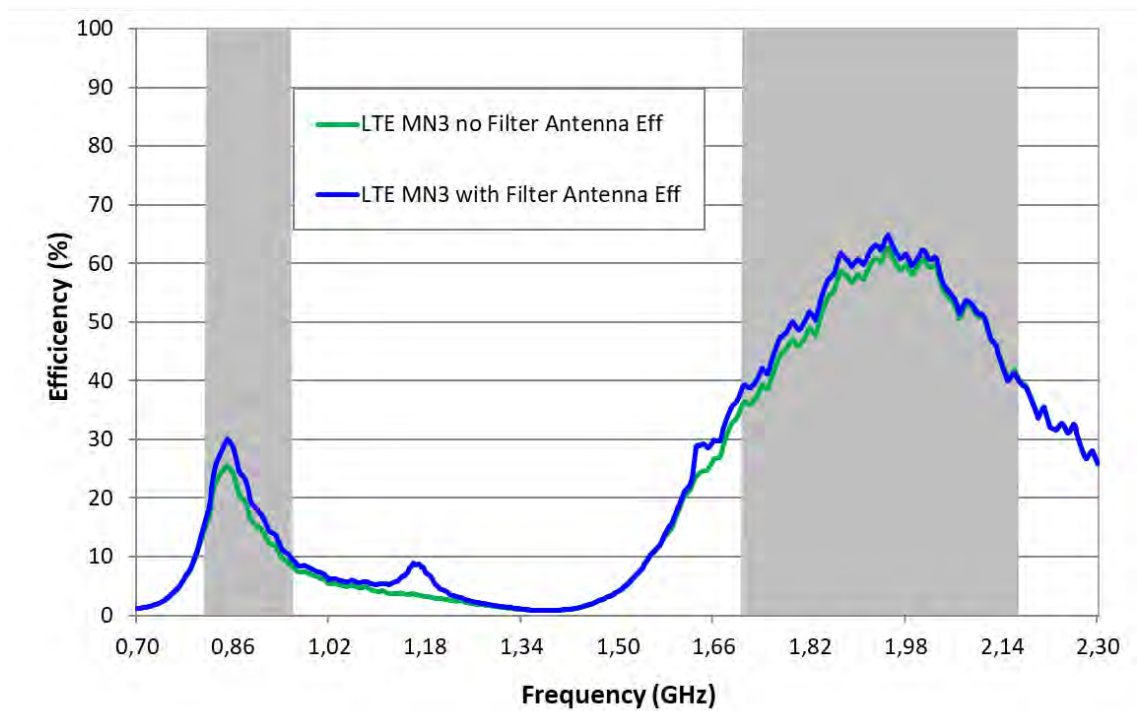


Figure 78 Antenna Efficiency Comparison between the Experiment 2 MN3 at LTE, considering the SAW filter and without considering the SAW filter.

To clearly determine the difference between both traces, see Table 46 shown below. The difference between both cases are slightly different, around a 3% better at the LFR and 2% better at HFR for the scenario including the filter. The values obtained from the MN3 without the filter are different to the previously shown at Table 43, due to the number of points used to calculate, first in the S parameters and then, in the Antenna and Radiation Efficiency are lower (to calculate the s₂₁ and S₁₁ in the Network Analyzer, the number of points must be reduce to 1/4 of the

original number of points). For this reason, the number of samples are lower and the average calculated is slightly different to the previous one.

LTE	ANTENNA EFFICIENCY (%)					
	824MHz	960MHz	Avg 824-960MHz	1710MHz	2170MHz	Avg 1710-2170MHz
MN3 – Without SAW Filter	15.7	8.6	17.1	36.0	40.8	51.4
MN3 – With SAW Filter	16.8	9.9	19.9	38.9	40.4	53.3

Table 46 Antenna Efficiency values for Experiment 2 MN3 without considering the SAW filter and MN3 considering the SAW filter at the LFR (824MHz-960MHz) and HFR (1710MHz-2170MHz) of the LTE band.

4.4 DUO mXTEND™ PROTOTYPE

Two prototypes using DUO mXTEND™ antenna have been designed, using a PCB with the same dimensions as the TRIO mXTEND™ Experiments, 69mm x 61mm, and two one antenna per application has been used. The Clearance Area for LTE antennas considered is 30mm x 11mm meanwhile the Clearance Area considered for GNSS antennas is 4mm x 7.5mm. The same bands are covered by the two experiments: LTE B1, B3, B4, B5, B8 (824MHz-960MHz and 1710MHz-2170MHz) and GNSS (1561MHz-1606MHz).

4.4.1 Experiment 3: 30 x 11mm² Clearance Area and vertical pads for LTE and 7.5x4mm Clearance Area for GNSS

In this Chapter it can be observed a solution working with two antennas, one DUO mXTEND™ placed at the top right corner for LTE band and another DUO mXTEND™ at the bottom center for GNSS band. The reason why the placement of the GNSS antenna is different to the LTE antenna or different to placement of the Experiments 1 and 3 antennas, is due to the working methodology is not the same.

Meanwhile all the antennas placed at the corner (this includes the TRIO mXTEND™ and the DUO mXTEND™) are working like a monopole, the DUO mXTEND™ is working like a slot antenna. That is the reason why as the more centered the antenna is the more performance will be achieved by the antenna.

For the LTE antenna the feeding line used has a dimension of 6mm x 9mm, and the GNSS antenna is directly connected to the matching network.

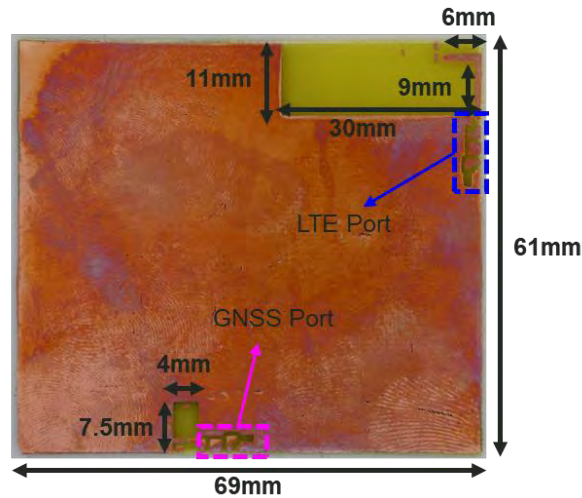


Figure 79 PCB in house used for Experiment 3. LTE port is placed at the top right corner and GNSS port is placed at the bottom middle.

The antenna booster DUO mXTEND™ has been soldered to the board using a hot gun like is explained in the methodology process (1.3 Methodology), but it is important to note that in comparison to the TRIO mXTEND™ the antenna requires more precision to be soldered on the board or the antenna performance could change a lot.

In order to tune the interest bands at the minimum Reflection Coefficient possible, it has been measured the antenna 0 ohms response in each port.

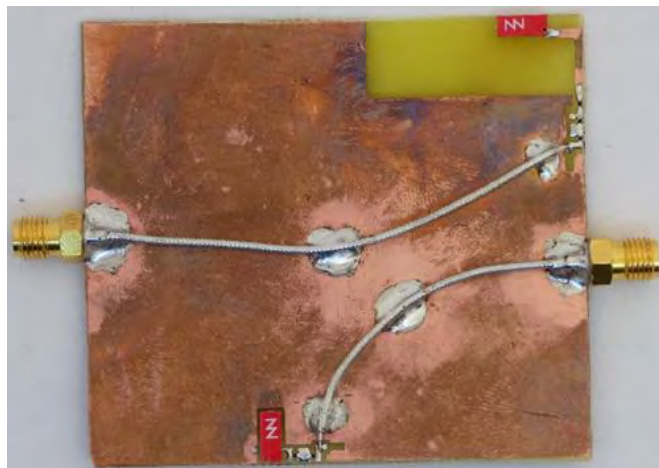


Figure 80 PCB in house used for Experiment 3, with the DUO mXTEND™ antenna booster (7mm x 3mm x 1mm) and 0 ohms matching network connected to the SMA connectors [23].

As it is shown in Figure 81, the 0 ohms antenna response has changed in comparison to the 0 ohms antenna response from Experiment 1 and 2, in both bands. At GNSS band the change is

more notorious due the working methodology is totally different. As it can be seen at Figure 56 and Figure 68, the trace described in the GNSS band is capacitive, as well as the LTE band, but for the Experiment 3 GNSS 0 ohms response, the trace described is inductive.

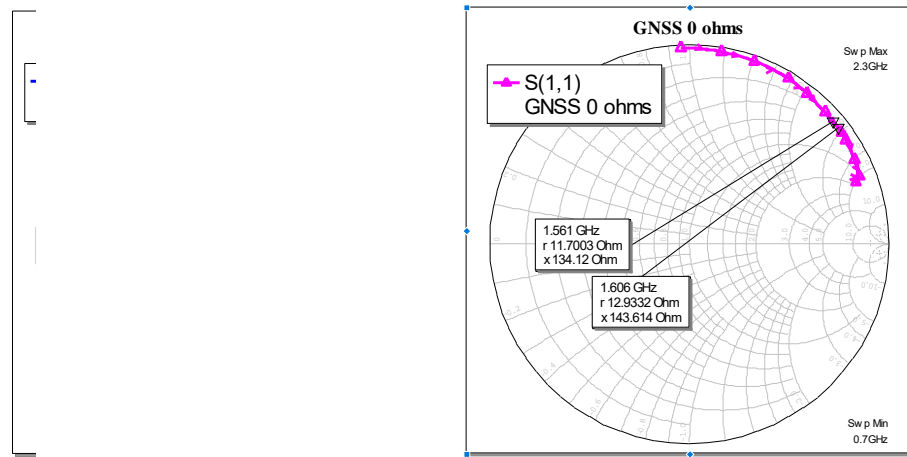


Figure 81 0 ohms antenna response measured in the Network Analyzed and the phase corrected for Experiment 3. At the left it is shown LTE port, at right GNSS port.

This is caused by the slot behavior, as smaller is the loop formed by the slot, more similar to a short circuit is going to be the antenna response. On the other hand, as bigger is the loop formed by the slot, is going to be like an open circuit.

The LTE difference between the TRIO mXTEND™ 0 ohms response and the DUO mXTEND™ 0 ohms response, is caused by the fact that the first antenna acts like a bigger monopole than the second one. This can be observed in the lower bands which are close to the open circuit Smith Chart.

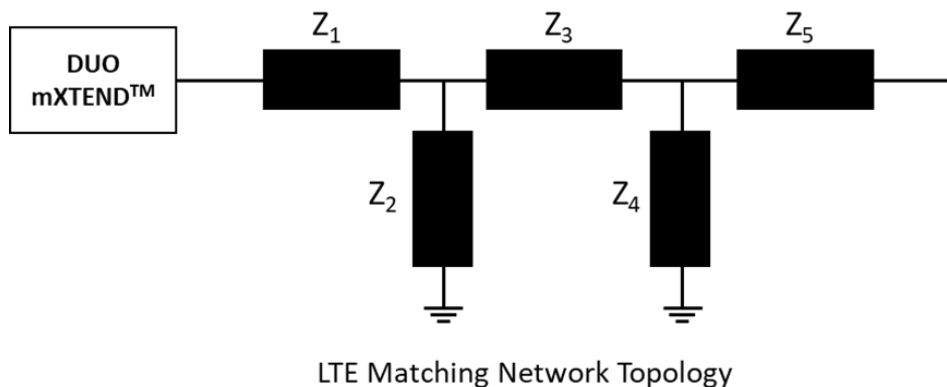


Figure 82 Matching network topology for Experiment 3 at LTE band

One matching network has been tested for LTE band, changing the matching network topology in comparison to the Experiment 1 and 2. It has been measured the Reflection Coefficient and the Antenna and Radiation Efficiency:

MN	Component	Value	Part Number
MN1	Z1	24nH	LQW15AN24NG80
	Z2	16nH	LQW15AN16NG80
	Z3	0.9pF	GJM1555C1HR90WB01
	Z4	1.5pF	GJM1555C1H1R5WB01
	Z5	0Ω Resistor	-

Table 47 Build of materials (BoM) used to obtain MN1 for Experiment 3 at LTE band

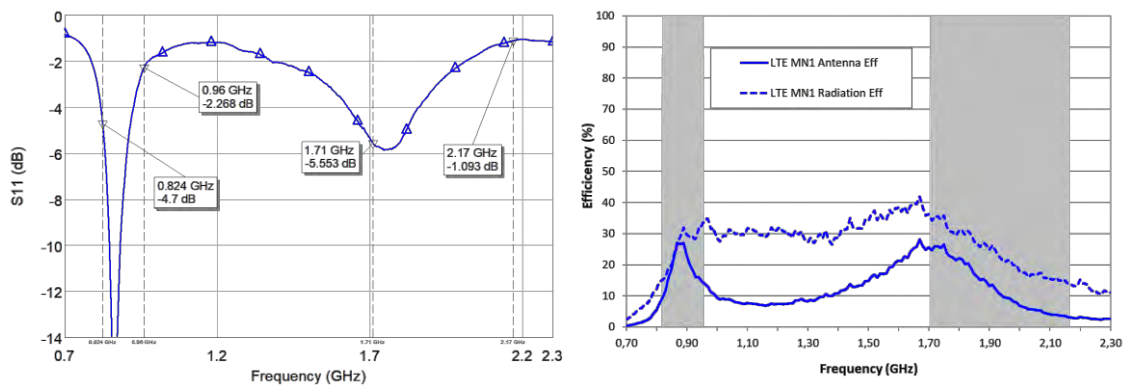


Figure 83 S₁₁ at left and Antenna and Radiation Efficiency at right, for Experiment 3 MN1 at LTE band.

LTE	ANTENNA EFFICIENCY (%)					
	824MHz	960MHz	Avg 824-960MHz	1710MHz	2170MHz	Avg 1710-2170MHz
MN1	9.2	14.3	19.3	25.2	3.1	12.8

Table 48 Antenna Efficiency values for Experiment 3 at the LFR (824MHz-960MHz) and HFR (1710MHz-2170MHz) of the LTE band.

As it is shown in Figure 83, it has been prioritized the lower band in front of the higher band in the tuning of the matching network due to the difficulty the tune both bands at the same time. The values for the lower band are comparable to the values obtained in Experiment 1 and 2, but when is compared to the higher, the values of Experiment 3 are much lowers, specially at 2170MHz.

On the other hand, for GNSS band, two scenarios have been designed. First, the original design seen in Figure 80 named as Scenario 1, and another design changing the coaxial cable location, named as Scenario 2 (see Figure 84). Ideally the difference between both designs

should be zero, but as a consequence of how the slot propagates the fields through the pcb, the first design presents a lot of losses. So, a comparison between both scenarios has been done in order to observe the importance of the introduced losses in the device.

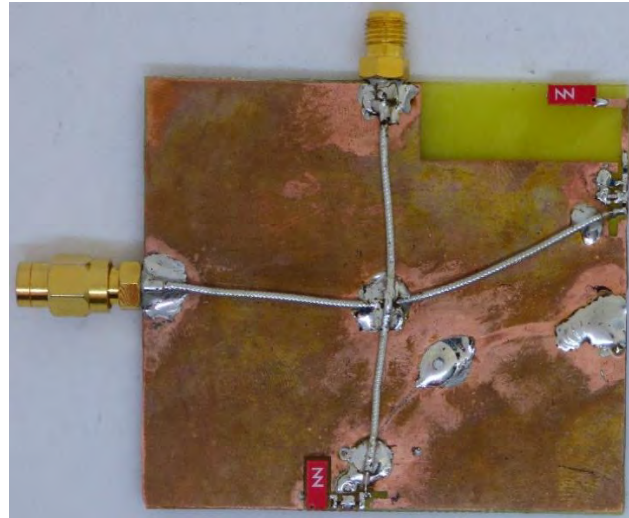


Figure 84 PCB in house used for Experiment 3, with the DUO mXTEND™ antenna booster (7mm x 3mm x 1mm) and 0 ohms matching network connected to the SMA connectors with a vertical cable location.

One Matching network has been tested for Scenario 1 and another Matching network has been tested for Scenario 2. Both scenarios share the same matching network topology:

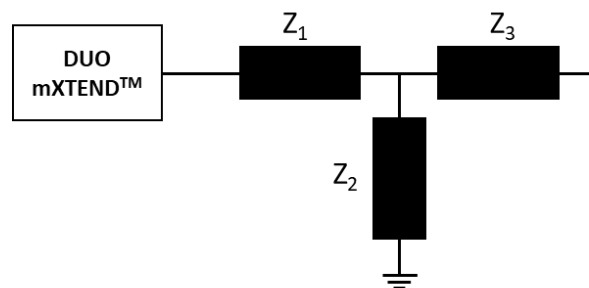


Figure 85 Matching network topology for Experiment 3 at GNSS band

Design	MN	Component	Value	Part Number
Scenario 1	MN1	Z1	1.0pF	GJM1555C1H1R0WB01
		Z2	4.9pF	GJM1555C1H4R9WB01
		Z3	0Ω Resistor	-

Table 49 Build of materials (BoM) used to obtain MN1 in Scenario 1 for Experiment 3 at GNSS band

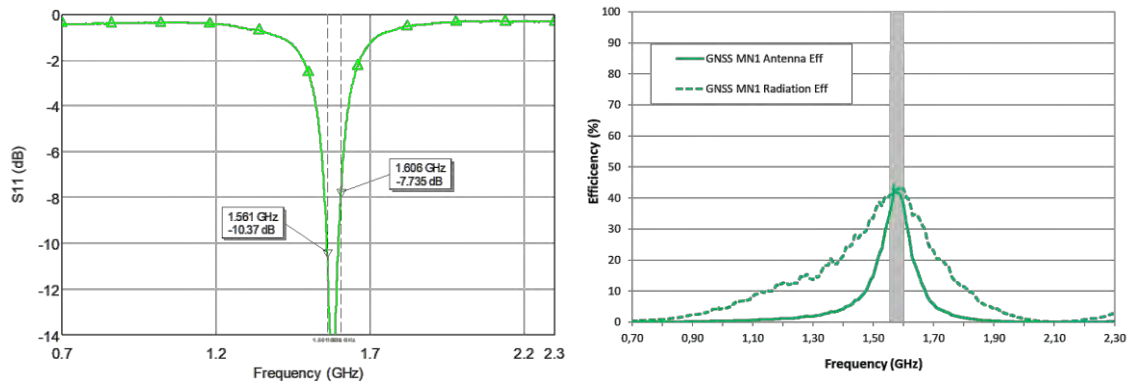


Figure 86 S_{11} at left and Antenna and Radiation Efficiency at right, for Experiment 3 MN1 in Scenario 1 at GNSS band.

Design	MN	Component	Value	Part Number
Scenario 2	MN2	Z1	1.2pF	GJM1555C1H1R2WB01
		Z2	3.8pF	GJM1555C1H3R8WB01
		Z3	0Ω Resistor	-

Table 50 Build of materials (BoM) used to obtain MN2 in Scenario 2 for Experiment 3 at GNSS band

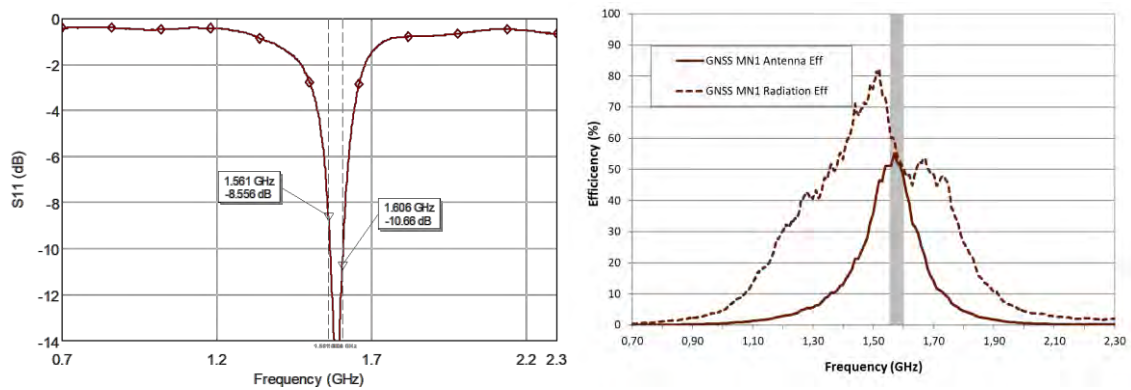


Figure 87 S_{11} at left and Antenna and Radiation Efficiency at right, for Experiment 3 MN2 in Scenario 2 at GNSS band.

To see clearly which performance will be better, it is important to do a comparison in Reflection Coefficient (see Figure 88) and Antenna Efficiency (see in Figure 89) between the two performances obtained.

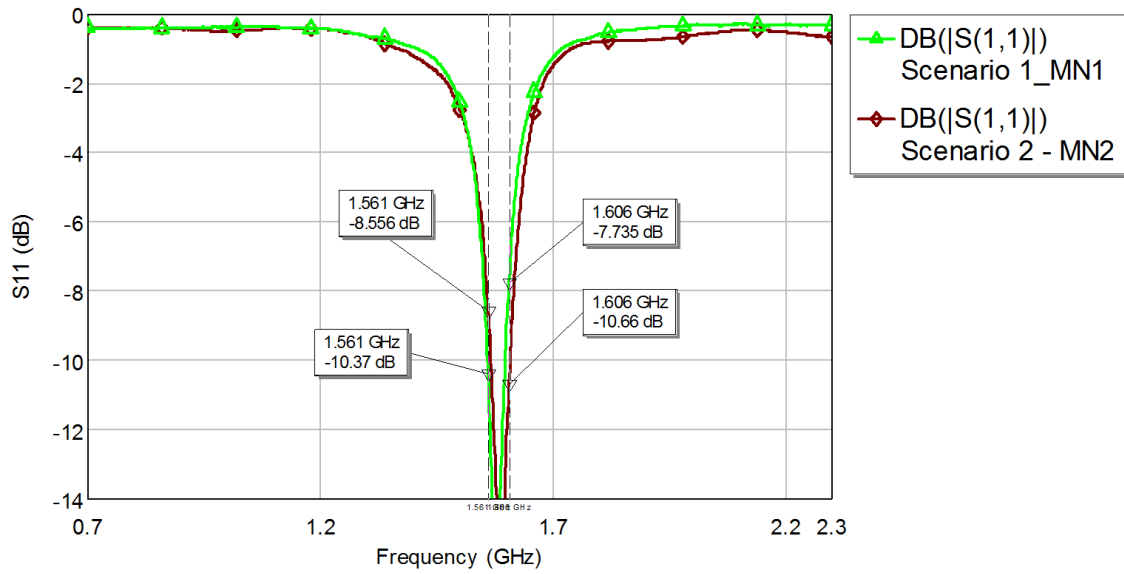


Figure 88 S parameters comparison between the two scenarios matching networks for Experiment 3 at GNSS band.

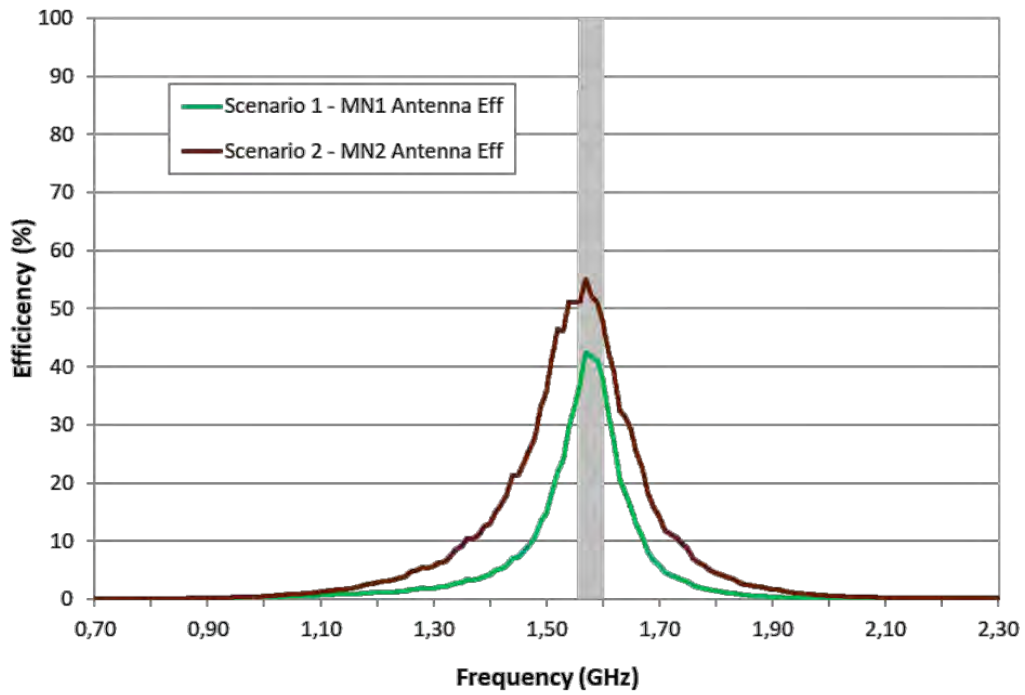


Figure 89 Antenna Efficiency comparison between the two scenarios matching networks for Experiment 3 at GNSS band.

GNSS	ANTENNA EFFICIENCY (%)		
	1561MHz	1575MHz	Avg 1598-1606MHz
Scenario 1 - MN1	35.5	42.5	38.9
Scenario 2 - MN2	51.2	55.2	48.8

Table 51 Antenna Efficiency values for both scenarios of Experiment 3 at 1561MHz (BeiDou E1 band), 1575 MHz (GPS L1 band) and from 1598 MHz to 1606 MHz (GLONASS L1 band).

As it can be seen in Table 51, between both scenarios there is a big difference in antenna efficiency values when Figure 88 shows a Reflection coefficient between both scenarios very similar. The matching network number of components is also the same and between components, do not exist a big difference between quality values. Considering the set-up analyzed for both cases are completely the same and the only change between scenarios is the coaxial cable position, is clear that the Scenario 1 presents a lot of losses for the cable position.

It is important to note the SMA connector and the coaxial cable are only a support to measure as precise as it can be possible the antenna performance. So, the losses seen in the change of the coaxial cable (Figure 80 and Figure 84) will disappear in a theoretical real case where the matching network is directly connected to the RF module.

4.4.2 Experiment 4: 30 x 11mm² Clearance Area and horizontal pads for LTE and 7.5x4mm Clearance Area for GNSS

In this Chapter it can be observed a solution working with two antennas, one DUO mXTEND™ placed at the top right corner for LTE band and another DUO mXTEND™ at the bottom center for GNSS band.

There are two design changes respect Experiment 2 set-up. The first design change is the LTE pads orientation which now are horizontally placed, and the other design change is the pads dimensions which now all the pads measures 2mm x 2mm like Experiment 1 and 2. It was observed some components (0603 metric) were not able to be soldered in the previous Experiment 3 pads (1mm x 1mm) and a solution with worse Q components was done. So, in order to maximize the antennas efficiencies, the recommended 2mm x 2mm pads dimensions has been made for both bands.

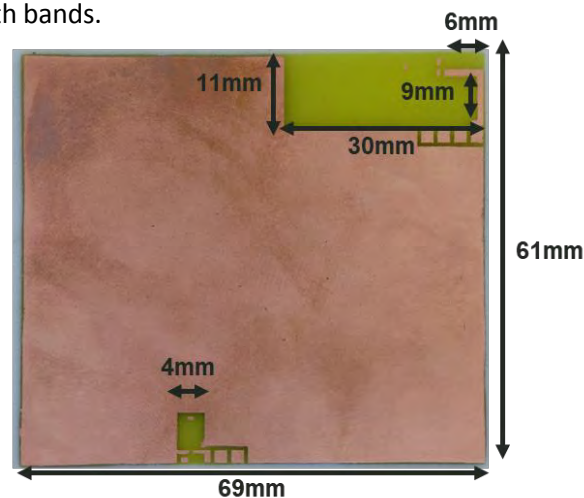


Figure 90 PCB in house used for Experiment 4. LTE port is placed at the top right corner and GNSS port is placed at the bottom middle.

As it is shown in Figure 91, the 0 ohms antenna response has changed a little bit in comparison to the 0 ohms antenna response from Experiment 3 (see Figure 81), in both bands. The changes in the 0 ohms response at LTE band is notorious than at GNSS because the pads orientation has changed, but the fact the pads now are higher than Experiment 3 pads, means an inductive effect is bigger due to the pads row act like a little transmission line, the more pads, more effect it will be seen.

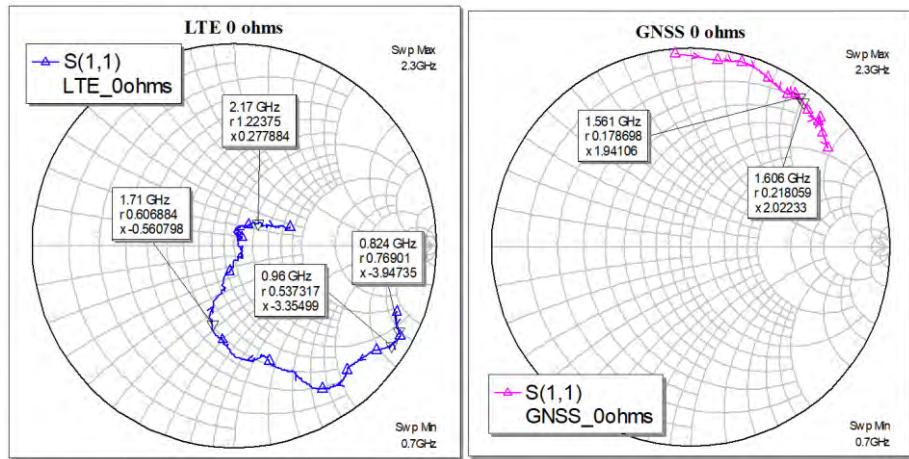


Figure 91 0 ohms antenna response measured in the Network Analyzed and the phase corrected for Experiment 4. At the left it is shown LTE port, at right GNSS port.

Three matching networks have been tested for LTE band, considering the same matching network topology for each band (the same as Experiment 1 and Experiment 2, see Figure 58). For every matching network obtained, it has been measured the Reflection Coefficient and the Antenna and Radiation Efficiency:

MN	Component	Value	Part Number
MN1	Z1	0Ω Resistor	-
	Z2	18nH	LQW18AN18NG10
	Z3	0.6pF	GJM1555C1HR60WB01
	Z4	12nH	LQW18AN12NG10
	Z5	1.0pF	GJM1555C1H1R0WB01
	Z6	7.5nH	LQW15AN7N5G80
	Z7	0Ω Resistor	-

Table 52 Build of materials (BoM) used to obtain MN1 for Experiment 4 at LTE band

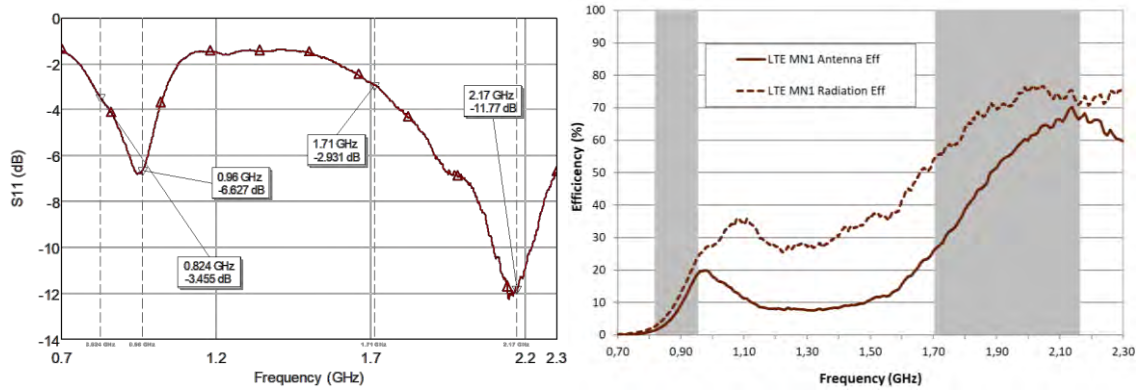


Figure 92 S_{11} at left and Antenna and Radiation Efficiency at right, for Experiment 4 MN1 at LTE band.

MN	Component	Value	Part Number
MN2	Z1	0Ω Resistor	-
	Z2	18nH	LQW18AN18NG10
	Z3	0.75pF	GJM1555C1HR75WB01
	Z4	2.3pF	GJM1555C1H2R3WB01
	Z5	0Ω Resistor	-
	Z6	6.0nH	LQW18AN6NG80
	Z7	0Ω Resistor	-

Table 53 Build of materials (BoM) used to obtain MN2 for Experiment 4 at LTE band

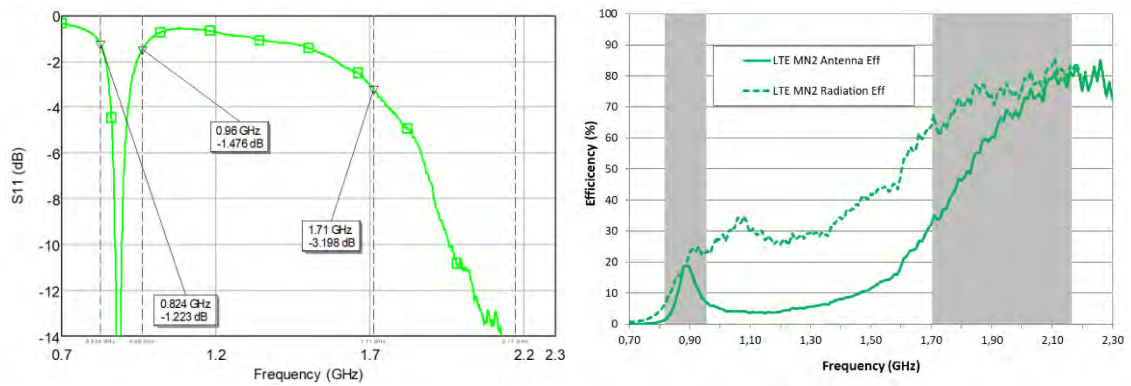


Figure 93 S_{11} at left and Antenna and Radiation Efficiency at right, for Experiment 4 MN2 at LTE band.

MN	Component	Value	Part Number
MN3	Z1	0Ω Resistor	-
	Z2	18nH	LQW18AN18NG10
	Z3	0.75pF	GJM1555C1HR75WB01
	Z4	2.3pF	GJM1555C1H2R3WB01
	Z5	0Ω Resistor	-
	Z6	6.0nH	LQW18AN6NG80
	Z7	3.0pF	GJM1555C1H3R0WB01

Table 54 Build of materials (BoM) used to obtain MN3 for Experiment 4 at LTE band

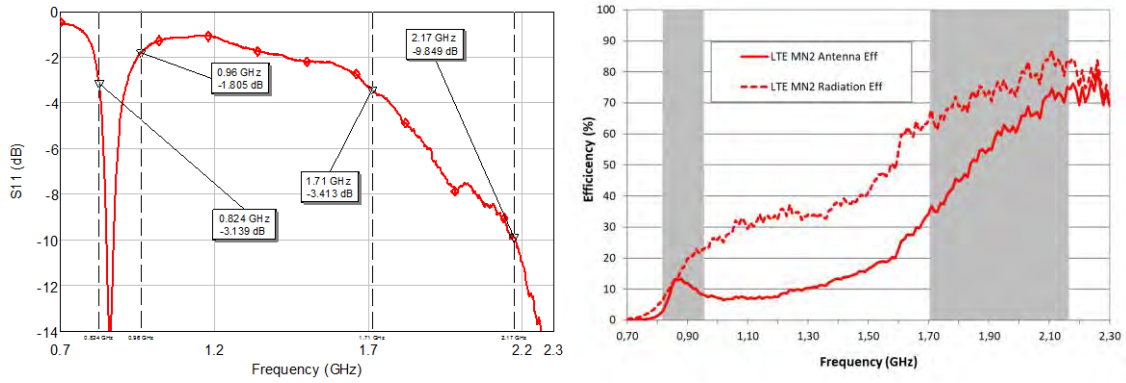


Figure 94 S_{11} at left and Antenna and Radiation Efficiency at right, for Experiment 4 MN3 at LTE band.

To clearly determinate which performance will be better, it is important to do a comparison in Reflection Coefficient (see Figure 95) and Antenna Efficiency (see in Figure 96) between all the performances obtained.

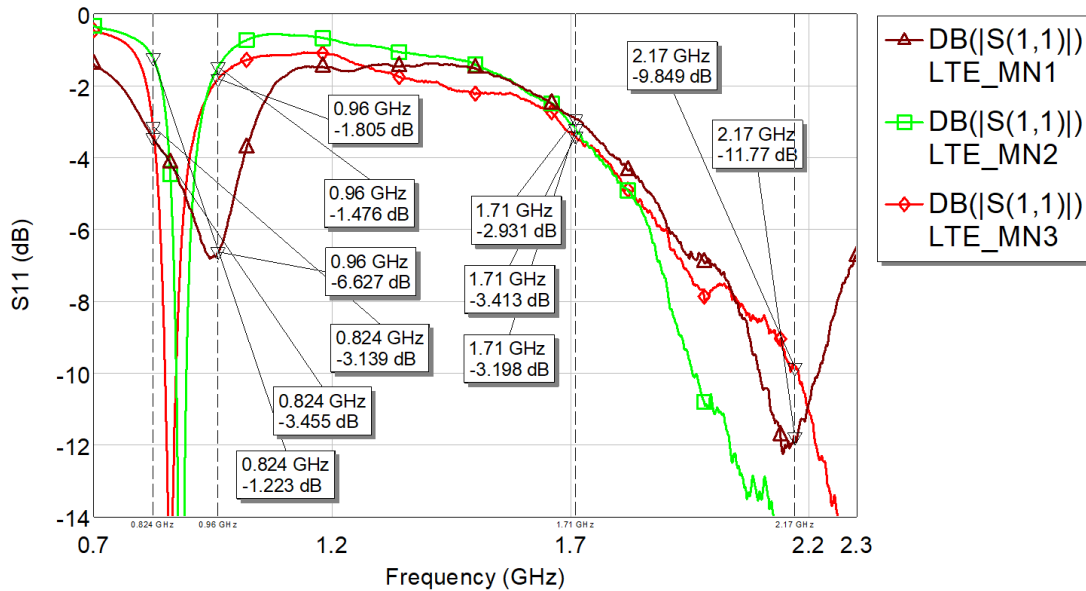


Figure 95 S parameters comparison between all the matching networks for Experiment 4 at LTE band.

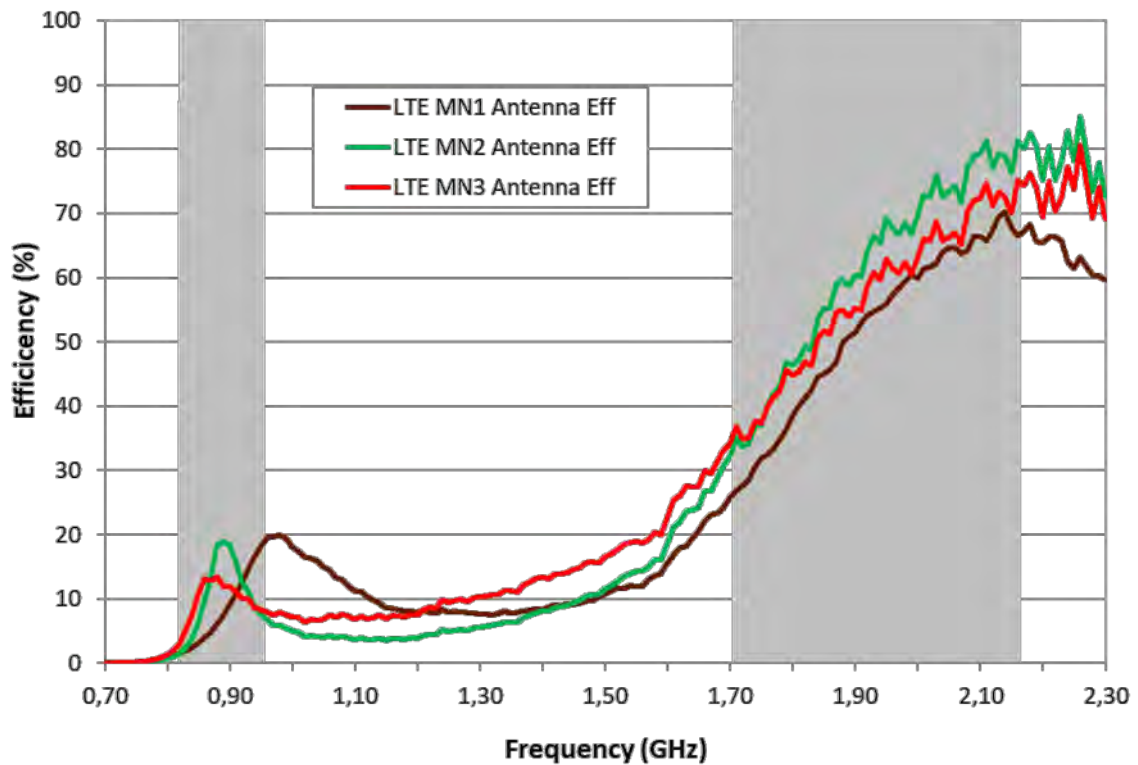


Figure 96 Antenna Efficiency comparison between all the matching networks for Experiment 4 at LTE band.

LTE	ANTENNA EFFICIENCY (%)					
	824MHz	960MHz	Avg 824-960MHz	1710MHz	2170MHz	Avg 1710-2170MHz
MN1	1.4	18.9	8.3	26.3	66.9	52.0
MN2	1.4	7.2	10.8	33.6	80.7	61.5
MN3	2.9	8.1	10.0	35.5	74.7	57.1

Table 55 Antenna Efficiency values for Experiment 4 at the LFR (824MHz-960MHz) and HFR (1710MHz-2170MHz) of the LTE band.

As it can be seen in Table 55 the three matching networks tested have a very good performance in the higher band (1710MHz-2170MHz), although in the 1710MHz frequency the performance is lower than the average efficiency at the band. For the lower band, the average efficiency is very low in comparison to all the other experiments done, overload the 824MHz frequency were the efficiency obtained is a very low value. In MN3 it has been prioritized the Uplink frequencies for B5 (824MHz-849MHz) but the values obtained remain too low.

On the other hand, for GNSS band two matching networks have been tested with the Scenario 2 set-up shown at Figure 84 and the same matching network topology as Experiment 3 seen in Figure 85.

MN	Component	Value	Part Number
MN1	Z1	1.2pF	GJM1555C1H1R2WB01
	Z2	3.8pF	GJM1555C1H3R8WB01
	Z3	0Ω Resistor	-

Table 56 Build of materials (BoM) used to obtain MN1 for Experiment 4 at GNSS band

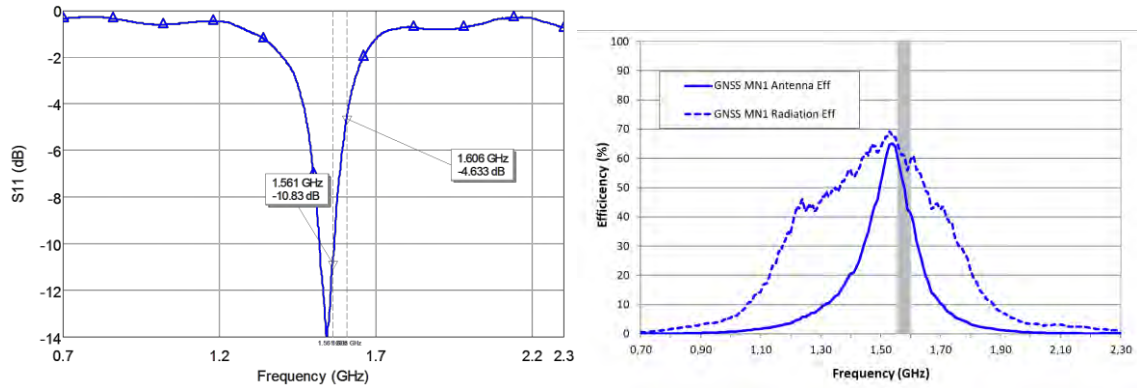


Figure 97 S_{11} at left and Antenna and Radiation Efficiency at right, for Experiment 4 MN1 at GNSS band.

MN	Component	Value	Part Number
MN2	Z1	1.2pF	GJM1555C1H1R2WB01
	Z2	3.6pF	GJM1555C1H3R6WB01
	Z3	0Ω Resistor	-

Table 57 Build of materials (BoM) used to obtain MN2 for Experiment 4 at GNSS band

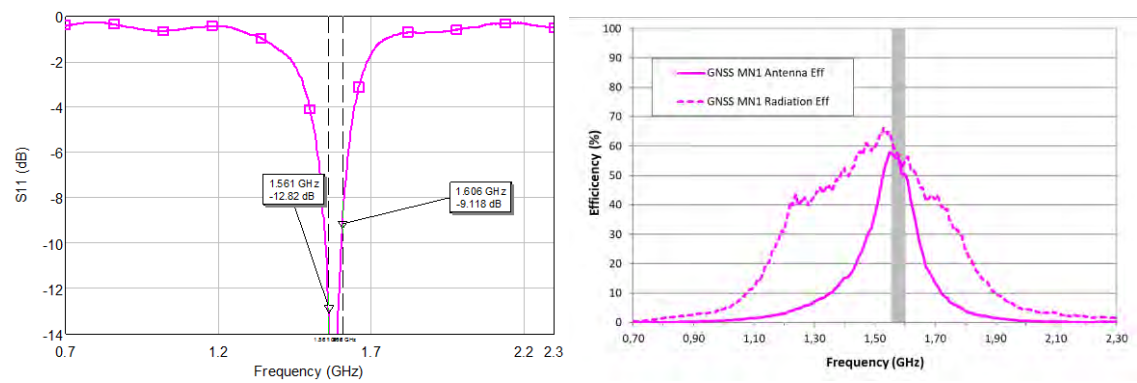


Figure 98 S_{11} at left and Antenna and Radiation Efficiency at right, for Experiment 4 MN2 at GNSS band.

To see clearly which performance will be better, it is important to do a comparison in Reflection Coefficient (see Figure 99) and Antenna Efficiency (see in Figure 100Figure 96) between all the performances obtained.

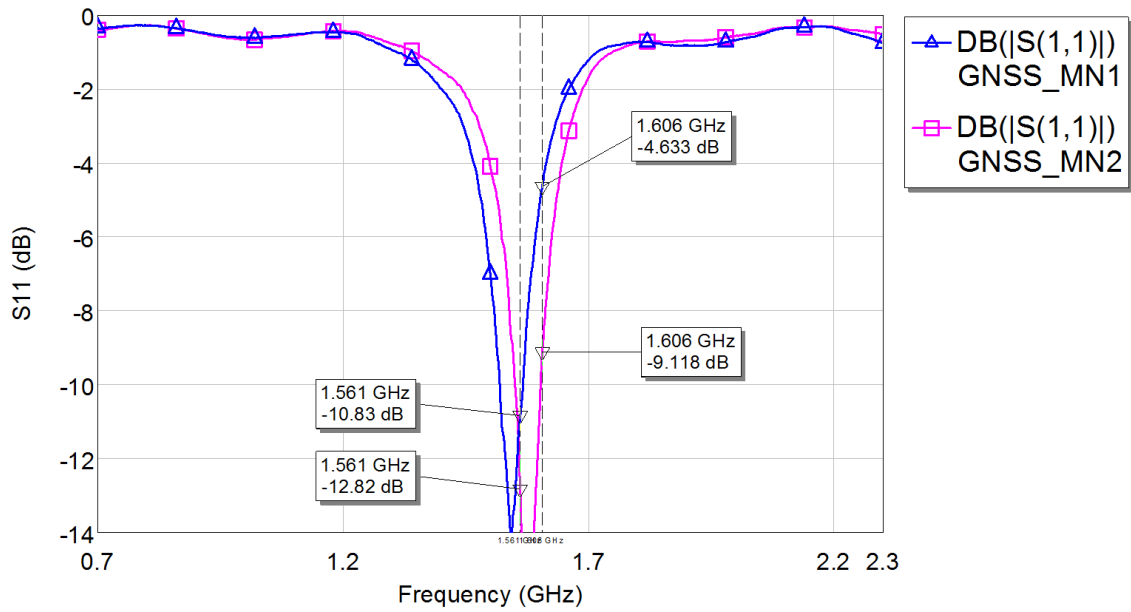


Figure 99 S parameters comparison between all the matching networks for Experiment 4 at GNSS band.

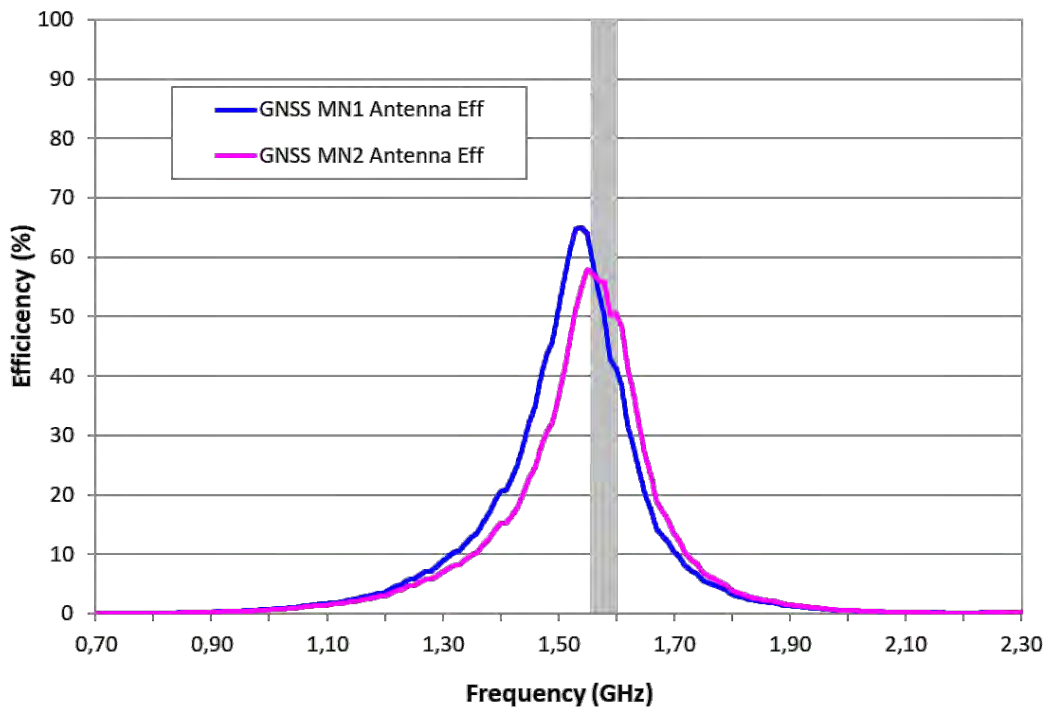


Figure 100 Antenna Efficiency comparison between all the matching networks for Experiment 4 at GNSS band.

GNSS	ANTENNA EFFICIENCY (%)		
	1561MHz	1575MHz	Avg 1598-1606MHz
MN1	61.0	54.0	41.7
MN2	57.5	56.1	50.5

Table 58 Antenna Efficiency values for both scenarios of Experiment 4 at 1561MHz (BeiDou E1 band), 1575 MHz (GPS L1 band) and from 1598 MHz to 1606 MHz (GLONASS L1 band).

Both matching networks designs have good performance at GNSS band (>40% in both cases), but MN1 has the response shifted to the left making the performance at GLONASS (1561MHz-1606MHz) much lower than the obtained in MN2. On the other hand, at BeiDou band (1561MHz) is higher in MN1 but the difference between both matching networks is not so big as in GLONASS band.

4.4 COMPARISON BETWEEN EXPERIMENTS

To know which Experiment and which matching network it has been the one embedded in the mangOH™ RED device, a comparison between experiments has been done. So, first of all, for every Experiment it has been selected the best matching network considering the performance achieved. For Experiment 1 and Experiment 2, there is only one matching network for each Experiment at GNSS application.

In LTE application, due to the good results achieved at the high band in almost every experiment, the lower band is the most critical band. So, a further comparison between the matching networks at the low band (824MHz-960MHz) has been done analyzing the efficiency values at the Uplink bands and Downlink bands for B5 and B8. As already it has been said, is important to prioritize the Uplink, so the objective is to select the matching network with the better efficiency values at the two Uplink bands.

ANTENNA EFFICIENCY (%)				
LTE	B5 Uplink (824-849 MHz)	B5 Downlink (869-894 MHz)	B8 Uplink (880-915 MHz)	B8 Downlink (925-960 MHz)
MN1	11,85	28,22	35,41	37,29
MN2	15,75	25,85	26,05	19,06
MN3	23,10	22,03	19,69	13,84

Table 59 Antenna Efficiency values for Experiment 1 at LTE lower band (824MHz-960MHz)

For Experiment 1, the matching network 3 has the better result for the lower band due to both Uplink bands have the better efficiency values. Furthermore, as it can be seen in Figure 64, the LTE higher band performance is also good (48.1% average efficiency).

ANTENNA EFFICIENCY (%)				
LTE	B5 Uplink (824-849 MHz)	B5 Downlink (869-894 MHz)	B8 Uplink (880-915 MHz)	B8 Downlink (925-960 MHz)
MN1	14,80	23,77	26,95	26,38
MN2	15,10	15,23	15,02	13,95
MN3	21,95	19,70	16,71	10,62
MN4	14,59	12,23	9,65	5,36

Table 60 Antenna Efficiency values for Experiment 2 at LTE lower band (824MHz-960MHz)

For Experiment 2, the matching network 3 has the better result for the lower band due to both Uplink bands have the better efficiency values. On the other hand, as it can be seen in Figure 74, the LTE higher band performance is the best between all the matching networks working with the TRIO mXTEND™ antenna (51.4% average efficiency).

Then, regarding Experiments 3 and Experiments 4, apart from LTE, the GNSS matching networks must be compared too.

ANTENNA EFFICIENCY (%)				
LTE	B5 Uplink (824-849 MHz)	B5 Downlink (869-894 MHz)	B8 Uplink (880-915 MHz)	B8 Downlink (925-960 MHz)
MN1	12,88	26,55	24,90	16,00

Table 61 Antenna Efficiency values for Experiment 3 at LTE lower band (824MHz-960MHz)

For Experiment 3 at LTE band, only one matching network has been done. The results achieved at the lower band are very good but it is important to note the LTE higher band (1710MHz-2170MHz) has a bad performance as it is shown in Figure 83 (12.8% average efficiency). As far as GNSS, as it is shown in Figure 89, matching network 2 has better efficiency values (51.7% average efficiency).

ANTENNA EFFICIENCY (%)				
LTE	B5 Uplink (824-849 MHz)	B5 Downlink (869-894 MHz)	B8 Uplink (880-915 MHz)	B8 Downlink (925-960 MHz)
MN1	2,05	5,63	7,86	15,86
MN2	2,88	15,84	17,99	9,74
MN3	5,76	12,96	12,26	9,18

Table 62 Antenna Efficiency values for Experiment 4 at LTE lower band (824MHz-960MHz)

For Experiment 4, the matching network 3 has the better result for the lower band due to both Uplink bands have the better efficiency values. On the other hand, as it can be seen in Figure 96, the LTE higher band performance very also good (57.1% average efficiency). Regarding the GNSS band, as it can be seen in Figure 100, matching network 1 is a shifted to the left in comparison to matching network 2, so in BeiDou (1561MHz) matching network 1 has better efficiency meanwhile matching network 2 has better efficiency values for GPS (1575MHz) and GLONASS (1598MHz-1606MHz). Matching network 2 has a better average efficiency at GNSS band (54.1%).

Once one matching network for each application has been selected for every Experiment, a comparison between the four Experiments has been done for LTE and GNSS.

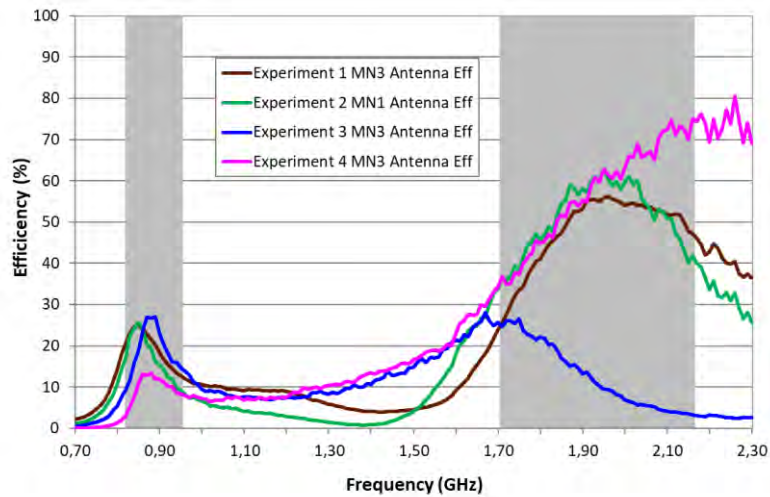


Figure 101 Antenna Efficiency comparison between the matching networks chosen for each Experiment at LTE.

ANTENNA EFFICIENCY (%)						
LTE	824MHz	960MHz	Avg 824-960MHz	1710MHz	2170MHz	Avg 1710-2170MHz
Exp1	20.3	12.4	19.4	24.7	46.6	48.1
Exp2	16.9	8.7	17.3	35.1	40.9	51.4
Exp3	9.2	14.3	19.3	25.2	3.1	12.8
Exp4	2.9	8.1	10.0	35.5	74.7	57.1

Table 63 Antenna efficiency values for the four Experiments matching networks chosen for LTE

Regarding the performance at LTE, Experiment 1 has the better efficiency values at the lower band, especially at 824MHz and has a good performance at the LTE higher band. On the other hand, Experiment 4 has the better efficiency values at high band but has a low performance at the lower band in comparison to the other Experiments.

The difference at the lower band between the TRIO mXTEND™ and the DUO mXTEND™ is notorious, in particular at the 824MHz frequency which is understandable if the electrical size between antennas is compared.

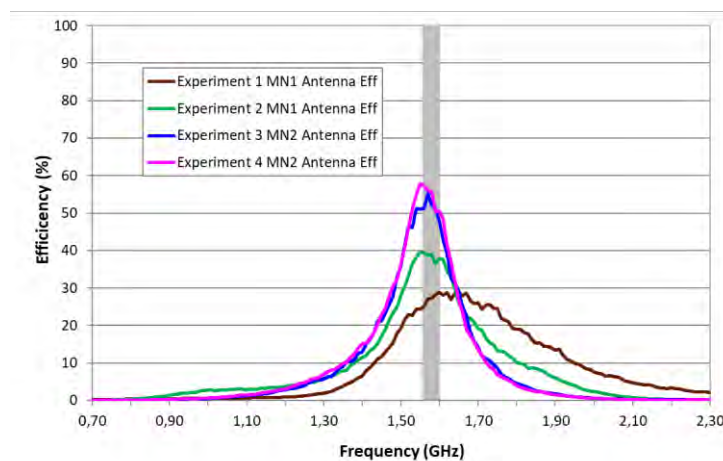


Figure 102 Antenna Efficiency comparison between the matching networks chosen for each Experiment at GNSS.

GNSS	ANTENNA EFFICIENCY (%)		
	1561MHz	1575MHz	Avg 1598-1606MHz
Exp1	24.7	27.1	28.6
Exp2	39.5	38.7	37.4
Exp3	51.2	55.2	48.8
Exp4	57.5	56.1	50.5

Table 64 Antenna efficiency values for the four Experiments matching networks chosen for GNSS

On the other hand, for GNSS band the DUO mXTEND™ Experiments have better performance than the TRIO mXTEND™. It is important to note, the Experiment 1 and Experiment 2 only use a single antenna for both bands meanwhile Experiment 3 and Experiment 4 use two antennas, one per application.

Comparing the two TRIO mXTEND™ Experiments 1 and 2, Experiment 2 has clearly a better efficiency at GNSS band.

As a conclusion, the Experiment selected to be embedded on the mangOH™ RED device has been the Experiment 2 which has a very good performance at all the LTE bands and a good GNSS performance, furthermore, is the most compact solution as far as surface occupied which is very important in order to maintain the original device as much as can be done.

4.5 EMBEDDING THE SOLUTION IN THE mangOH™ RED

Experiment 2 it has been, finally, the Experiment chosen for be embedded into mangOH™ RED. In order to embed the TRIO mXTEND™ into the mangOH™ RED an additional Experiment 2 PCB in house has been done. The objective is to change the minimum the original device in order to do the most accurate possible measure, so the first step is to remove the RF Module and the RF components on the board where the coaxial cables and the SMA connectors has been placed.

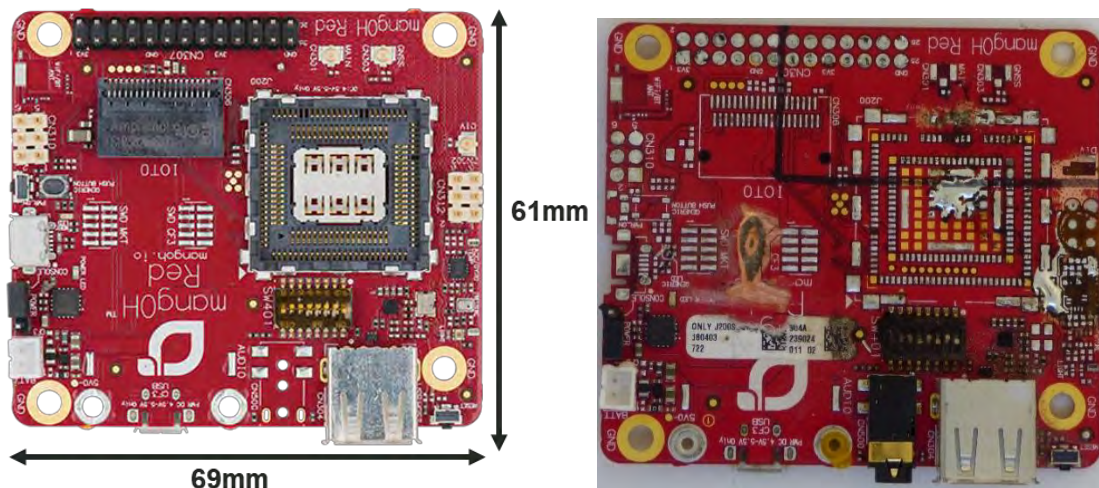


Figure 103 At left the original mangOH™ RED device, at right the mangOH™ RED after remove all the necessary components to locate the connectors and with the TRIO mXTEND™ surface necessary marked.

As it is shown in Figure 103, the surface area marked is the one that it has been removed in order to embed to Experiment 2 into the device. In this area is included the necessary space to place all the Clearance Area antenna, due to the mangOH™ RED device does not have this Clearance Area considered, the matching network pads, and a piece of Experiment 2 ground plane area to make connectivity between both ground planes.

To ensure the stability of the additional board added to the original device and ensure the connectivity between ground plane areas, it has been used a sticky copper strip on the top layer and American tape on the bottom layer. Then, once the additional PCB it has been added, the coaxial cables and the SMA connectors it has been placed on a similar position as the Experiment 2 ones, to simulate the most similar set-up.

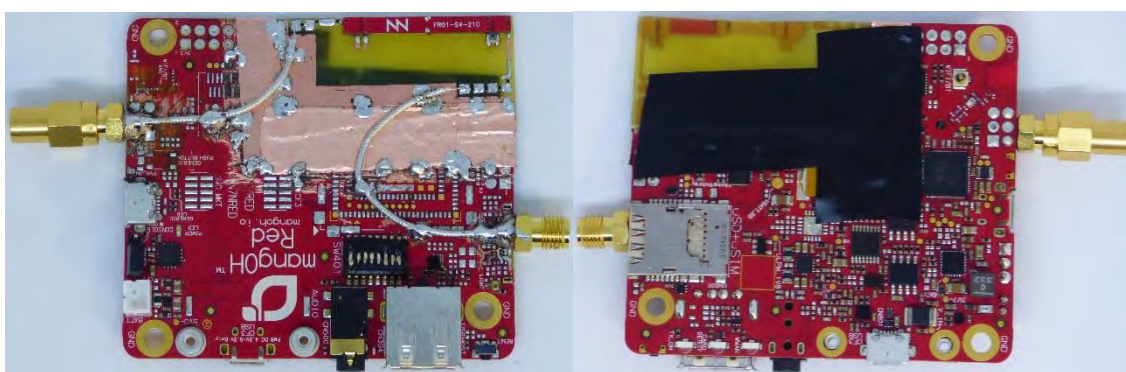


Figure 104 mangOH™ RED device with the Experiment 2 additional PCB embedded. At left the top view with a sticky copper strip to ensure the connectivity and the stability, and at right the bottom view with an American tape to ensure the stability of the additional PCB.

As it is shown in Figure 105, the 0 ohms antenna response has changed in comparison to the 0 ohms antenna response from Experiment 1, in both bands (see Figure 68). Usually exist a difference between the PCB in house scenario and the final device due to the ground plane area of the device could not be totally continuous, the components on the top and bottom layer affect to the antenna performance, and the ground plane connection could not be as precise as it would like to be.

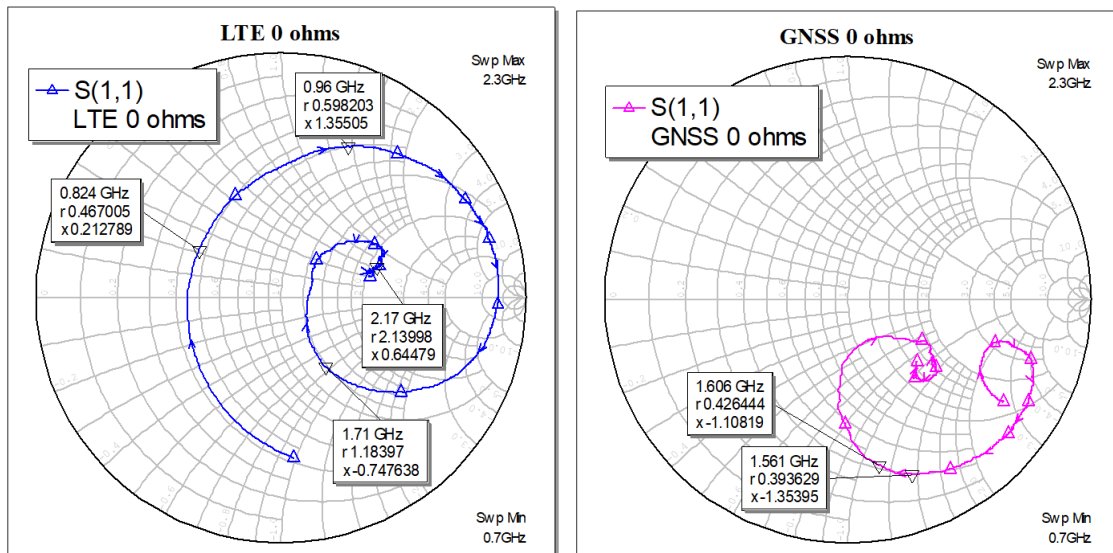


Figure 105 0 ohms antenna response measured in the Network Analyzed and the phase corrected the mangOH™RED device with the Experiment 2 embedded. At the left it is shown LTE port, at right GNSS port.

So, the final step is to tune the matching network as it has been done in Experiment 2. One matching network for LTE Section A (Figure 57), and another one for GNSS have been tested, with the same matching network topologies as Experiment 2 (see Figure 58 for LTE and Figure 65 for GNSS) and the same matching network components as matching network 3 for LTE (see Table 41) and the same matching network components as matching network 1 for GNSS (see Table 45).

For both matching networks, it has been measured the Reflection Coefficient and the Antenna and Radiation Efficiency:

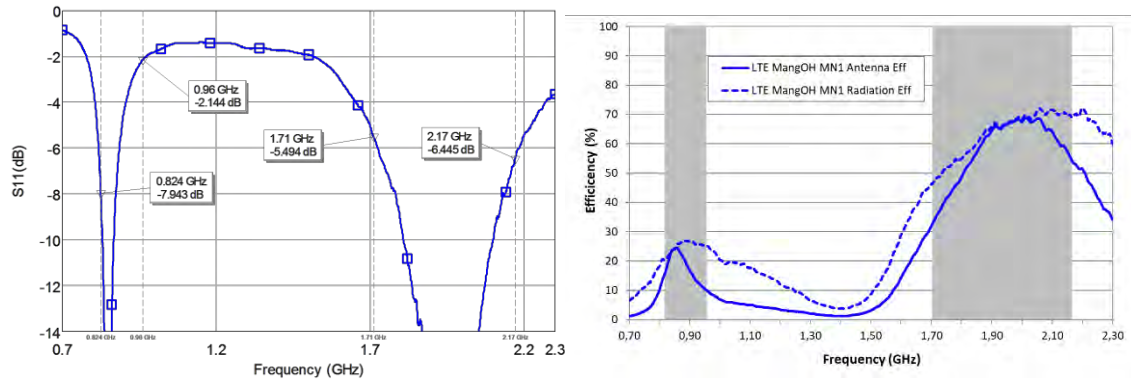


Figure 106 S_{11} at left and Antenna and Radiation Efficiency at right, for mangOH™ RED device at LTE band.

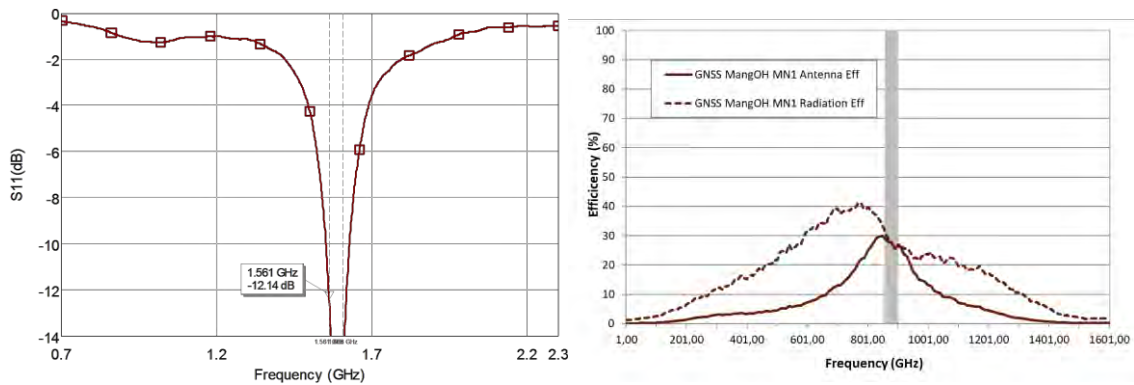


Figure 107 S_{11} at left and Antenna and Radiation Efficiency at right, for mangOH™ RED device at GNSS band.

As the matching networks tested for LTE and GNSS are the same as the tested in Experiment 2 (Figure 67), a comparison between performance has been done.

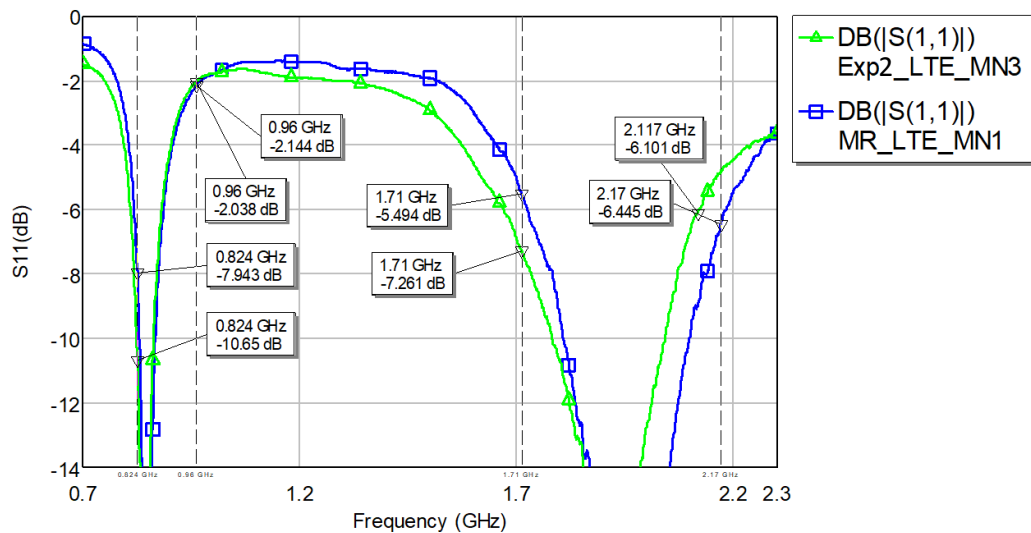


Figure 108 S parameters comparison between Experiment 2 and mangOH™ RED with the same matching network at LTE band.

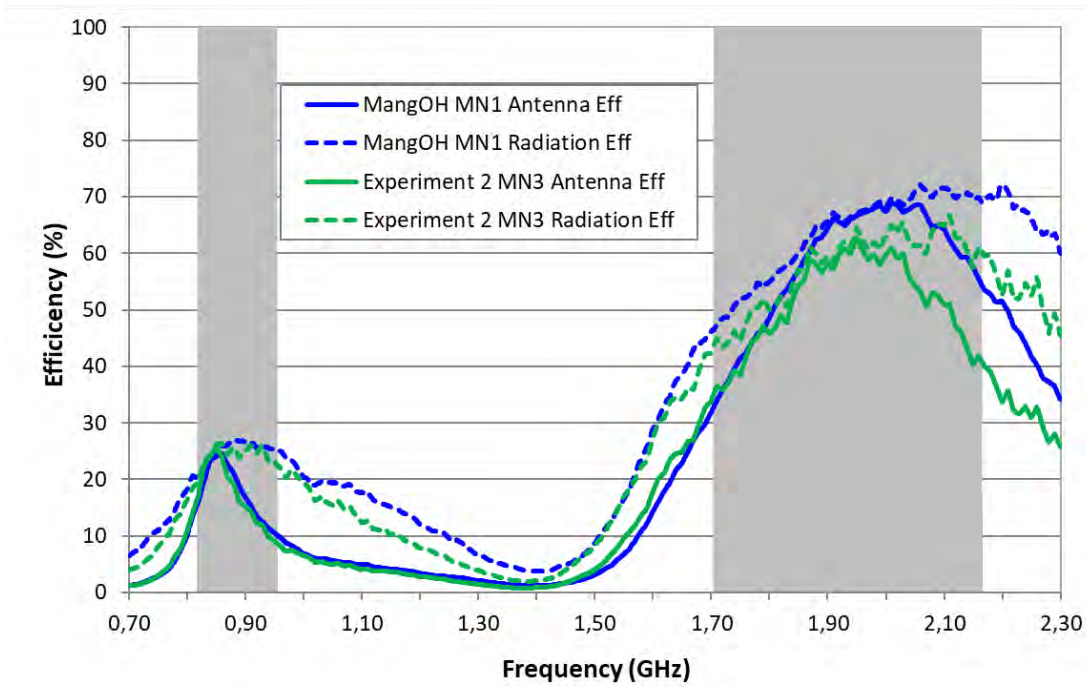


Figure 109 Antenna and Radiation Efficiency comparison between Experiment 2 and mangOH™ RED with the same matching network at LTE band.

LTE	ANTENNA EFFICIENCY (%)					
	824MHz	960MHz	Avg 824-960MHz	1710MHz	2170MHz	Avg 1710-2170MHz
Experiment 2	16.9	8.7	17.3	35.1	40.9	51.4
MangOH™ RED	15.8	10.2	17.9	32.9	54.5	58.3

Table 65 Antenna efficiency values for Experiment 2 and mangOH™ RED with the same matching network at LTE band.

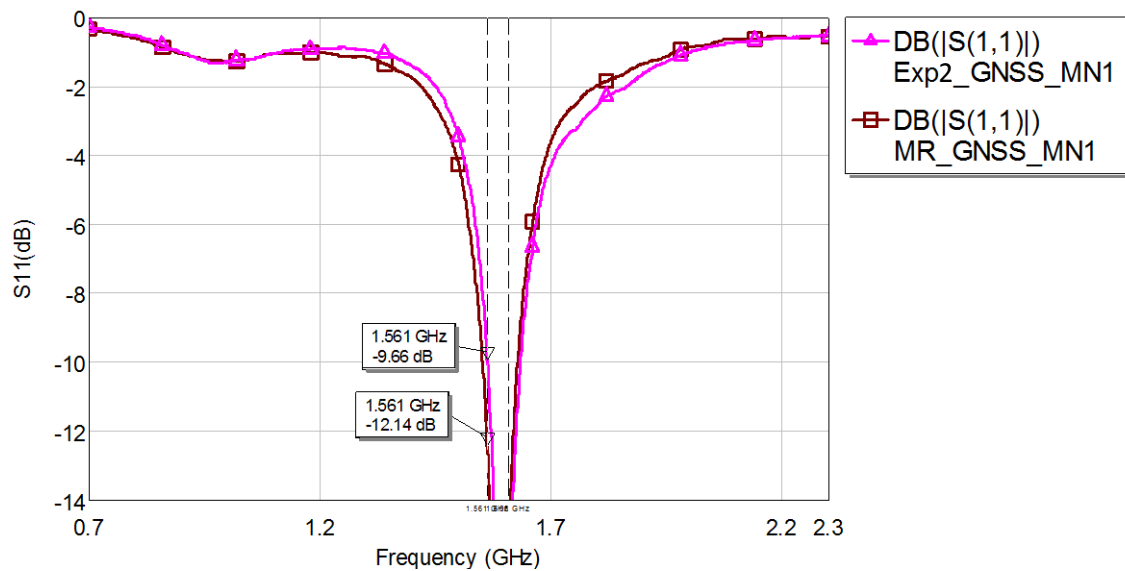


Figure 110 S parameters comparison between Experiment 2 and mangOH™ RED with the same matching network at GNSS band.

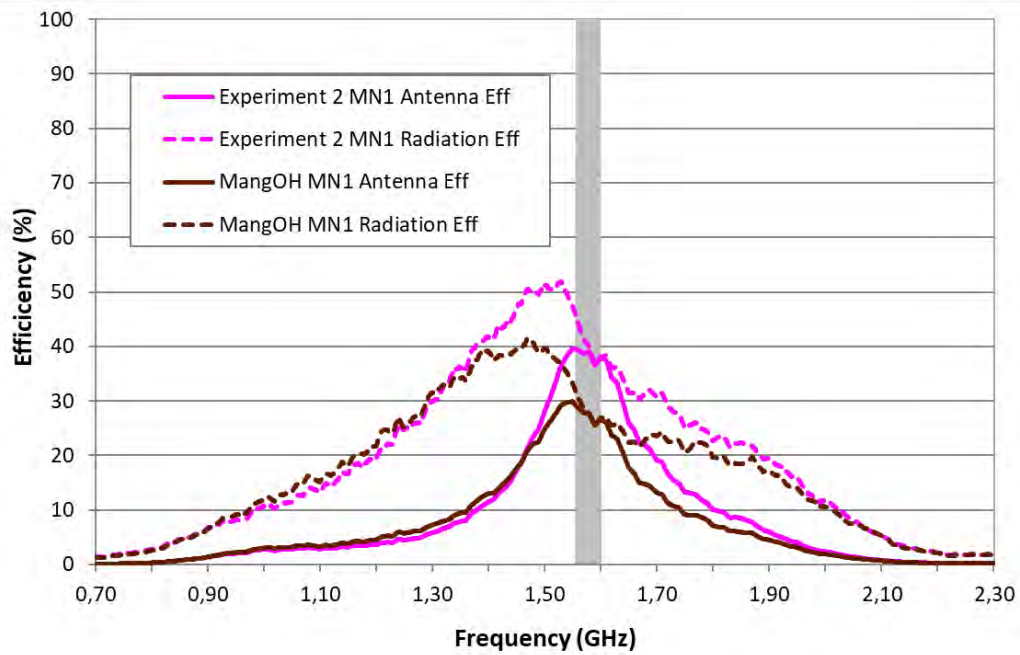


Figure 111 Antenna and Radiation Efficiency comparison between Experiment 2 and mangOH™ RED with the same matching network at GNSS band.

GNSS	ANTENNA EFFICIENCY (%)		
	1561MHz	1575MHz	Avg 1598-1606MHz
Experiment 2	39.5	38.7	37.4
MangOH™ RED	29.2	27.9	26.2

Table 66 Antenna efficiency values for Experiment 2 and mangOH™ RED with the same matching network at LTE band.

As it is shown in Figure 108 and Figure 110, the Reflection Coefficient obtained in the mangOH™ RED device is very similar to the obtained in the Experiment 2 PCB in house with the same matching network components and topology, which it means the results obtained in the Experiments done with the PCB's in house are very reliable to what it can be expected to achieved in the final device.

Otherwise, the efficiency values achieved in the mangOH™ RED device are slightly different in both applications. Meanwhile the efficiency for LTE band, both low band (824MHz-960MHz) and high band (1710MHz-2170MHz), have higher values for the mangOH™ RED set-up as it can be seen in Table 65, the GNSS values obtained for this final set-up are lowers than the achieved in Experiment 2 scenario, as it is shown in Table 66.

Due to low band is pretty equal in both cases and the differences appear in the high band, the most likely case is that the device is experimenting a coupling effect between the high band

LTE and the GNSS band which is affecting more the mangOH™ RED device than the Experiment 2 set-up.

Another possible problem, it could be than the ground plane where the GNSS SMA connector is placed does not have a continuous ground plane area, making the connection to ground worse than the Experiment 2 set-up studied and provoking losses in the band. It is important to note, the mangOH™ RED device does not have a continuous ground plane at the lateral connectors to place their respective footprint, so the scenario studied in all the Experiments is not completely the same, is a very similar one.

Although some changes appears between both set-ups performance, it is important to note the matching network soldered is completely the same and the embedding of the Experiment 2 into the mangOH™ RED device, has been realized by cutting a piece of the final device and replacing it for the equivalent part of a PCB in house with the Experiment 2 set-up mounted. So, considering the scenario mounted is not ideal one, achieving a performance very equal between scenarios demonstrate all Experiments realized with PCB's in house are very likely to have a similar performance in a real scenario.

5. CONCLUSIONS

The technology and specially, the IoT field are evolving to small devices with a massive life-time battery able to connect to other devices or able to be tracked. Therefore, the antennas and specially, the embedded antennas, are growing in relevance for the IoT devices designs.

The performance of the antenna will have a huge impact in the battery lifetime and the frequency range which the antenna is able to cover has a big importance in the versatility of the device. Consequently, the optimal situation is to have an antenna the smaller possible, with the best performance and which can cover the most applications and bands.

The Virtual Antenna™ technology studied in this project demonstrates is possible to achieve a good antenna performance in a small device with a small antenna and also, is able to cover the most used bands with only a tuning of the matching network. To test the antenna performance, it has been chosen the mangOH™ RED device from Sierra Wireless, an already commercialized top IoT device which is focalized in the Industry 4.0 market.

In this project it has been studied the steps to follow in order to implement an antenna into a device correctly:

1. Study of the bands to cover with the antenna.
2. Electromagnetic simulations with various antennas, design placement of the antenna in the device and performance comparison between the scenarios simulated.
3. Prototyping with the best simulated designs and comparison between the set-ups mounted.
4. Embedding into the original device to test the real performance achievable.

The electromagnetic simulations have been tested 3 different antennas. Two of them, the TRIO mXTEND™ and the DUO mXTEND™, operating at LTE bands (824MHz-960MHz and 1710MHz-2170MHz) and GNSS (1561MHz-1606MHz), and the other one, the RUN mXTEND™, only operating at LTE bands. A comparison between the best experiments for each antenna is shown in Table 67.

The better scenarios for the two antennas operating in LTE and GNSS have been implemented physically in a pcb in-house prototype with a variant of each, considering the matching network at LTE port horizontally to reduce the dimensions occupied. Furthermore, regarding the TRIO mXTEND™ chip antenna, alongside the change in the matching network position it has been changed the GNSS feeding line and matching network to improve the results obtained in the first experiment. From these four scenarios mounted it has been chosen the best case and then embedded into the mangOH™ RED device. A comparison between the best prototype for the DUO mXTEND™, the TRIO mXTEND™ and the embedded solution into the mangOH™ RED device it can be seen in the Table 68. The solution chosen for the embedding into the final device it has been the TRIO mXTEND™ best case scenario, so in the same Table 68 it can be observed the different between the same solution in a prototype and a real device.

	RUN mXTEND™ – Experiment 3	TRIO mXTEND™ – Experiment 3	DUO mXTEND™ - Experiment 3																																																						
Scenario																																																									
LTE Efficiency																																																									
Result Table	<table border="1"> <thead> <tr> <th colspan="6">ANTENNA EFFICIENCY (%)</th> </tr> <tr> <th>824MHz</th> <th>960MHz</th> <th>Avg 824-960MHz</th> <th>1710MHz</th> <th>2170MHz</th> <th>Avg 1710-2170MHz</th> </tr> </thead> <tbody> <tr> <td>30.3</td> <td>15.6</td> <td>26.8</td> <td>74.5</td> <td>62.3</td> <td>73.4</td> </tr> </tbody> </table>	ANTENNA EFFICIENCY (%)						824MHz	960MHz	Avg 824-960MHz	1710MHz	2170MHz	Avg 1710-2170MHz	30.3	15.6	26.8	74.5	62.3	73.4	<table border="1"> <thead> <tr> <th colspan="6">ANTENNA EFFICIENCY (%)</th> </tr> <tr> <th>824MHz</th> <th>960MHz</th> <th>Avg 824-960MHz</th> <th>1710MHz</th> <th>2170MHz</th> <th>Avg 1710-2170MHz</th> </tr> </thead> <tbody> <tr> <td>23.1</td> <td>9.0</td> <td>24.2</td> <td>54.5</td> <td>69.0</td> <td>75.1</td> </tr> </tbody> </table>	ANTENNA EFFICIENCY (%)						824MHz	960MHz	Avg 824-960MHz	1710MHz	2170MHz	Avg 1710-2170MHz	23.1	9.0	24.2	54.5	69.0	75.1	<table border="1"> <thead> <tr> <th colspan="6">ANTENNA EFFICIENCY (%)</th> </tr> <tr> <th>824MHz</th> <th>960MHz</th> <th>Avg 824-960MHz</th> <th>1710MHz</th> <th>2170MHz</th> <th>Avg 1710-2170MHz</th> </tr> </thead> <tbody> <tr> <td>8.6</td> <td>12.9</td> <td>22.7</td> <td>49.3</td> <td>15.3</td> <td>39.2</td> </tr> </tbody> </table>	ANTENNA EFFICIENCY (%)						824MHz	960MHz	Avg 824-960MHz	1710MHz	2170MHz	Avg 1710-2170MHz	8.6	12.9	22.7	49.3	15.3	39.2
ANTENNA EFFICIENCY (%)																																																									
824MHz	960MHz	Avg 824-960MHz	1710MHz	2170MHz	Avg 1710-2170MHz																																																				
30.3	15.6	26.8	74.5	62.3	73.4																																																				
ANTENNA EFFICIENCY (%)																																																									
824MHz	960MHz	Avg 824-960MHz	1710MHz	2170MHz	Avg 1710-2170MHz																																																				
23.1	9.0	24.2	54.5	69.0	75.1																																																				
ANTENNA EFFICIENCY (%)																																																									
824MHz	960MHz	Avg 824-960MHz	1710MHz	2170MHz	Avg 1710-2170MHz																																																				
8.6	12.9	22.7	49.3	15.3	39.2																																																				
GNSS Efficiency	-																																																								
Results Table	-	<table border="1"> <thead> <tr> <th colspan="3">ANTENNA EFFICIENCY (%)</th> </tr> <tr> <th>1561MHz</th> <th>1575MHz</th> <th>Avg 1598-1606MHz</th> </tr> </thead> <tbody> <tr> <td>36.7</td> <td>31.0</td> <td>16.2</td> </tr> </tbody> </table>	ANTENNA EFFICIENCY (%)			1561MHz	1575MHz	Avg 1598-1606MHz	36.7	31.0	16.2	<table border="1"> <thead> <tr> <th colspan="3">ANTENNA EFFICIENCY (%)</th> </tr> <tr> <th>1561MHz</th> <th>1575MHz</th> <th>Avg 1598-1606MHz</th> </tr> </thead> <tbody> <tr> <td>81.1</td> <td>78.5</td> <td>64.8</td> </tr> </tbody> </table>	ANTENNA EFFICIENCY (%)			1561MHz	1575MHz	Avg 1598-1606MHz	81.1	78.5	64.8																																				
ANTENNA EFFICIENCY (%)																																																									
1561MHz	1575MHz	Avg 1598-1606MHz																																																							
36.7	31.0	16.2																																																							
ANTENNA EFFICIENCY (%)																																																									
1561MHz	1575MHz	Avg 1598-1606MHz																																																							
81.1	78.5	64.8																																																							

Table 67 Comparison between the best solutions simulated for the RUN mXTEND™ (left), TRIO mXTEND™ (middle) and DUO mXTEND™ (right)



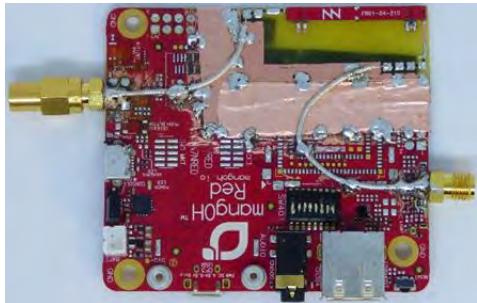
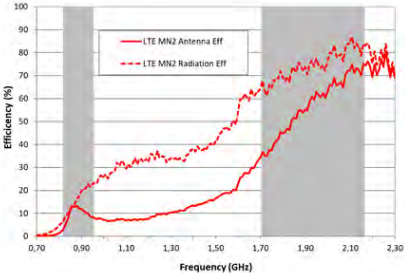
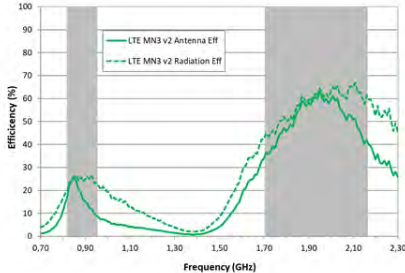
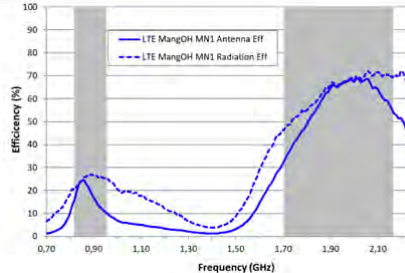
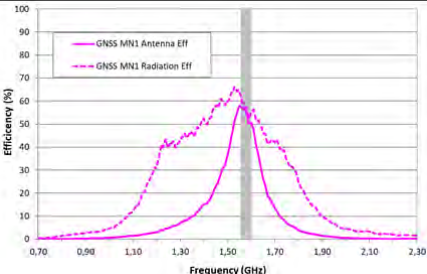
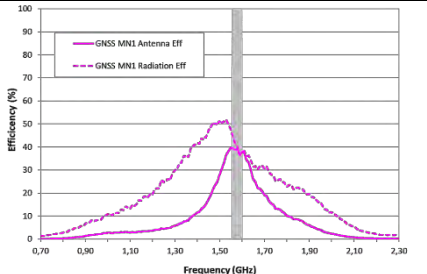
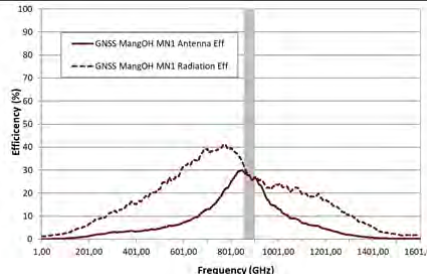
	DUO mXTEND™ – Experiment 1	TRIO mXTEND™ – Experiment 2	mangOH™ RED																																																						
Scenario																																																									
LTE Efficiency																																																									
Results Table	<table border="1"> <thead> <tr> <th colspan="6">ANTENNA EFFICIENCY (%)</th> </tr> <tr> <th>824MHz</th> <th>960MHz</th> <th>Avg 824-960MHz</th> <th>1710MHz</th> <th>2170MHz</th> <th>Avg 1710-2170MHz</th> </tr> </thead> <tbody> <tr> <td>30.3</td> <td>15.6</td> <td>26.8</td> <td>74.5</td> <td>62.3</td> <td>73.4</td> </tr> </tbody> </table>	ANTENNA EFFICIENCY (%)						824MHz	960MHz	Avg 824-960MHz	1710MHz	2170MHz	Avg 1710-2170MHz	30.3	15.6	26.8	74.5	62.3	73.4	<table border="1"> <thead> <tr> <th colspan="6">ANTENNA EFFICIENCY (%)</th> </tr> <tr> <th>824MHz</th> <th>960MHz</th> <th>Avg 824-960MHz</th> <th>1710MHz</th> <th>2170MHz</th> <th>Avg 1710-2170MHz</th> </tr> </thead> <tbody> <tr> <td>16.9</td> <td>8.7</td> <td>17.3</td> <td>35.1</td> <td>40.9</td> <td>51.4</td> </tr> </tbody> </table>	ANTENNA EFFICIENCY (%)						824MHz	960MHz	Avg 824-960MHz	1710MHz	2170MHz	Avg 1710-2170MHz	16.9	8.7	17.3	35.1	40.9	51.4	<table border="1"> <thead> <tr> <th colspan="6">ANTENNA EFFICIENCY (%)</th> </tr> <tr> <th>824MHz</th> <th>960MHz</th> <th>Avg 824-960MHz</th> <th>1710MHz</th> <th>2170MHz</th> <th>Avg 1710-2170MHz</th> </tr> </thead> <tbody> <tr> <td>15.8</td> <td>10.2</td> <td>17.9</td> <td>32.9</td> <td>54.5</td> <td>58.3</td> </tr> </tbody> </table>	ANTENNA EFFICIENCY (%)						824MHz	960MHz	Avg 824-960MHz	1710MHz	2170MHz	Avg 1710-2170MHz	15.8	10.2	17.9	32.9	54.5	58.3
ANTENNA EFFICIENCY (%)																																																									
824MHz	960MHz	Avg 824-960MHz	1710MHz	2170MHz	Avg 1710-2170MHz																																																				
30.3	15.6	26.8	74.5	62.3	73.4																																																				
ANTENNA EFFICIENCY (%)																																																									
824MHz	960MHz	Avg 824-960MHz	1710MHz	2170MHz	Avg 1710-2170MHz																																																				
16.9	8.7	17.3	35.1	40.9	51.4																																																				
ANTENNA EFFICIENCY (%)																																																									
824MHz	960MHz	Avg 824-960MHz	1710MHz	2170MHz	Avg 1710-2170MHz																																																				
15.8	10.2	17.9	32.9	54.5	58.3																																																				
GNSS Efficiency																																																									
Results Table	<table border="1"> <thead> <tr> <th colspan="3">ANTENNA EFFICIENCY (%)</th> </tr> <tr> <th>1561MHz</th> <th>1575MHz</th> <th>Avg 1598-1606MHz</th> </tr> </thead> <tbody> <tr> <td>57.5</td> <td>56.1</td> <td>50.5</td> </tr> </tbody> </table>	ANTENNA EFFICIENCY (%)			1561MHz	1575MHz	Avg 1598-1606MHz	57.5	56.1	50.5	<table border="1"> <thead> <tr> <th colspan="3">ANTENNA EFFICIENCY (%)</th> </tr> <tr> <th>1561MHz</th> <th>1575MHz</th> <th>Avg 1598-1606MHz</th> </tr> </thead> <tbody> <tr> <td>39.5</td> <td>38.7</td> <td>37.4</td> </tr> </tbody> </table>	ANTENNA EFFICIENCY (%)			1561MHz	1575MHz	Avg 1598-1606MHz	39.5	38.7	37.4	<table border="1"> <thead> <tr> <th colspan="3">ANTENNA EFFICIENCY (%)</th> </tr> <tr> <th>1561MHz</th> <th>1575MHz</th> <th>Avg 1598-1606MHz</th> </tr> </thead> <tbody> <tr> <td>29.2</td> <td>27.9</td> <td>26.2</td> </tr> </tbody> </table>	ANTENNA EFFICIENCY (%)			1561MHz	1575MHz	Avg 1598-1606MHz	29.2	27.9	26.2																											
ANTENNA EFFICIENCY (%)																																																									
1561MHz	1575MHz	Avg 1598-1606MHz																																																							
57.5	56.1	50.5																																																							
ANTENNA EFFICIENCY (%)																																																									
1561MHz	1575MHz	Avg 1598-1606MHz																																																							
39.5	38.7	37.4																																																							
ANTENNA EFFICIENCY (%)																																																									
1561MHz	1575MHz	Avg 1598-1606MHz																																																							
29.2	27.9	26.2																																																							

Table 68 Comparison between the best solutions mounted for the DUO mXTEND™ (left), TRIO mXTEND™ (middle) and mangOH™ RED device (right)

6. BIBLIOGRAPHY

- [1]. <http://www.accountancyresourcinggroup.co.uk/news-and-insights/industry-40-impact-of-digitization-on-finance-and-accountancy/>
- [2]. J. Anguera, A. Andújar, C. Puente, J. Mumbrú, "Antennaless Wireless Device", US Patent 8,203,492, August 2008.
- [3]. J. Anguera, A. Andújar, C. Puente, and J. Mumbrú, "Antennaless Wireless Device capable of Operation in Multiple Frequency regions," US. Patent 8,736,497, August 4, 2008.
- [4]. A. Andújar, J. Anguera, and C. Puente, "Ground Plane Boosters as a Compact Antenna Technology for Wireless Handheld Devices," *IEEE Trans. Antennas Propag.*, vol.59, no.5, pp.1668-1677, May 2011.
- [5]. Jaume Anguera and Aurora Andújar, "Ground Plane Contribution in Wireless Handheld Devices using Radar Cross Section Analysis", *Progress In Electromagnetics Research M*, vol.26, pp-101-114, 2012
- [6]. Jaume Anguera, Aurora Andújar, and Carlos García, "Multiband and Small Coplanar Antenna System for Wireless Handheld Devices", *IEEE Transactions on Antennas and Propagation*, vol.61, no. 7, pp. 3782-3789, July 2013.
- [7]. J. Anguera, N. Toporcer, and A. Andújar, "Slim bar booster for electronics devices," US Patent 9960478 (B2), July 2014.
- [8]. J. Anguera, A. Andújar, and C. Puente, "Antenna-Less Wireless: A Marriage Between Antenna and Microwave Engineering," *Microwave Journal*, vol.60, no.10, October 2017, pp.22-36.
- [9]. Aurora Andújar and Jaume Anguera, "MIMO Multiband Antenna System Combining Resonant and Non-Resonant Elements", *Microwave and Optical Technology Letters*, vol.56, no. 5, pp.1076-1084, May 2014.
- [10]. A. Andújar and J. Anguera, "Integration of a Non-Resonant Antenna in a Smartphone for Multiband Operation," European Conference on Antennas and Propagation, EUCAP 2018, London, UK, April 2018.
- [11]. J. Anguera, A. Andújar, J. L. Leiva, C. Schepens, R. Gaddi, and S. Kahng, "Multiband Antenna Operation with a Non-Resonant Element Using a Reconfigurable Matching Network," European Conference on Antennas and Propagation, EUCAP 2018, London, UK, April 2018.
- [12]. J. Anguera, C. Picher, A. Bujalance, and A. Andújar, "Ground Plane Booster Antenna Technology for Smartphones and Tablets," *Microwave and Optical Technology Letters*, vol.58, no. 6, pp.1289-1294, June 2016.
- [13]. A. Andújar, J. Anguera, and R. M^a Mateo, "Multiband Non-Resonant Antenna System with Reduced Ground Clearance," European Conference on Antennas and Propagation, EUCAP 2017, Paris, France, April 2017.
- [14]. Cristina Picher, Jaume Anguera, Aurora Andújar, Carles Puente, and Adrián Bujalance, "Concentrated Ground Plane Booster Antenna Technology for Multiband Operation in Handset Devices", *Radioengineering*, Vol. 23, no. 4, Dec. 2014. pp.1061-1070.
- [15]. Jaume Anguera, Aurora Andújar, Jussi Rahola, Jaakko Juntunen, "Synthesis of Multiband Matching Networks for Non-Resonant Antennas", *Computing and Electromagnetics CEM'17*, Barcelona, Spain, June 2017.
- [16]. Jaume Anguera, Aurora Andújar, Guzmán Mestre, Jussi Rahola, Jaakko Juntunen, "Design of Multiband Antenna Systems for Wireless Devices Using Antenna Boosters", *IEEE Microwave Magazine*, accepted paper, 2019.
- [17]. <https://www.awr.com/resource-library/virtual-antenna-matching-circuit-design-and-integration-iot-devices>

- [18]. J. Anguera, N. Toporcer, and A. Andújar, "Slim bar booster for electronics devices," US Patent 9960478 (B2), July 2014.
- [19]. J. Anguera, A. Andújar, C. Puente, and R. Mateos, "Modular multi-stage antenna system and component for wireless communications", patent App. US62/529,032
- [20]. J. Anguera and A. Andújar, C. Puente, "Compact Antenna Technology for Wireless Communications", patent app. US 62870837
- [21]. J. Anguera, A. Andújar, C. Puente, "Wireless Handheld Devices, Radiation Systems and manufacturing Methods", CN104508905 (B); US9331389 (B2); US9865917 (B2);
- [22]. J. Anguera, A. Andújar, C. Puente, and R. Mateos, "Modular multi-stage antenna system and component for wireless Communications" PCT/EP2018/068436
- [23]. Jaume Anguera, Aurora Andújar, Carles Puente, "Compact Antenna Technology for Wireless Communications", Pat. App. US62870837, EP19184772.2